Translational Medicine Communications

RESEARCH Open Access

Anglemetry of neural axis cell differentiation genes by structural pressurotopy of DNA loop strand segment tropy in reference to tissue macro-compliance

Hemant Sarin

Abstract

Background: Even as the eukaryotic stranded DNA is known to heterochromatinize at the nuclear envelope in response to mechanical strain, the precise mechanistic basis for alterations in chromatin gene transcription in differentiating cell lineages has been difficult to determine due to limited spatial resolution for detection of shifts in reference to a specific gene in vitro. In this study, heterochromatin shift during euchromatin gene transcription has been studied by parallel determinations of DNA strand loop segmentation tropy nano-compliance (*esebssiwaagoT*$_Q$ units, linear nl), gene positioning angulation in linear normal two-dimensional (2-D) *z*, *y*-vertical plane (anglemetry, ^{0}), horizontal alignment to the *z*, *x*-plane (vectormetry; m_A, m_M, a.u.), and by pressuromodulation mapping of differentiated neuron cell sub-class operating range for neuroaxis gene expression in reference to tissue macro-compliance (P_{eff}).

Methods: The *esebssiwaagoT*$_Q$ effective pressure unit (P_{eff}) maxima and minima for horizontal gene intergene base segment tropy loop alignment were determined ($n = 224$); the P_{eff} *esebssiwaagoT*$_Q$ quotient were determined ($n = 28$) for analysis of gene intergene base loop segment tropy structure nano-compliance ($n = 28$; $n = 188$); and gene positioning anglemetry and vectormetry was performed ($n = 42$). The sebs intercept-to-sebssiwa intercept quotient for linear normalization was determined ($b_{sebs}/b_{sebssiwa}$) by exponential plotting of sub-episode block sum (sebs) (x_1, y_1; x_2, y_2) and sub-episode block sum split integrated weighted average (sebssiwa) functions was performed, and the sebs – sebssiwa function residuals were determined. The effective cell pressure (P_{eff})-to-angle conversion factor was determined, $\Theta_A = (1E + 02)\ \{0.90 - [(0.000 + a \geq x < 0.245)\ (1.208)]$ form was applied for anisotropic gene anglemetry, and the $\Theta_M = (1E + 02)\ \{0.90 - [1.208\ (0.245 \geq x \leq m)]$ form was applied for mesotropic gene anglemetry. Two-step Tukey range t-test was performed for inter-group comparisons of $b_{sebs}/b_{sebssiwa}$ quotients and sebs – sebssiwa normalized residuals between tier 1 ($P_{eff} \leq 0.200$; $n = 11$) and tier 2 ($P_{eff} > 0.200 \leq 0.300$; $n = 6$), between tier 1 and tier 3 ($P_{eff} > 0.300$; $n = 8$), and between tier 3 and tier 2 ($\alpha = 0.05$).

(Continued on next page)

Correspondence: hemantsarin74@gmail.com
Freelance Investigator in Translational Science and Medicine (unaffiliated), 833 Carroll Road, Charleston, West Virginia, USA

(Continued from previous page)

Results: Based on the results of this study, I) heterochromatin strand DNA loop micro-segmentation structural nano-compliance is either amorphousity, anisotropy or mesotropy loop segment forms perceiving various grades of the asymmetric tropy viscosity effect, where between 3-to-5 and 8-to-11 genes are arranged as one or two in-tandem alternating anisotropic and mesotropic gene(s), or as in-tandem anisotropic or mesotropic genes in juxtaposition separated by intergene tropy base distance; for example, the anisotropy loop segment form between positions − 12 to + 15 in reference *LMNA* (P_{eff}, 0.184; $\theta_{\text{A}} = 68.4^0$) on human 1q22 (+) is: **5′**-0.234-(a_{-12})-0.272 (m_{-11})-0.229 (a_{-10})-0.211 (a_{-9})-0.269 (m_{-8})-0.144 (a_{-7})-0.314 (m_{-6})-0.268 (m_{-5})-0.176 (a_{-4})-0.260 (m_{-3})-0.259 (m_{-2})-0.270 (m_{-1})-0.184 (a_0)-0.135 (m_{+1})-0.395 (m_{+2})-0.146 (a_{+3})-0.212 (a_{+4})-0.336 (m_{+5})-0.287 (m_{+6})-0.153 (a_{+7})-0.283 (m_{+8})-0.193 (a_{+9})-0.269 (m_{+10})-0.199 (a_{+11})-0.146 (a_{+12})-0.190 (a_{+13})-0.188 (a_{+14})-0.243 (a_{+15})-**3′**, which begins at the **5′** end with *DAP3* (P_{eff} 0.234); II) mesotropy loop form genes are positioned between 11.7 and 60.4^0 (*CD34*) in the *z*, *y*-vertical plane, whereas anisotropy loop form genes positioned between 60.5 and 82.3^0 (*MIR4537*) in the *z*, *y*-vertical plane; III) the relationship between effective pressure and momentum is inverse proportionality, P_{eff} ($0.064 \geq x < 0.245$) · $\boldsymbol{m}_{\text{A}} = P_{\text{eff}}$ ($0.245 \geq x \leq 0.648$) · $\boldsymbol{m}_{\text{M}}$; IV) the interval for peripheral lower motor neuron (lmn) gene expression is definable as being between a P_{eff} of 0.434 and 0.311 (> 0.305), between a P_{eff} of 0.305 and 0.213 for cerebrocortical upper motor neurons, between a P_{eff} of 0.318 and 0.203 for hippocampocortical neurons, and between a P_{eff} of 0.298 and 0.217 for basal ganglia spiny neurons; therefore, there exists an inverse relationship between effective range of whole cell compliance and tissue macro-compliance ($R_{\text{effective whole cell compliance}} \cdot T_{\text{macro-compliance}} = \text{k}$), in which case the range for mesenchymal cell (MSC) gene expression is delineable as being between a Peff of 0.648 and <= 0.118 esebssiwaagoTQ units; and V) *RGS18* (P_{eff} 0.205; $\theta_{\text{M}} = 65.2^0$), *RGS16* ($P_{eff}$ 0.251; $\theta_{\text{M}} = 59.7^0$; human paralog of murine *RGS4*), *lnc-RXFP4–5* (P_{eff}, 0.314; $\theta_{\text{M}} = 52.1^0$; pituit), *RGS13* ($P_{eff}$, 0.360, $\theta_{\text{M}} = 46.5^0$), *CEACAM1* ($P_{eff}$, 0.384; $\theta_{\text{M}} = 43.6^0$), *SLC25A44* ($P_{eff}$, 0.395; $\theta_{\text{M}} = 42.3^0$) and *RGS21* ($P_{eff}$, 0.413; $\theta_{\text{M}} = 40.1^0$) are expressed within the lower motor neuron (lmn)-upper motor neuron (umn) neural cell axis; and *TSACC* (P_{eff}, 0.336; $\theta_{\text{M}} = 49.4^0$) and *JUND* ($P_{eff}$, 0.344; $\theta_{\text{M}} = 48.4^0$) are non-cell specific developmental biomarkers.

Conclusions: Based on the findings of this study considered together, the precise mechanistic basis for alterations in chromatin gene transcription eukaryotic stranded heterochromatin arranged by structural pressurotopy nano-compliance in DNA stand loop segments is effective cell pressure (P_{eff}) regulated shifting of transcriptionally active DNA in-between the inner nuclear envelope margin and the peripheral nucleoplasm edge and the *z*, *x*-plane horizontal alignment of a gene by gene specific P_{eff} within the cell specific effective range of whole cell compliance in reference to tissue macro-compliance. The findings of this study are therefore applicable to the further study of changes in gene transcription in response to applied mechanical strain-mediated alterations in nuclear envelope deformability in silico.

Keywords: Membrane proteins, Lamins, Nuclear pore, Mechanical loading, Substrate stiffness, Viscosity, Growth factor, Small molecule, Stem cell, Cell differentiation

Introduction

Non-constitutively less active heterochromatin and constitutively more active heterochromatin commonly known as euchromatin are the two forms of eukaryotic euchromatic chromatins [1–5]. Adenine and thymine nucleobase-rich G-banded DNA of heterochromatin binds to less hydrophilic staining dyes such as 4′,6-diamidino-2-phenylindole (DAPI; -4.37 nm^{-1}) with cationicity sufficiently separated in space (1+ SS 1+), whereas guanine and cytosine nucleobase-rich R-banded DNA of constitutive heterochromatin (euchromatin) binds to more hydrophilic dyes such as Oligomycin (-6.75 nm^{-1}) with polyhydroxylated hydrophilicity sufficiently separated in space (OH SS OH), which is more transcriptionally-active due to protein affinity interactions of the same [5, 6], both of which are loosely wound around the nucleosome core histone proteins in the pressurized state of a cell. Adenine and T-rich G-banded non-constitutive heterochromatin resides in affinity with non-histone polypeptides lamin A/C or B1/B2 [7–13], from which genes are episodically-transcribed in fully-differentiated cells [1–5], in contrast to G and C-rich R-banded constitutive heterochromatin resides in affinity with nuclear pore complex subunits rather than in affinity with the lamins and lamin-associated proteins, from which regulatory housekeeping genes are transcribed [1–5, 11]. During the G_o resting transcriptionally active cell stage, both of the chromatins are located in one of two locations in the nucleus, either at the inner nuclear membrane-bound to lamins A/C or B1/B2 via lamin-associated polypeptides (LAP) polypeptides (LAP) 1 and 2 isoforms and emerin (EMD), or closer to the center at peripheral edge central nucleoplasm interface during the non-transcription of lamin/lamin-associated polypeptides [14–18], during which there is differential gene transcription [15] in comparison to that at the inner nuclear membrane in apposition to nuclear pore complex subunits [16].

During the DNA synthesis stage [1–3], both forward and reverse strands of early and late-replicating

chromatins become DNA polymerase substrates when replication forks form at defined intervals resembling radial loops at the inner nuclear membrane [19–22], a process that continues at the nuclear envelope to the point of MKI67 protein expression [23], which is a 359 kDa G_2 interphase enzyme involved in translocation of tetraploid chromatin from the inner nuclear membrane to the nuclear center by mass effect, as the nuclear envelope dissolutes and chromatids align at the metaphase plate. A mass effect mechanism has been suggested for horizontal alignment of DNA during the S phase is the 900 kDa molecular weight of multi-subunit DNA polymerase during which multiple assembled DNA polymerases simultaneously walk forward (+) or reverse (-) strand intergene segments at replication forks based on recent determinations that during the process of gene transcription the DNA synthesis (S_1) phase begins when effective cell pressure (P_{eff}) increases into the 0.261 to 0.283 (*PCNA*) pressure units range [24–28].

Nuclear envelope elastance (*E*) responses to pressure application and alterations in initial envelope elastance to tonicity or dynamic strain over time have been studied by micropipette aspiration techniques in *LMNA* (-/-) or emerin (*EMD*, -/y) gene-deficient cells (*J*, creep compliance; $kpa^{-1}{\cdot}sec^{-1}$; α power) [29–35]; cell morphology alterations in response to grades of substrate stiffness have been studied by spectrophotometry of gel viscoelasticity (G'; Pa) and cell tissue tensional homeostasis by traction force microscopy [36, 37]; and cell mechanosensitivity changes and nuclear deformability alterations in response to mechanical loading during pharmacological application *in vitro* studied by the chromatin condensation parameter (CCP, %) and the nucleus deformability index (NDI, %; NAR, a.u.) [38–41], in addition to differential gene transcription in mesenchymal stem and transformed cells studied *in situ* by qRT-PCR mRNA expression, based on the findings of which mechanoforce transduction can be defined as downstream molecular signaling events that result in alterations in chromatin gene transcription [28].

It has been recently hypothesized that alterations in cell membrane compliance in relation to mitochondrial membrane compliance results in increases or decreases in effective cell pressure secondary to that alterations in cell membrane compliance by membrane domain-binding of growth factors and small molecule ligand binding to cell surface receptors [24–27]. The modes of cellular pressurization in the biological system *in vivo* is have been further defined as the combination of (a) synergistic positive macro-pressuromodulation due to the presence of a rigidified extracellular matrix or cortical bone, which increases effective cell pressure, or non-synergistic negative macro-pressuromodulation due to the presence of surrounding cells, which decreases effective cell pressure; and (b) positve or negative micro-pressuromodulation at cell membrane domains by way of endocrine, paracrine and autocrine small molecule hormones, growth factors and cytokines, which either increases or decreases effective cell pressure. Therefore, the effective cell pressure for horizontal alignment of gene tropy and maximal gene transcription is related to cell compliance by $Compliance_{\text{cell membrane micro-pressuromulation}} + Elastance_{\text{cell membrane integrin-to-collagen or sub-cortical bone macro-pressuromodulation}}$ $Pressure_{\text{effective intracellular}} = k$ during synergistic macro-pressuromodulation, and by $Compliance_{\text{cell membrane micro--pressuromulation}} - Elastance_{\text{cell junction-to-cell junction macro-pressuromodulation}}$ $Pressure_{\text{effective intracellular}} = k$ during non-synergistic macro-pressuromodulation, where $P_{\textit{effective intracellular}}$ $(P_{\text{eff}}) = P_{\textit{effective intranuclear}}$.

A fractional measure has been recently developed to quantify the effective intracellular pressure required to horizontally align a gene for its maximal transcription, as there are non-specific avidity associations of nuclear protoplasm proteins and non-coding RNAs in a tropic manner with the intergene segment bases of genes located upstream and downstream *with respect to* a gene; and represents the 5' → 3' reading direction intergene distance tropy that needs to be overcome for a gene to horizontally align for transcription and has a specificity and sensitivity of 100% as validated [25]. This measure, the episodic sub-episode block sums split-integrated weighted average-averaged gene overexpression tropy quotient ($esebssiwaagoT_Q$). The $esebssiwaagoT_Q$, a physical property of a gene, is less than 0.245 units for infra-pressuromodulated anisotropic genes, and in between 0.245 and 0.745 units for supra-pressuromodulated mesotropic genes.

Even as the eukaryotic stranded chromatin has shown to be heterochromatinized to various degrees at the nuclear envelope in response to application of mechanical strain *in vitro*, the precise mechanistic basis for alterations in chromatin gene transcription in differentiating cell lineages has been difficult to determine due to limited spatial resolution for detection of shifts in reference to specific genes *in vitro*. Therefore, in this study heterochromatin DNA strand loop structure gene positioning angulation in the *z*, *y*-vertical plane is studied by segmentation of DNA strand loops in terms of mesotropy and anisotropy utilizing the sebs intercept-to-sebssiwa intercept linearization quotient, $b_{\text{sebs}}/b_{\text{sebssiwa}}$, for validation of linear normalization and the effective cell pressure unit (P_{eff}) -to-gene angulation conversion factor for gene anglemetry and momentum vectormetry analysis in linear nl two-dimensional (2-D) protoplasmic cell space; henceforth, these normalized heterochromatin gene angulation parameters are applied for determination of the

esebssiwaagoT$_Q$-based pressuromodulation map for gene expression of the subtypes of neuronal cells that constitute the peripheral to central nervous system neuroaxis in correlation with changes in tissue macro-compliance.

Methods

Selection of genes for study

Human chromatin forward and reverse strand genes were sampled from 17 of 24 chromosome loci for determination of minima and maxima effective intracellular pressure unit (P_{eff}) for the episodic sub-episode block sums split-integrated weighted average-averaged gene overexpression tropy quotient (*esebssiwaagoT*$_Q$), n = 224 [25–27]; the sampled representative genes include ch 14 (n = 188, heavy chain immunoglobin locus, native and recombined) [26, 27], ch 1 (*PDPN*, *S100A2*, *S100A14*, *CDH11*, *SELE*, *CD34*, *PTPRC* and *CR2*; n = 8), ch 2 (*TGFA*), ch 3 (*ACPP*), ch 4 (*CD38*), ch 6 (*PRR3*, *PRDM1*, *ENPP1*), ch 7 (*ABCB1*, *FOXP2*), ch 10 (*MRC1*, *MKI67*), ch 11 (*SORL1*, *MS4A1*, *RAG1*, *RAG2*), ch 12 (*BTG1*, *CD27*, *AICDA*, *ESPL1*), ch 14 (*IFI27*), ch 16 (*CDH11*, *CD19*), ch 17 (*CD79B*), ch 16 (*PHLPP*, *ZCCHC2*), ch 19 (*CD79A*), ch 20 (*CD20*, *PCNA*), ch 22 (*APOBEC3A*, *APOBEC3*, *APOBEC3H*) and ch 23-X (*DMD*) [25–27]. Three different sets of additional genes were selected for study: 1) twenty-eight sequentially located protein coding and non-coding RNA genes in native positions on the Ch 1 q arm forward (+) strand in reference to *LMNA* for the P_{eff} *esebssiwaagoT*$_Q$-based sub-analysis study of native intergene base loop segment tropy structure nano-compliance (n = 28); 2) protein coding genes located on various chromosomes and overexpressed during cell differentiation were selected for P_{eff} *esebssiwaagoT*$_Q$-based sub-analysis study of gene angulation positioning in the linear normalized z, y-vertical plane and momentum vectormetry to the z, x-horizontal plane (n = 28), and include genes involved in cell membrane adhesion (*CD34*, *CEACAM1*), cell membrane ligand binding (*INSL3*, *ENPP1*), extracellular matrix formation (*COL1A1*, *COL2A1*, *COL6A1*, *CCN2*), cell cycle regulation (*RGS13*, *RGS4*, *RGS1*), inner nuclear envelope matrix stabilization (*LMNA*, *LMNB1*, *LMNB2*, *EMD*, *NUMA1*), transcriptional regulation (*MYC*, *JUND*, *SOX18*, *PRKCH*, *EGR1*, *ESRRB*, *GABPA*, *NFE2L2*), NFκB survival pathway (*IER3*), oxygen sensing (*CYGB*), and in B-cell function (*PRDM1*, *MIR4537*); and 3) protein coding genes located on various chromosomes and overexpressed during central-to-peripheral neural cell differentiation were selected for predictive sub-analysis study of neural axis gene overexpression in reference to tissue macro-compliance by *esebssiwaagoT*$_Q$-based effective intracellular pressure units (n = 14), and include genes involved in neurotransmitter ligand binding (*DRD1*, *DRD2*, DRD3, *GRIN1*), synaptic cleft stabilization (*UNC13A*, *SHANK2*), cell cycle regulation (*RGS21*, *RGS2*, *RGS16*, *RGS18*), nuclear RNA splicing (*RBFOX3*), transcriptional regulation (*SOX1*, *SOX14*), and in oxygen sensing (*NGB*).

Gene locus coordinates were mined as per the GRch38/hg38 gene location classification system at Gene Cards (https://www.genecards.org) and LNCipedia (https://lncipedia.org). Genes were stratified by gene locus episode and initial sub-episode block structure (SEB) as either Episode 2 (> 11,864 ≤ 265,005 bases; 5 SEB), Episode 3 (≤ 11,864; 7 SEB) and for Episode 4 (>265, 005 <607,463; 9 SEB), Episode 5 (≥ 607,463 < 2,242, 933; 11 SEB) or Episode 6 (≥ 2,242,933; 13 SEB) to determine the initial sub-episode block structure count for determination of the episodic sub-episode block sums split-integrated weighted average-averaged gene overexpression tropy quotient were determined [25–27].

Determination of native gene location intergene base segment loop tropy and strand loop structure in reference to *LMNA*

The sequentially located gene locus gene loop segment tropies in reference to *LMNA* on ch 1q22 (+) for sub-group structural analysis included *DAP3*, *MSTO2P*, *PIR32612*, *LOC100132108*, *SYT11*, *GC01P155896*, *lnc-RXFP4-5*, *RXFP4*, *lnc-RXFP4-2*, *ENSG00000224276* / *LOC105371729*, *GC01P156042* (*LAMTOR2*), *RAB25*, *LMNA*, *SEMA4A*, *SLC25A44*, *PMF1-BGLAP*, *TMEM79*, *TSACC*, *RHBG*, *ENSG00000237390*, *lnc-TTC24-5*, *lnc-TTC24-4*, *ENSG00000260460*, *lnc-TTC24-1*, *GC01P156524*, *TTC24*, *NAXE*, *HALPN2* and *BCAN* from 5' to 3' end (n = 28).

The *esebssiwaagoT*$_Q$-based Σ intergene base segment tropy was determined as the integrated upstream part anisotropic sub-episode block sum (*uppasebs*), downstream part anisotropic sub-episode block sum (*dppasebs*), the upstream part mesotropic sub-episode block sum (*uppmsebs*) and the downstream part anisotropic sub-episode block sum (*dppasebs*) by the final sequentially integrated (∫) paired point tropy quotient (*prpT*$_Q$) point of final sub-episode block structure based on which the gene intergene base segment loop structure was determined in terms of segmental anisotropy, segmental mesotropy or segmental amorphousosity for the respective genes in native configuration in reference to the *LMNA* gene locus.

Determination of the linearization quotient for *z*, *y*-plane gene anglemetry by exponential function plotting of sebs and sebssiwa

Genes selected for sub-group analysis anglemetry include episode 2 (n = 14), episode 3 (n = 11), episode 4 (n = 2) and episode 6 (n = 1), n = 28. Episode 2 genes selected for sub-group study include (ch, strand) *LMNA* (1q22, +), *RGS13* (1q31.2, +), *CD34* (1q32.2, -), *LMNB1*

(5q23.2, +), *PRDM1* (6q21, +), *ENPP1* (6q23.2, +), *NUMA1* (11q13.3-q13.4, -), *COL2A1* (12q13.11, -), *ESRRB* (14q24.3, +), *COL1A1* (17q21.33, -), *CYGB* (17q25.1, -), *CEACAM1* (19q13.2, -), *GABPA* (21q21.3, +) and *COL6A1* (21q22.3, +); episode 3 genes selected for sub-group study include *RGS4* (1q23.3, +), *RGS1* (1q31.2, +), *EGR1* (5q31.2, +), *IER3* (6q21.33, -), *CCN2* (6q23.2, -), *MYC* (8q24.21, +), *MIR4537* (14q32.3, -), *INSL3* (19q13.11, -), *JUND* (19q13.11, -), *SOX18* (20q13.33, -) and *EMD* (Xq28, +); the episode 4 genes selected for sub-group study include *LMNB2* (19q13.3, -) and *PRKCH* (14q32.2, +); and the episode 6 gene(s) selected for sub-group study include *NFE2L2* (2q31.2, -).

The *esebssiwaagoT*$_Q$-based *uppasebs*, *dppasebs*, *uppmsebs*, and *dppasebs* and the correlate upstream part anisotropic sub-episode block sum split integrated weighted average (*uppasebssiwa*), downstream part anisotropic sub-episode block sum split integrated weighted average (*dppasebssiwa*), the upstream part mesotropic sub-episode block sum split integrated weighted average (*uppmsebssiwa*), and the downstream part anisotropic sub-episode block sum split integrated weighted average (*dppasebssiwa*) were determined. The *y*-intercept exponential function for each sub-group analysis gene locus sub-episode block sum (sebs; upstream part, *upp*; downstream part, *dpp*) and sub-episode block sum split integrated weighted average (sebssiwa; upstream, downstream) was plotted (x_1, y_1; x_2, y_2) for determination of the normalized *uppasebs*, *uppmsebs*::*uppasebssiwa*, *uppmsebssiwa* effect; the *x*-intercept plot was utilized for determination of the normalized *dppasebs*, *dppmsebs*::*dppasebssiwa*, *dppmsebssiwa* effect when the *uppasebs* and *uppmsebs* sums part-effect was equivalent; and a hybrid intercept plot was utilized in case of equivalent magnitude ratio *uppasebs* : *dppasebs* and *uppmsebs* : *dppmsebs* sums part-effects. Each function is represented in form, $b{\cdot}e^{m{\cdot}x}$, *where b* represents the downstream anisotropic effect. The *y*- or *x*-sebs intercept to sebssiwa intercept quotient for linearization was determined in form, $b_{sebs}/b_{sebssiwa}$. The sub-episode block sum (sebs) - sub-episode block sum split integrated weighted average (sebssiwa) was determined as the normalized subtractive residual for each function, adjusted residual.

3-tier pairwise statistical comparison of $b_{sebs}/b_{sebssiwa}$ linearization quotients and sebs - sebssiwa residuals by *esebssiwaagoT*$_Q$ stratum

Sub-group analysis genes were stratified by P_{eff} interval in ≤ 0.200, > 0.200 ≤ 0.300 and > 0.300 tiers for pairwise comparisons of the $b_{sebs}/b_{sebssiwa}$ intercept linearization quotient and subtractive residual determinations of *uppasebs*, *dppasebs*, *uppmsebs*, *dppmsebs* and correlate *uppasebssiwa*, *dppasebssiwa*, *uppmsebssiwa*, *dppmsebssiwaa* as independent sums and averages for genes with non-*nil* residual normalizing adjustments. Two-step Tukey range t-test was performed for inter-group comparisons of $b_{sebs}/b_{sebssiwa}$ quotients and sebs – sebssiwa normalized residuals between tier 1 ($P_{eff} \leq 0.200$; $n = 11$) and tier 2 ($P_{eff} > 0.200 \leq 0.300$; $n = 6$), between tier 1 and tier 3 ($P_{eff} > 0.300$; $n = 8$), and between tier 3 and tier 2 ($\alpha = 0.05$); likewise comparisons were performed for determination of differences in Σ intergene tropy between the tiers ($\alpha = 0.05$).

Determination of the effective pressure unit quotient to angle conversion factor gene anglemetry from the *z*, *y*-vertical to *z*, *x*-horizontal plane

The pressure unit to angle conversion factor was determined in reference to the *z*, *x*-axis horizontal plane and two-dimensional gene anglemetry analysis was performed for the sub-group analysis genes ($n = 28$; $n = 14$). The $\Theta_A = (1E + 02)\ \{0.90 - [(0.000 + a \geq x < 0.245)\ (1.208)]$ form was applied for anisotropic gene anglemetry, *where a* is the minimum pressure for anisotropic gene expression, and the $\Theta_M = (1E + 02)\ \{0.90 - [1.208\ (0.245 \geq x \leq m)]$ form was applied for mesotropic gene anglemetry, *where m* is the maximum pressure for mesotropic gene expression ($n = 224$), based on linear regression of the *esebssiwaagoT*$_Q$s of the gene set of the study ($R^2 = 1$). Gene position arc distance in the *z*, *y*-vertical plane in reference to the *z*, *x*-horizontal plane was defined for anisotropic and mesotropic genes based on gene anglemetry thetas, Θ_A and Θ_M. The hypotenusal intergene tropy base distance for anisotropic genes was then defined as d_A for anisotropic genes, and as d_M for mesotropic genes, in which case *d* is the final sub-episode block sum of intergene tropy base distance for anisotropic genes (ASEB) or for mesotropic genes (MESEB). The Σ intergene base tropy distance is defined in reference to the horizontal line of unity (H_0) as either $d_A{\cdot}\sin\ \Theta_A$ for anisotropic genes and as $d_M{\cdot}\sin\ \Theta_M$ for mesotropic genes, *wherein* the arc gene tropy intergene base distance is definable as $d_M{\cdot}\sin\ \Theta_M$ in reference to the line of unity; and *wherein* the Σ hypotenusal gene intergene tropy distance d_A (or d_M) is defined as a non-component scalar at $H_0 = 0^0$ in which case $d_{A\ (or\ M)}{\cdot}\cos\ \Theta_{A\ (or\ M)} + x_{A\ (or\ M)}$.

Vectormetry for z, x-plane horizontal alignment of anisotropic and mesotropic genes

Vectormetry for horizontal alignment of anisotropic and mesotropic genes was performed empirically for anisotropic and mesotropic genes based on the *z*, *y*-vertical plane position angle, Θ_A for anisotropic genes and Θ_M for mesotropic genes, and effective cell pressure (P_{eff}) for horizontal alignment, P_{eff} $(0.000 + a \geq x < 0.245)$ for anisotropic and P_{eff} $(0.245 \geq x \leq 0.745 - m)$ for

mesotropic. Defined knowns were applied for vectormetry, *where* momental vector, $\boldsymbol{m}$, is a product of the mass of DNA-associated nuclear proteins (m) and the velocity of gene tropy to horizontal (v). The origination momentum vector for chromatin-associated protein viscosity at intergene segment effect was then defined as $\boldsymbol{m}_{\text{ch tropy}}$; the initial origination momentum vector for nuclear membrane nucleoplasm chromatin-associated protein viscosity at intergene segment effect was then defined as $\boldsymbol{m}_{\text{ch nmn tropy}}$; and the origination gravitational momentum vector was then defined as $\boldsymbol{m}_{\text{pro-grav ch tropy}}$. The effective momentum, $\boldsymbol{m}_{\text{eff}}$, for *z, x*-horizontal plane alignment of anisotropic gene tropy was then defined, $\boldsymbol{m}_{\text{A}}$ ($\boldsymbol{m}_{\text{ch tropy}}$ - $\boldsymbol{m}_{\text{pro-grav ch tropy}}$); and the effective momentum for *z, x*-horizontal plane alignment of mesotropic gene tropy was then defined, $\boldsymbol{m}_{\text{M}}$ [$\boldsymbol{m}_{\text{ch tropy}}$ + $\boldsymbol{m}_{\text{ch nmn tropy}}$ (- $\boldsymbol{m}_{\text{pro-grav ch tropy}}$)]. The relationship between effective pressure ($\boldsymbol{P}_{\text{eff}}$) and momentum ($\boldsymbol{m}_{\text{eff}}$) was definable for anisotropic gene horizontal alignment ($\boldsymbol{m}_{\text{A}}$) and mesotropic gene horizontal alignment ($\boldsymbol{m}_{\text{M}}$).

Determination of the heterochromatinization parameters for neural axis cell differentiation genes

Genes selected for sub-group analysis include episode 2 (n = 5), episode 3 (n = 5) and episode 4, 5 or 6 (n = 4), *n* = 14. Episode 2 genes selected for sub-group study include (ch, strand) *UNC13A* (19p13.11, -), *RGS21* (1q31.2, +), *SOX1* (13q34, +), *DRD2* (11q23.2, -), *GRIN1* (9q34.3, +); episode 3 genes selected for sub-group study include *NGB* (14q24.3, -), *RGS2* (1q31.2, +), *RGS16* (1q23.3, -), *SOX14* (3q22.3, +), *DRD1* (5q35.2, +) and *EGR1* (5q31.2, +); the Episode 4 genes selected for sub-group study include *RGS18* (1q31.2, +) and *DRD3* (3q13.31, -); and the Episode 5 to 6 genes selected for sub-group study include *RBFOX3* (17q25.3, -) and *SHANK2* (11q13.3-q13.4, -).

The *uppasebs*, *dppasebs*, *uppmsebs*, *dppasebs*, *uppasebssiwa*, *dppasebssiwa*, *uppmsebssiwa* and *dppasebssiwa* were determined as per the *esebssiwaagoT*$_{\text{Q}}$ method and its adjusted residual (x_1, y_1; x_2, y_2). The exponential function pair was *y*-intercept or reverse *x*-intercept plotted for determination of the sebs-to-sebssiwa intercept linearization quotient ($b_{\text{sebs}}/b_{\text{sebssiwa}}$). The *uppesebssiwaa*/*dppesebssiwaa* quotient effective intracellular pressure (P_{eff}) was then determined for classifying of predicted gene overexpression of the genes selected for neural axis cell differentiation. Two-dimensional gene anglemetry analysis was performed for the mesotropic and anisotropic gene set by effective pressure for gene expression for determination of gene position in the *z, y*-vertical plane position angle (Θ_{A}, Θ_{M}). The tropy of the intergene base segments and interposed gene segment bases was determined as the hypotenusal Σ gene intergene base segment tropy for *z, y*-plane to *z, x*-horizontal plane alignment.

Results

Sequentially located forward strand native genes in 5′→3′ chronology on ch 1q22 in reference to *LMNA* by P_{eff} *esebssiwaagoT*$_{\text{Q}}$ units

DAP3 is a 2 A 5 initial and final SEB gene locus with a Σ intergene base segment tropy of 3.09108E + 05 bases at position -12. Sequential integration (∫) to the final *esebssiwaagoT*$_{\text{Q}}$ for *DAP3* is 0.093, 0.157, 0.210, 0.247. The final *uppesebssiwaa* and *dppesebssiwaa* for *DAP3* are 1.1196E + 04 and 4.7835E + 04 intergene bases. The P_{eff} for gene locus *DAP3* is 0.234 *esebssiwaagoT*$_{\text{Q}}$ units.

MSTO2P is a 3 M 7 initial and final SEB gene locus with a Σ intergene base segment tropy of 5.94486E + 05 bases at position -11. Sequential integration (∫) to the final *esebssiwaagoT*$_{\text{Q}}$ for *MSTO2P* is 0.680, 0.417, 0.358, 0.340, 0.309, 0.269 (DfC). The final *uppesebssiwaa* and *dppesebssiwaa* for *MSTO2P* are 1.8354E + 04 and 6.7448E + 04 intergene bases. The P_{eff} for gene locus *MSTO2P* is 0.272 *esebssiwaagoT*$_{\text{Q}}$ units (Table 1; Figs. 1, 2 and 3).

PIR32612 is a 3 A 7 initial and final SEB gene locus with a Σ intergene base segment tropy of 5.26775E + 05 intergene bases at position -10. Sequential integration (∫) to the final *esebssiwaagoT*$_{\text{Q}}$ for *PIR32612* is 0.0002, 0.242, 0.261, 0.247, 0.279, 0.248. The final *uppesebssiwaa* and *dppesebssiwaa* for *PIR32612* are 1.3367E + 04 and 5.8380E + 04 intergene bases. The P_{eff} for gene locus *PIR32612* is 0.229 *esebssiwaagoT*$_{\text{Q}}$ units (Table 1; Figs. 1, 2 and 3).

LOC100132108 is a 3 A 7 initial and final SEB gene locus with a Σ intergene base segment tropy of 5.82948E + 05 intergene bases at position -9. Sequential integration (∫) to the final *esebssiwaagoT*$_{\text{Q}}$ for *LOC100132108* is 0.262, 0.357, 0.258, 0.198, 0.225, 0.205. The final *uppesebssiwaa* and *dppesebssiwaa* for *LOC100132108* are 1.4504E + 04 and 6.8778E + 04 intergene bases. The P_{eff} for gene locus *LOC100132108* is 0.211 *esebssiwaagoT*$_{\text{Q}}$ units (Table 1; Figs. 1, 2 and 3).

SYT11 is a 2 A 5 initial and final SEB gene locus with a Σ intergene base segment tropy of 4.15371E + 05 intergene bases at position -8. Sequential integration (∫) to the final *esebssiwaagoT*$_{\text{Q}}$ for *SYT11* is 0.166, 0.401, 0.333, 0.266. The final *uppesebssiwaa* and *dppesebssiwaa* for *SYT11* are 1.8089E + 04 and 6.7250E + 04 intergene bases. The P_{eff} for gene locus *SYT11* is 0.269 *esebssiwaagoT*$_{\text{Q}}$ units (Table 1; Figs. 1, 2 and 3).

GC01P155896 is a 3 A 7 (+1) ACM final SEB gene locus with a Σ intergene base segment tropy of 1.201927E + 06 intergene bases at position -7. Sequential integration (∫) to the final *esebssiwaagoT*$_{\text{Q}}$ for *GC01P155896* is 0.188, 0.330, 0.205, 0.198, 0.144, 0.138, 0.131. The final *uppesebssiwaa* and *dppesebssiwaa* for *GC01P155896* are 1.8900E + 04 and 1.31341E + 05 intergene bases. The P_{eff} for gene locus *GC01P155896* is 0.144 *esebssiwaagoT*$_{\text{Q}}$ units (Table 1; Figs. 1, 2 and 3).

Table 1 Sequentially located forward strand native genes of human chromosome 1 q arm locus 22 in reference to *LMNA* within intergene loop tropy segments with nano-compliance of the same with respect to the gene

	Germline gene locus[a]	Episode category (sub-episode block structure)[b, c]	Gene locus start and end base location (no of locus bases; Σ intergene base segment tropy)	Sequential integration (∫) to final $esebssiwaagoT_Q$ (fract)[d]	Final *uppesebssiwaa*, *dppesebssiwaa*	P_{eff} $esebssiwaagoT_Q$ (fract)[e]
-12	*DAP3*, death associated protein 3	2 A 5	5′-155,687,960 – 155,739,010 (51,051; 3.09108E + 05)	0.093, 0.157, 0.210, 0.247	1.1196E + 04, 4.7835E + 04	0.234
-11	*MSTO2P*, misato family member, pseudogene	3 M 7	155,745,768 – 155,750,688 (4,921; 5.94486E + 05)	0.680, 0.417, 0.358, 0.340, 0.309, *0.269*	1.8354E + 04, 6.7448E + 04	0.272
-10	*PIR32612*	3 A 7	155,750,710 – 155,750,759 (30; 5.26775E + 05)	0.0002, 0.242, 0.282, 0.218, 0.232, 0.224	1.3367E + 04, 5.8380E + 04	0.229
-9	*LOC100132108*	3 A 7	155,845,340 – 155,847,270 (1,931; 5.82948E + 05)	0.262, 0.357, 0.258, 0.198, 0.225, 0.205	1.4504E + 04, 6.8778E + 04	0.211
-8	*SYT11*, synaptotagmin 11	2 A 5	155,859,469 – 155,885,199 (25,731; 4.15371E + 05)	0.166, 0.401, 0.333, 0.266	1.8089E + 04, 6.7250E + 04	0.269
iiii-7	*GC01P155896*	3 A 7 (+ 1) ACM	155,894,280 – 155,894,386 (107; 1.201927E+ 06)	0.188, 0.330, 0.205, 0.198, 0.144, 0.138, 0.131	1.8900E + 04, 1.31341E + 05	0.144
-6	*lnc-RXFP4–5*	3 M 7 (− 2) NCA	155,934,457 – 155,936,536 (2,080; 5.72477E + 05)	0.335, 0.274, 0.292, 0.233, *0.314*, 0.272, 0.250	2.6779E + 04, 8.5304E + 04	0.314
-5	*RXFP4*, relaxin family peptide//INSL5 receptor 4	3 A 7	155,941,689 – 155,942,949 (1,261; 4.25027E + 05)	0.144, 0.453, 0.451, 0.376, 0.299, 0.260	1.2920E + 04, 4.8207E + 04	0.268
-4	*lnc-RXFP4–2* (ENSG00000273002)	3 M 7	155,978,659 – 155,983,018 (4,380; 1.210734E+ 06)	0.551, 0.184, 0.225, 0.208, 0.199, 0.162	2.7911E + 04, 1.58180E + 05	0.176
-3	*ENSG00000224276/ LOC105371729*	2 M 5	155,991,390 – 156,033,225 (41,836; 3.67426E + 05)	0.527, 0.209, 0.211, 0.236, 0.*260*, 0.247	1.4498E + 04, 5.5694E + 04	0.260
-2	*GC01P156042* (*LAMTOR2*, late endosomal/lysosomal adaptor, MAPK and MTOR activator 2)	2 M 5 (−2) NCA	156,042,571 – 156,060,811 (18,241; 2.91985E + 05)	0.358, 0.278, *0.259*, 0.273	1.3666E + 04, 5.2795E + 04	0.259
-1	*RAB25*, member RAS oncogene family	3 A 7 (−2) ACM	156,061,160 – 156,070,514 (9,355; 6.29741E + 05)	0.030, 0.356, 0.297, 0.434, *0.270*, 0.242, 0.233	2.6153E + 04, 9.7028E + 04	0.270
	LMNA, prelamin-A/C	2 A 5	156,082,156 – 156,140,089 (57,934; 9.51609E + 05)	0.156, 0.206, 0.162, 0.240	2.8948E + 04, 1.57549E + 04	0.184
1	*SEMA4A*, semaphorin 4A	2 M 5	156,147,359 – 156,177,752 (30,394; 2.95365E + 05)	0.449, 0.170, 0.173, 0.136	7.891E + 03, 5.8332E + 04	0.135
2	*SLC25A44*, solute carrier family 25 member 44	2 A 5	156,193,932 – 156,212,796 (18,865; 3.62292E + 05)	0.184, 0.226, 0.268, 0.399, *0.395*, 0.378, 0.270	2.1658E + 04, 5.4827E + 04	0.395
3	*PMF1-BGLAP*, PMF1 (polyamine modulated factor 1)-BGLAP (bone gamma-carboxyglutamate protein) readthrough	2 A 5	156,212,982 – 156,243,332 (27,090; 3.92203E + 05)	0.005, 0.230, 0.161, 0.133	9.594E + 03, 6.5791E + 04	0.146

Table 1 Sequentially located forward strand native genes of human chromosome 1 q arm locus 22 in reference to *LMNA* within intergene loop tropy segments with nano-compliance of the same with respect to the gene *(Continued)*

	Germline gene locus[a]	Episode category (sub-episode block structure)[b, c]	Gene locus start and end base location (no of locus bases; Σ intergene base segment tropy)	Sequential integration (∫) to final $esebssiwaagoT_Q$ (fract)[d]	Final *uppesebssiwaa*, *dppesebssiwaa*	P_{eff} $esebssiwaagoT_Q$ (fract)[e]
4	*TMEM79*, transmembrane Protein 79	3 A 7 (+1) ACM	156,282,913 – 156,293,185 (10,273; 1.848556E + 06)	0.335, 0167, 0.208, 0.194, 0.247, 0.245, 0.228	4.0434E + 04, 1.90636E + 05	0.212
5	*TSACC*, TSSK6 activating cochaperone	3 A 7	156,337,314 – 156, 346,395 (9,682; 7.43872E + 05)	0.028, 0.250, 0.327, 0.340, 0.364, 0.318	2.7118E + 04, 8.0818E + 04	0.336
6	*RHBG*, Rh family B glycoprotein	2 M 5	156,366,043 – 156,385,234 (19,192; 6.05950E + 05)	0.419, 0.280, 0.315, 0.302	2.6125E + 04, 9.1097E + 04	0.287
7	*ENSG00000237390*	3 A 7	156,388,226 – 156,395,609 (7,384; 9.58633E + 05)	0.020, 0.110, 0.164, 0.154, 0.137, 0.144	1.7374E + 04, 1.13726E + 05	0.153
8	*lnc-TTC24–5*	3 M 7	156,500,997 – 156,502,475 (1,479; 9.02656E + 05)	0.369, 0.321, 0.355, 0.242, 0.267, 0.290	4.1211E + 04, 9.6908E + 04	0.283
9	*lnc-TTC24–4*	3 A 7 (+2) ACM	156,503,086 – 156,503,834 (749; 1.138955E + 05)	0.055, 0.276, 0.152, 0.193, 0.223, 0.235, 0.194	2.3007E + 04, 1.19362E + 05	0.193
10	*lnc-TTC24–1*	3 M 7	156,509,584 – 156,513,960 (4,377; 4.86984E + 05)	0.544, 0.097, 0.267, 0.342, 0.312, 0.264	1.4861E + 04, 5.5298E + 04	0.269
11	*GC01P156524*	3 A 7 (+ 2) ACM	156,524,535 – 156,525,810 (476; 1.492171E + 06)	0.141, 0.225, 0.162, 0.212, 0.223, 0.217, 0.232, 0.217, *0.199*, 0.196, 0.205	2.6686E + 04, 1.34141E + 053 A 7	*0.199*
12	*TTC24*, tetratricopeptide repeat domain 24	3 M 7	156,579,727 – 156,587,797 (8,071; 8.54954E + 05)	0.406, 0.197, 0.184, 0.116, 0.145, 0.159	1.6633E + 04, 1.14108E + 05	*0.146*
13	*NAXE*, NAD(P) HX epimerase	3 A 7	156,591,762 – 156,594,299 (2,538; 1.422774E + 06)	0.125, 0.218, 0.153, 0.144, 0.159, 0.187	2.7892E + 04, 1.61601E + 05	*0.190*
14	*HAPLN2*, hyaluronan and proteoglycan link protein 2	*3 M 7*	156,618, 801–3 M 7 156,625,725 (6,925; 7.92243E + 05)	0.636 0.505, 0.456, 0.243, 0.209, 0.211, *0.188*, 0.209, 0.194	1.8695E + 04, 9.9190E + 04	*0.188*
15	*BCAN*, brevican	*2 M 5*	156,641,390 – 156,659,532–3′ (18,143; 7.28923E + 05)	0.389, 0.212, 0.235, 0.262	2.7104E + 04, 1.11335E + 05	*0.243*

[a)] RNA genes included are protein encoding genes, non-coding GC_, PIR_, ENSG_ and long non-coding *lnc-* naming convention mRNA genes including functional pseudogenes; [b)] Gene loci episodic structure sub-episode block categories include Episode 2 (> 11,864 ≤ 265,005 bases; 5 SEB), Episode 3 (≤ 11,864; 7 SEB), Episode 4 (>265,005 < 607,463; 9 SEB), Episode 5 (≥ 607,463 < 2,242,933; 11 SEB) or Episode 6 (≥ 2,242,933; 13 SEB); [c)] Gene loci sub-episode block structure variations include non-contributory anisotropy (NCA), anisotropy converted to mesotropy (ACM), and/or 0.5-factor adjusted stabilizing mesotropy or anisotropy converted to stabilizing isotropy for anisotropy or mesotropy (stlAfM, stlMfA or stlMfM) that result in initial to final SEB conversion; [d)] Integration is in underlined italics where the sequential sub-episode block structure is deviation from constancy (DfC) [25], as in the cases of gene locuses *MSTO2P* (pos − 11), *lnc-RXFP4–5* (pos −6), *ENSG00000224276 / LOC105371729* (pos −3), *GC01P156042* (pos − 2), *RAB25* (pos − 1), *SLC25A44* (pos + 2), *GC01P156524* (pos + 11) and *HALPN2* (pos + 14); and [e)] P_{eff} $esebssiwaagoT_Q$ is in italics where three (3) or more anisotropic or mesotropic genes are situated in tandem within the intergene tropy of the same in reference to *LMNA* located in native configuration

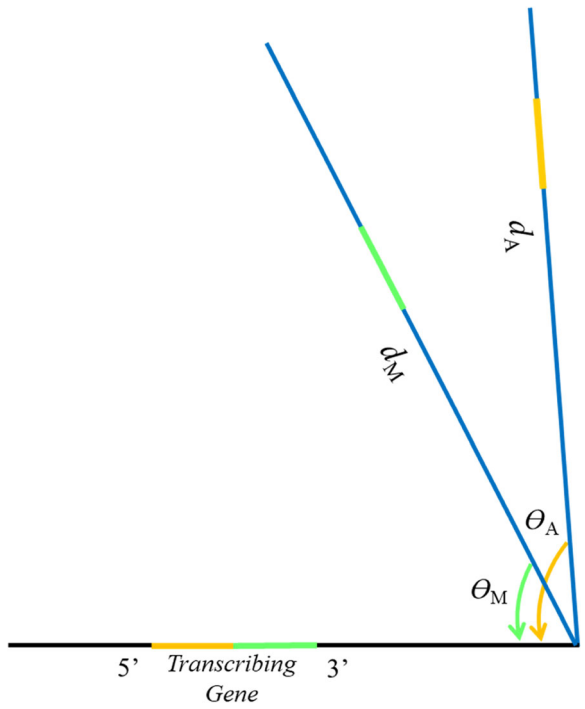

Fig. 1 Angulation of intergene base arc distance tropy in reference to the *z*, *x*-axis horizontal plane for amorphous heterochromatin loop segment genes. Amorphous heterochromatin strand loop micro-structural segmentation is a series of intergene base distance-separated alternating anisotropic (a) and mesotropic genes (m) in the form of one or two in-tandem anisotropic or mesotropic genes of the same at angulation (Θ_A, Θ_M) in the *z*, *y*-vertical axis plane. The prelamin-A/C gene (P_{eff}, 0.184)-containing amorphous form heterochromatin strand loop segment for example is arranged as *LMNA* ($\Theta_A = 67.8^0$)-*SEMA4A* ($\Theta_A = 73.7^0$)-*SLC25A44* ($\Theta_M = 42.3^0$)-*PMF1-BGLAP* ($\Theta_A = 72.4^0$)-*TMEM79* ($\Theta_A = 64.4^0$)-*TSACC* ($\Theta_M = 49.4^0$)-*RHBG* ($\Theta_M = 55.3^0$) in series from 5′ to 3′ on human ch 1q22 at positions +1 through +6 in reference to *LMNA*. As shown is an anisotropic gene within its hypotenusal gene intergene base distance tropy positioned at angulation, $\Theta_A \leq 82.3^0$ in the *z*, *y*-vertical plane with Σ gene + intergene base distance, d_A: sin Θ_A, juxtaposed to a mesotropic gene within its hypotenusal gene intergene base distance tropy positioned at angulation, $\Theta_M \geq 11.7^0$, from the horizontal line of unity in a heterochromatin strand amorphous form loop segment. A transcribable gene can be either an anisotropic segment loop gene (Θ_A) or a mesotropic gene segment loop gene (Θ_M) in an amorphous segment loop of alternating in-tandem genes. Legend. d_A, hypotenusal distance of anisotropic gene intergene tropy bases; d_M, hypotenusal distance of mesotropic gene intergene tropy bases. Note: 3′, downstream

lnc-RXFP4-5 is a 3 M 7 (-2) NCA final SEB gene locus with a Σ intergene base segment tropy of 5.72477E + 05 intergene bases at position -6. Sequential integration (∫) to the final $esebssiwaagoT_Q$ for *lnc-RXFP4-5* is 0.335, 0.274, 0.292, 0.233, 0.314 (DfC), 0.272, 0.250. The final *uppesebssiwaa* and *dppesebssiwaa* for *lnc-RXFP4-5* are 2.6779E + 04 and 8.5304E + 04 intergene bases. The P_{eff} for gene locus *lnc-RXFP4-5* is 0.314 $esebssiwaagoT_Q$ units (Table 1; Figs. 1, 2 and 3).

RXFP4 is a 3 A 7 initial and final SEB gene locus with a Σ intergene base segment tropy of 4.25027E + 05 intergene bases at position -5. Sequential integration (∫) to the final $esebssiwaagoT_Q$ for *RXFP4* is 0.144, 0.453, 0.451, 0.376, 0.299, 0.260. The final *uppesebssiwaa* and *dppesebssiwaa* for *RXFP4* are 1.2920E + 04 and 4.8207E + 04 intergene bases. The P_{eff} for gene locus *RXFP4* is 0.268 $esebssiwaagoT_Q$ units (Table 1; Figs. 1, 2 and 3).

lnc-RXFP4-2 is a 3 M 7 initial and final SEB gene locus with a Σ intergene base segment tropy of 1.210734E + 06 intergene bases at position -4. Sequential integration (∫) to the final $esebssiwaagoT_Q$ for *lnc-RXFP4-2* is 0.551, 0.184, 0.225, 0.208, 0.199, 0.162. The final *uppesebssiwaa* and *dppesebssiwaa* for *lnc-RXFP4-2* are 2.7911E + 04 and 1.58180E + 05 intergene bases. The P_{eff} for gene locus *lnc-RXFP4* is 0.176 $esebssiwaagoT_Q$ units (Table 1; Figs. 1, 2 and 3).

ENSG00000224276 / *LOC105371729* is a 2 M 5 initial and final SEB gene locus with a Σ intergene base segment tropy of 3.67426E + 05 intergene bases at position -3. Sequential integration (∫) to the final $esebssiwaagoT_Q$ for *ENSG00000224276* / *LOC105371729* is 0.527, 0.209, 0.211, 0.236, 0.260 (DfC), 0.247. The final *uppesebssiwaa* and *dppesebssiwaa* for *ENSG00000224276 / LOC105371729* are 1.4498E + 04 and 5.5694E + 04 intergene bases. The P_{eff} for gene locus *ENSG00000224276/LOC105371729* is 0.260 $esebssiwaagoT_Q$ units (Table 1; Figs. 1, 2 and 3).

GC01P156042 (*LAMTOR2*) is a 2 M 5 (-2) ACM final SEB gene locus with a Σ intergene base segment tropy of 2.91985E + 05 intergene bases at position -2. Sequential integration (∫) to the final $esebssiwaagoT_Q$ for *GC01P156042* (*LAMTOR2*) is 0.358, 0.278, 0.259 (DfC), 0.273. The final *uppesebssiwaa* and *dppesebssiwaa* for *GC01P156042* (*LAMTOR2*) are 1.3666E + 04 and 5.2795E + 04 intergene bases. The P_{eff} for gene locus *GC01P156042* (*LAMTOR2*) is 0.259 $esebssiwaagoT_Q$ units (Table 1; Figs. 1, 2 and 3).

RAB25 is a 3 A 7 (-2) ACM final SEB gene locus with a Σ intergene base segment tropy of 6.29741E + 05 intergene bases at position -1. Sequential integration (∫) to the final $esebssiwaagoT_Q$ for *RAB25* is 0.030, 0.356, 0.297, 0.434, 0.270 (DfC), 0.242, 0.233. The final *uppesebssiwaa* and *dppesebssiwaa* for *RAB25* are 2.6153E + 04 and 9.7028E + 04 intergene bases. The P_{eff} for gene locus *RAB25* is 0.270 $esebssiwaagoT_Q$ units (Table 1; Figs. 1, 2 and 3).

LMNA is a 2 A 5 initial and final SEB gene locus with a Σ intergene base segment tropy of 9.51609E + 05 intergene bases at position 0. Sequential integration (∫) to the final $esebssiwaagoT_Q$ for *LMNA* is 0.156, 0.206, 0.162, 0.240. The final *uppesebssiwaa* and *dppesebssiwaa* for *LMNA* are 2.8948E + 04 and 1.57549E + 04 intergene bases. The P_{eff} for gene locus *LMNA* is 0.184 $esebssiwaagoT_Q$ units (Table 1; Figs. 1, 2 and 3).

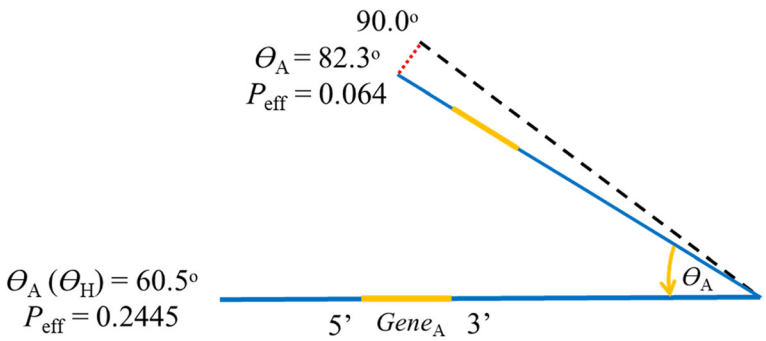

Fig. 2 Angulation of intergene base arc distance tropy in reference to the *z*, *x*-axis horizontal plane for anisotropic heterochromatin loop segment genes. Anisotropic heterochromatin strand loop micro-structural arrangement is a series of ≥ 3 intergene base distance-separated genes perceiving the asymmetric tropy viscosity effect with nano-compliance of the same, Θ_A, lncRNA class gene *GC01P156524* (P_{eff}, 0.199)-containing anisotropic form heterochromatin strand loop segment for example is arranged as *GC01P156524* ($\Theta_A = 66^0$)-*TTC24* ($\Theta_A = 72.4^0$)-*NAXE* ($\Theta_A = 67.0^0$)-*HALPN2* ($\Theta_A = 67.3^0$)-*BCAN* ($\Theta_A = 60.6^0$) in series from 5′ to 3′ on human ch 1q22 at positions +11 through +15 in reference to *LMNA*. As shown is a gene of an anisotropic heterochromatin segment loop positioned at $\Theta_A = 60.49^0$ (P_{eff}, 0.2445) in the *z*, *y*-axis plane is transcriptionally active at $\Theta_A = \Theta_H$, and ch 14q32.3 reverse strand (-) *IGH_* immunoglobin heavy chain locus gene, *MIR4537*, positioned at the upper limit of angulation $\Theta_A = 82.3^0$, aligns for *z*, *x*-horizontal plane transcription at a $P_{eff} = 0.064$ *esebssiwaagoT*$_Q$ units. Legend. Θ_H, zero degree horizontal axis line of unity; d_A, hypotenusal distance of anisotropic gene intergene tropy bases; d_A sin Θ_A, distance to horizontal for anisotropic gene intergene tropy distance; d_A at $H_0 = 0^0$, d_A·cos $\Theta_A + x_A$; $P_{effective\ intracellular\ pressure}$ (P_{eff}) = $P_{effective\ intranuclear\ pressure}$

SEMA4A is a 2 M 5 initial and final SEB gene locus with a Σ intergene base segment tropy of 2.95365E + 05 intergene bases at position +1. Sequential integration (∫) to the final *esebssiwaagoT*$_Q$ for *SEMA4A* is 0.449, 0.170, 0.173. The final *uppesebssiwaa* and *dppesebssiwaa* for *SEMA4A* are 7.891E + 03 and 5.8332E + 04 intergene bases. The P_{eff} for gene locus for *SEMA4A* is 0.135 *esebssiwaagoT*$_Q$ units (Table 1; Figs. 1, 2 and 3).

SLC25A44 is a 2 A 5 initial and final SEB gene locus with a Σ intergene base segment tropy of 3.62292E + 05 intergene bases at position +2. Sequential integration (∫) to the final *esebssiwaagoT*$_Q$ for *SLC25A44* is 0.184,

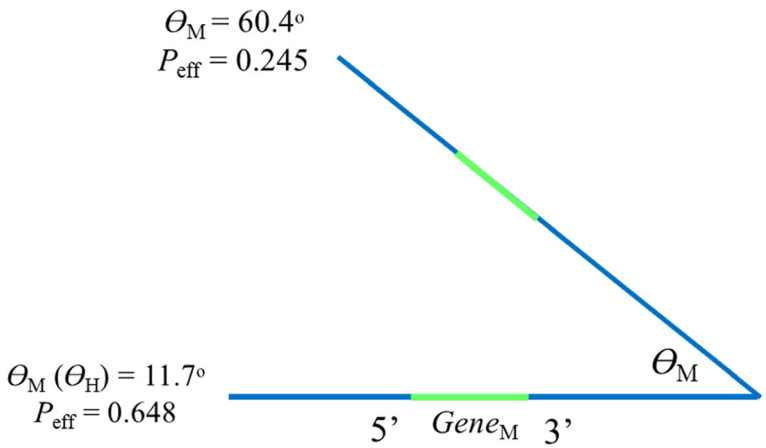

Fig. 3 Angulation of intergene base arc distance tropy in reference to the *z*, *x*-axis horizontal plane mesotropic heterochromatin loop segment genes. Mesotropic heterochromatin strand loop micro-structural arrangement is a series of ≥ 3 intergene base distance-separated genes perceiving the lesser grade asymmetric tropy viscosity effect with nano-compliance of the same, Θ_M, RNA/ncRNA class gene locus *ENSG00000224276* / *LOC105371729* (P_{eff}, 0.260)-containing mesotropic form heterochromatin strand loop segment consisting of three genes in-series is arranged as *ENSG00000224276* / *LOC105371729* ($\Theta_M = 58.6^0$)-*GC01P156042* (*LAMTOR2*) ($\Theta_M = 58.7^0$)-*RAB25* ($\Theta_M = 57.4^0$) from 5′ to 3′ on the forward (+) strand of human ch 1q22 at positions -3 through -1 in reference to *LMNA*; and the heavy chain immunoglobin gene locus (*IGH_*) containing mesotropic form heterochromatin strand loop segment consisting of 8 diversity genes in-series is arranged as *IGHD1-20* (*nf*) ($\Theta_M = 41^0$)-*IGHD6-19* ($\Theta_M = 52.7^0$)-*IGHD5-18* ($\Theta_M = 59.3^0$)-*IGHD4-17* ($\Theta_M = 52.5^0$)-*IGHD3-16* ($\Theta_M = 52.8^0$)-*IGHD2-15* ($\Theta_M = 54.5^0$)-*IGHD1-14* ($\Theta_M = 54.7^0$)-*IGHD6-13* ($\Theta_M = 55.4^0$) from 3′ to 5′ on the reverse (-) strand of human ch 14q32.3 in native configuration. As shown is a gene of a mesotropic heterochromatin segment loop positioned at the lower limit of angulation $\Theta_M = 11.7^0$ in the *z*, *y*-vertical plane that horizontally aligns for transcription in *z*, *x*-axis at a P_{eff} of 0.648 *esebssiwaagoT*$_Q$ units. Legend. Θ_H, zero degree horizontal; d_M, hypotenusal distance of anisotropic gene intergene tropy bases; d_M sin Θ_M, distance to horizontal for anisotropic gene intergene tropy distance; d_M at $H_0 = 0^0$, d_M·cos $\Theta_M + x_M$; $P_{effective\ intracellular\ pressure}$ (P_{eff}) = $P_{effective\ intranuclear\ pressure}$

0.226, 0.268, 0.399, 0.395 (DfC), 0.378, 0.270. The final *uppesebssiwaa* and *dppesebssiwaa* for *SLC25A44* are 2.1658E + 04 and 5.4827E + 04 intergene bases. The P_{eff} for gene locus for *SLC25A44* is 0.395 *esebssiwaagoT*$_Q$ units (Table 1; Figs. 1, 2 and 3).

PMF1-BGLAP is a 2 A 5 initial and final SEB gene locus with a Σ intergene base segment tropy of 3.92203E + 05 intergene bases at position +3. Sequential integration (∫) to the final *esebssiwaagoT*$_Q$ for *PMF1-BGLAP* is 0.005, 0.230, 0.161, 0.133. The final *uppesebssiwaa* and *dppesebssiwaa* for *PMF1-BGLAP* are 9.594E + 03 and 6.5791E + 04 intergene bases. The P_{eff} for gene locus for *PMF1-BGLAP* is 0.146 *esebssiwaagoT*$_Q$ units (Table 1; Figs. 1, 2 and 3).

TMEM79 is a 3 A 7 (+1) ACM final SEB gene locus with a Σ intergene base segment tropy of 1.848556E + 06 intergene bases at position +4. Sequential integration (∫) to the final *esebssiwaagoT*$_Q$ for *TMEM79* is 0.335, 0167, 0.208, 0.194, 0.247, 0.245, 0.228. The final *uppesebssiwaa* and *dppesebssiwaa* for *TMEM79* are 4.0434E + 04 and 1.90636E + 05 intergene bases. The P_{eff} for gene locus for *TMEM79* is 0.212 *esebssiwaagoT*$_Q$ units (Table 1; Figs. 1, 2 and 3).

TSACC is a 3 A 7 initial and final SEB gene locus with a Σ intergene base segment tropy of 7.43872E + 05 intergene bases at position +5. Sequential integration (∫) to the final *esebssiwaagoT*$_Q$ for *TSACC* is 0.028, 0.250, 0.327, 0.340, 0.364, 0.318. The final *uppesebssiwaa* and *dppesebssiwaa* for *TSACC* are 2.7118E + 04 and 8.0818E + 04 intergene bases. The P_{eff} for gene locus for *TSACC* is 0.336 *esebssiwaagoT*$_Q$ units (Table 1; Figs. 1, 2 and 3).

RHBG is a 2 M 5 initial and final SEB gene locus with a Σ intergene base segment tropy of 6.05950E + 05 intergene bases at position +6. Sequential integration (∫) to the final *esebssiwaagoT*$_Q$ for *RHBG* is 0.419, 0.280, 0.315, 0.302. The final *uppesebssiwaa* and *dppesebssiwaa* for *RHBG* are 2.6125E + 04 and 9.1097E + 04 intergene bases. The P_{eff} for gene locus for *RHBG* is 0.287 *esebssiwaagoT*$_Q$ units (Table 1; Figs. 1, 2 and 3).

ENSG00000237390 is a 3 A 7 initial and final SEB gene locus with a Σ intergene base segment tropy of 9.58633E + 05 intergene bases at position +7. Sequential integration (∫) to the final *esebssiwaagoT*$_Q$ for *ENSG00000237390* is 0.020, 0.110, 0.164, 0.154, 0.137, 0.144. The final *uppesebssiwaa* and *dppesebssiwaa* for *ENSG00000237390* are 1.7374E + 04 and 1.13726E + 05 intergene bases. The P_{eff} for gene locus for *ENSG00000237390* is 0153 *esebssiwaagoT*$_Q$ units (Table 1; Figs. 1, 2 and 3).

lnc-TTC24-5 is a 3 M 7 initial and final SEB gene locus with a Σ intergene base segment tropy of 9.02656E + 05 intergene bases at position +8. Sequential integration (∫) to the final *esebssiwaagoT*$_Q$ for *lnc-TTC24-5* is 0.369, 0.321, 0.355, 0.242, 0.267, 0.290. The final *uppesebssiwaa* and *dppesebssiwaa* for *lnc-TTC24-5* are 4.1211E + 04 and 9.6908E + 04 intergene bases. The P_{eff} for gene locus for *lnc-TTC24-5* is 0.283 *esebssiwaagoT*$_Q$ units (Table 1; Figs. 1, 2 and 3).

lnc-TTC24-4 is a 3 A 7 (+1) ACM final SEB gene locus with a Σ intergene base segment tropy of 1.138955E + 05 intergene bases at position +9. Sequential integration (∫) to the final *esebssiwaagoT*$_Q$ for *lnc-TTC24-4* is 0.055, 0.276, 0.152, 0.193, 0.223, 0.235, 0.194. The final *uppesebssiwaa* and *dppesebssiwaa* for *lnc-TTC24-4* are 2.3007E + 04 and 1.19362E + 05 intergene bases. The P_{eff} for gene locus for *lnc-TTC24-4* is 0.193 *esebssiwaagoT*$_Q$ units (Table 1; Figs. 1, 2 and 3).

lnc-TTC24-1 is a 3 M 7 initial and final SEB gene locus with a Σ intergene base segment tropy of 4.86984E + 05 intergene bases at position +10. Sequential integration (∫) to the final *esebssiwaagoT*$_Q$ for *lnc-TTC24-1* is 0.544, 0.097, 0.267, 0.342, 0.312, 0.264. The final *uppesebssiwaa* and *dppesebssiwaa* for *lnc-TTC24-1* are 1.4861E + 04 and 5.5298E + 04 intergene bases. The P_{eff} for gene locus for *lnc-TTC24-1* is 0.269 *esebssiwaagoT*$_Q$ units (Table 1; Figs. 1, 2 and 3).

GC01P156524 is a 3 A 7 (+2) ACM final SEB gene locus with a Σ intergene base segment tropy of 1.492171E + 06 intergene bases at position +11. Sequential integration (∫) to the final *esebssiwaagoT*$_Q$ for *GC01P156524* is 0.141, 0.225, 0.162, 0.212, 0.223, 0.217, 0.232, 0.217, 0.199 (DfC), 0.196, 0.205. The final *uppesebssiwaa* and *dppesebssiwaa* for *GC01P156524* are 2.6686E + 04 and 1.34141E + 05 intergene bases. The P_{eff} for gene locus for *GC01P156524* is 0.199 *esebssiwaagoT*$_Q$ units (Table 1; Figs. 1, 2 and 3).

TTC24 is a 3 M 7 initial and final SEB gene locus with a Σ intergene base segment tropy of 8.54954E + 05 intergene bases at position +12. Sequential integration (∫) to the final *esebssiwaagoT*$_Q$ for *TTC24* is 0.406, 0.197, 0.184, 0.116, 0.145, 0.159. The final *uppesebssiwaa* and *dppesebssiwaa* for *TTC24* are 1.6633E + 04 and 1.14108E + 05 intergene bases. The P_{eff} for gene locus for *TTC24* is 0.146 *esebssiwaagoT*$_Q$ units (Table 1; Figs. 1, 2 and 3).

NAXE is a 3 M 7 initial and final SEB gene locus with a Σ intergene base segment tropy of 1.422774E + 06 intergene bases at position +13. Sequential integration (∫) to the final *esebssiwaagoT*$_Q$ for *NAXE* is 0.125, 0.218, 0.153, 0.144, 0.159, 0.187. The final *uppesebssiwaa* and *dppesebssiwaa* for *NAXE* are 2.7892E + 04 and 1.61601E + 05 intergene bases. The P_{eff} for gene locus for *NAXE* is 0.190 *esebssiwaagoT*$_Q$ units (Table 1; Figs. 1, 2 and 3).

HAPLN2 is a 3 M 7 initial and final SEB gene locus with a Σ intergene base segment tropy of 7.92243E + 05 intergene bases at position +14. Sequential integration (∫) to the final *esebssiwaagoT*$_Q$ for *HAPLN2* is 0.636, 0.505, 0.456, 0.243, 0.209, 0.211, 0.188 (DfC), 0.209, 0.194. The final *uppesebssiwaa* and *dppesebssiwaa* for

HAPLN2 are 1.8695E + 04 and 9.9190E + 04 intergene bases. The P_{eff} for gene locus for *HAPLN2* is 0.188 *esebssiwaagoT*$_Q$ units (Table 1; Figs. 1, 2 and 3).

BCAN is a 2 M 5 initial and final SEB gene locus with a Σ intergene base segment tropy of 7.28923E + 05 intergene bases at position +15. Sequential integration (∫) to the final *esebssiwaagoT*$_Q$ for *BCAN* is 0.389, 0.212, 0.235, 0.262. The final *uppesebssiwaa* and *dppesebssiwaa* for *BCAN* are 2.7104E + 04 and 1.11335E + 05 intergene bases. The P_{eff} for gene locus for *BCAN* is 0.243 *esebssiwaagoT*$_Q$ units (Table 1; Figs. 1, 2 and 3).

Anisotropic gene intergene tropy sub-episode block sum for linear two-dimensional *z*, *y*-plane anglemetry

The *uppasebs*, *dppasebs*, *uppmsebs* and *dppasebs* for anisotropic gene locus *MIR4537* are 7.232E + 03, 1.72400E + 05, 5.896E + 03 and 1.1694E + 04. The *uppasebssiwa*, *dppasebssiwa*, *uppmsebssiwa* and *dppasebssiwa* for anisotropic gene locus *MIR4537* are 2.411E + 03, 5.7467E + 04, 1.474E + 03 and 2.934E + 03. The sebs and sebssiwa exponential function pair for anisotropic gene locus *MIR4537* is 5.799E+03 e^{8E-03x} and 1.424E+03 $e^{1.72E+02x}$. The $b_{sebs}/b_{sebssiwa}$ linearization quotient for anisotropic gene locus *MIR4537* is 4.07. The sebs - sebssiwa residual for anisotropic gene locus *MIR4537* is 4,821, 114,933, 4,422 and 8,770. The *uppesebssiwaa* and *dppesebssiwaa* for anisotropic gene *MIR4537* are 1.942E + 03 and 3.0195E + 04. The *esebssiwaagoT*$_Q$ for anisotropic gene locus *MIR4537* is 0.064. Anisotropic gene locus *MIR4537* is positioned at angle $\Theta_A = 82.2^0$ in the *z*, *y*-axis vertical plane.

The *uppasebs*, *dppasebs*, *uppmsebs* and *dppasebs* for anisotropic gene locus *COL2A1* are 9.2758E + 04, 1.390995E + 06, 6.4607E + 04 and 1.46229E + 05. The *uppasebssiwa*, *dppasebssiwa*, *uppmsebssiwa* and *dppasebssiwa* for anisotropic gene locus *COL2A1* are 3.0919E + 04, 4.63665E + 05, 3.2304E + 04 and 7.3115E + 04. The sebs and sebssiwa exponential function pair for anisotropic gene locus *COL2A1* is 6.1920E + 04 e^{3E-07x} and 2.8989E+04 e^{2E-06x}. The $b_{sebs}/b_{sebssiwa}$ linearization quotient for anisotropic gene locus *COL2A1* is 2.14. The sebs - sebssiwa residual for anisotropic gene locus *COL2A1* is 61,839, 927,330, 32,304 and 73,115. The *uppesebssiwaa* and *dppesebssiwaa* for anisotropic gene locus *COL2A1* are 3.1611E + 04 and 2.68390E + 05. The *esebssiwaagoT*$_Q$ for anisotropic gene locus *COL2A1* is 0.118. Anisotropic gene locus *COL2A1* is positioned at angle $_A = 75.8^0$ in the *z*, *y*-axis vertical plane (Table 2).

The *uppasebs*, *dppasebs*, *uppmsebs* and *dppasebs* for anisotropic gene locus *RGS4* are 8.1560E + 04, 1.196076E + 06, 1.01032E + 05 and 1.85608E + 05. The *uppasebssiwa*, *dppasebssiwa*, *uppmsebssiwa* and *dppasebssiwa* for anisotropic gene locus *RGS4* are 2.7187E + 04, 3.98692E + 05, 2.5258E + 04 and 4.6402E + 04. The sebs and sebssiwa exponential function pair for anisotropic gene locus *RGS4* is 7.8415E+04 e^{2E-07x} and 2.5014E+04 e^{2E-07x}. The $b_{sebs}/b_{sebssiwa}$ linearization quotient for anisotropic gene locus *RGS4* is 3.14. The sebs - sebssiwa residual for anisotropic gene locus *RGS4* is 54,373, 797,384, 75,774 and 139,206. The *uppesebssiwaa* and *dppesebssiwaa* for anisotropic gene locus *RGS4* are 2.6223E + 04 and 2.22547E + 05. The *esebssiwaagoT*$_Q$ for anisotropic gene locus *RGS4* is 0.118. Anisotropic gene locus *RGS4* is positioned at angle $\Theta_A = 75.8^0$ in the *z*, *y*-axis vertical plane (Table 2).

The *uppasebs*, *dppasebs*, *uppmsebs* and *dppasebs* for anisotropic gene locus *MYC* are 8.8269E + 04, 1.042981E + 06, 8.5825E + 04 and 2.27872E + 05. The *uppasebssiwa*, *dppasebssiwa*, *uppmsebssiwa* and *dppasebssiwa* for anisotropic gene locus *MYC* are 2.9423E + 04, 3.47660E + 05, 4.2913E + 04 and 1.13936E + 05. The sebs and sebssiwa exponential function pair for anisotropic gene locus *MYC* is 8.8964E+04 e^{3E-08x} and 2.4479E+04 e^{2E-06x}. The $b_{sebs}/b_{sebssiwa}$ linearization quotient for anisotropic gene locus *MYC* is 3.63. The sebs - sebssiwa residual for anisotropic gene locus *MYC* is 58, 846, 695,321, 42,913 and 113,936. The *uppesebssiwaa* and *dppesebssiwaa* for anisotropic gene locus *MYC* are 3.6168E + 04 and 2.30798E + 05. The *esebssiwaagoT*$_Q$ for anisotropic gene locus *MYC* is 0.157. Anisotropic gene locus *MYC* is positioned at angle $\Theta_A = 71.0^0$ in the *z*, *y*-axis vertical plane (Table 2).

The *uppasebs*, *dppasebs*, *uppmsebs* and *dppasebs* for anisotropic gene locus *LMNA* are 4.3403E + 04, 5.73397E + 05, 8.6878E + 04 and 2.47931E + 05. The *uppasebssiwa*, *dppasebssiwa*, *uppmsebssiwa* and *dppasebssiwa* for anisotropic gene locus *LMNA* are 1.4468E + 04, 1.91132E + 05, 4.3439E + 04 and 1.23966E + 05. The sebs and sebssiwa exponential function pair for anisotropic gene locus *LMNA* is 6.65237E+05 e^{2E-05x} and 1.92333E+05 e^{6E-06x}. The $b_{sebs}/b_{sebssiwa}$ linearization quotient for anisotropic gene locus *LMNA* is 3.46. The sebs - sebssiwa residual for anisotropic gene locus *LMNA* is 28,935, 382,265, 43,439 and 123,966. The *uppesebssiwaa* and *dppesebssiwaa* for anisotropic gene locus *LMNA* are 2.8995E + 04 and 1.57549E + 05. The *esebssiwaagoT*$_Q$ for anisotropic gene locus *LMNA* is 0.184. Anisotropic gene locus *LMNA* is positioned at angle $\Theta_A = 67.8^0$ in the *z*, *y*-axis vertical plane (Table 2).

The *uppasebs*, *dppasebs*, *uppmsebs* and *dppasebs* for anisotropic gene locus *CCN2* are 1.21423E + 05, 1.117098E + 06, 1.21173E + 05 and 3.42644E + 05. The *uppasebssiwa*, *dppasebssiwa*, *uppmsebssiwa* and *dppasebssiwa* for anisotropic gene locus *CCN2* are 3.0356E + 04, 2.79275E + 05, 3.0293E + 04 and 8.5661E + 04. The sebs and sebssiwa exponential function pair for anisotropic gene locus *CCN2* is 1.21063E+05 e^{3E-09x} and 3.0266E+04 e^{1E-08x}. The

Table 2 Angulation of anisotropic genes in reference to the horizontal for the linear normal *esebssiwaagoT*$_Q$ effective intracellular pressure unit

Gene (no. of locus bases; no. of gene bases or n/a)	Gene locus (strand)	Episode category (final SEB structure)	sebs $f(x)$[a]	sebssiwa $f(x)$[a]	$b_{sebs}/b_{sebssiwa}$[b]	sebs – sebssiwa (x_1, y_1; x_2, y_2), residual	*uppesebssiwaa*, *dppesebssiwaa* (P_{eff} *esebssiwaagoT*$_Q$)	Angulation (^{0})
MIR4537, microRNA 4537 (70; n/a)	14q32.3 (–)	3 A 7	5.799E+ 03 e^{8E-03x}	1.424E+ 03 $e^{1.72E+02x}$	4.07	4,821, 114,933; 4,422, 8,770	1,942, 30,195 (0.064[c])	82.3
COL2A1, collagen type VI alpha 1 chain (23,314; n/a)	12q13.11 (–)	2 A 5	6.1920E+ 04 e^{3E-07x}	3.2569E+ 04 e^{1E-07x}	1.90	61,839, 927,330; 32,304, 73,115	31,611, 268,390 (0.118)	75.8
RGS4, regulator of g protein signaling 4 (8,197; n/a)	1q23.3 (+)	3 M 7	7.8415E+ 04 $e^{-2E-07x}$	2.5014E+ 04 e^{2E-07x}	3.14	54,373, 797,384; 75,774, 139,206	26,223, 222,547 (0.118)	75.8
MYC, MYC proto-oncogene (6,001; n/a)	8q24.21 (+)	3 A 5	8.8964E+ 04 e^{3E-08x}	2.4479E+ 04 e^{2E-06x}	3.63	58,846, 695,321; 42,913, 113,936	36,168, 230,798 (0.157)	71
CCN2, cellular communication network factor 2 (3,203; n/a)	6q23.2 (–)	3 A 8	1.21063E+05 e^{3E-09x}	3.0266E+04 e^{1E-08x}	4.00	91,067, 837,824; 90,880, 256,983	30,325, 182,468 (0.166)	70
LMNB2, lamin B2 (288,491; 29,359)	19q13.3 (–)	4 A 7	3.0747E+04 e^{7E-07x}	1.1944E+04 e^{9E-06x}	2.57	18,824, 220,250; 19,549, 45,732	8,024, 48,141 (0.167)	69.8
ESRRB, Estrogen Related Receptor Beta (196,759; 191,128)	14q24.3 (+)	2 A 5	1.05918E+04 e^{1E-06x}	3.4501E+04 e^{2E-06x}	3.07	64,086, 539,533; 22,161, 45,003	27,102, 157,268 (0.172)	69.2
LMNA, lamin A/C (57,934; 57,544)	1q22 (+)	2 A 5	6.65237E+05 e^{2E-05x}	1.92333E+05 e^{6E-06x}	3.46	28,935, 382,265; 43,439, 123,966	28,945, 157,549 (0.184)	67.8
LMNB1, lamin B1 (60,398; n/a)	5q23.2 (+)	2 A 5	1.0E+05 e^{5E-07x}	2.96910E+05 e^{1E-05x}	3.37	32,013, 478,625; 58,014, 135,885	37,010, 187,599 (0.197)	66.2
EGR1, early growth response 1 (3,826; n/a)	5q31.2 (+)	3 M 7	7.93682E+05 e^{5E-06x}	4.04638E+05 e^{4E-05x}	1.96	18,244, 199,860; 39,226 88,802	28,735, 144,331 (0.199)	66.0
PRKCH, protein kinase C eta type (471,621; 363,422)	14q32.2 (+)	4 A 5	2.0E+06 e^{1E-05x}	3.86798E+05 e^{1E-05x}	5.17	35,062, 628,017; 76,455, 155,817	46,994, 234,912 (0.200)	65.8
IER3, immediate early response 3 (1,356; n/a)	6q21.33 (–)	3 M 5	6.75603E+05 e^{2E-05x}	3.08411E+05 e^{9E-06x}	2.78	11,982, 102,979; 35,375, 84,093	14,835, 72,513 (0.205)	65.3
EMD, emerin (2,327; n/a)	Xq28 (+)	3 A 5	2.70939E+05 e^{4E-06x}	8.5425E+04 e^{3E-06x}	3.17	7,078, 172,964; 39,612, 98,034	21,576,92,258 (0.234)	61.7

Table 2 Angulation of anisotropic genes in reference to the horizontal for the linear normal *esebssiwaagoT*$_Q$ effective intracellular pressure unit *(Continued)*

Gene (no. of locus bases; no. of gene bases or n/a)	Gene locus (strand)	Episode category (final SEB structure)	sebs *f(x)*[a]	sebssiwa *f(x)*[a]	$b_{sebs}/b_{sebssiwa}$[b]	sebs – sebssiwa (x_1, y_1; x_2, y_2), residual	*uppesebssiwaa*, *dppesebssiwaa* (P_{eff} *esebssiwaagoT*$_Q$)	Angulation (^{0})
COL6A1, collagen type VI alpha 1 chain (23,314; n/a)	21q22.3 (+)	2 A 4 q term	7.1790E+04 e^{1E-05x}	3.5895E+04 e^{3E-05x}	2.00	807, 36,660; 23,271, 65,941	12,039, 51,301 (0.235)	61.6
COL1A1, collagen type I alpha 1 chain (18,360; n/a)	17q21.33 (–)	2 A 5	3.1489E+04 e^{9E-07x}	1.5175E+04 e^{6E-06x}	2.08	20,066, 140,511; 13,062, 25,468	11,547,47,862 (0.241)	60.9

[a]$f(x) = b \cdot e^{m \cdot x}$, where *b* is the downstream anisotropic effect (intercept and slope are absolute values); [b]$b_{sebs}/b_{sebssiwa}$ is the linearization quotient; and [c]previously reported episode and sub-episode block structure and *esebssiwaagoT*$_Q$ value as per references, *MIR4537* [26, 27]. Note: [1)] Gene loci sub-episode block structure (SEB) variations include non-contributory anisotropy (NCA), anisotropy converted to mesotropy (ACM), and/or 0.5-factor adjusted stabilizing mesotropy or anisotropy converted to stabilizing isotropy for anisotropy or mesotropy (stIAfM, stIMfA or stIMfM) that result in an initial to final SEB conversion; [2)] Sub-episode block structures for initial to final SEB converted genes are *MYC*, 3 A 7 (−2); *CCN2*, 3 A 7 (+1) stIAfA; *LMNB2*, 4 A 9 (−2) NCA; *PRKCH*, 4 A 9 (−2) (−2) NCA ACM; *COL6A1*, 2 A 5 (−1) q terminal end; *IER3*, 3 M 7 (− 2) ACM; and *EMD*, 3 A 7 (− 2) stIAfA; and [3)] $b_{sebs}/b_{sebssiwa}$ for *MIR4357*, *COL2A1*, *RGS4*, *MYC*, *CCN2*, *LMNB2*, *ESRRB* and *COL1A1* is by reverse *x*-intercept plotting of the *uppasebs*, *uppamsebs*, *dppasebs* and *dppmsebs* and the corelate *uppasebssiwa*, *uppamsebssiwa*, *dppasebssiwa* and *dppmsebssiwa*; and the same for *LMNA* and *PRKCH* is by *x*-, *y*- function b_{sebs} and $b_{sebssiwa}$ intercept hybridization

$b_{sebs}/b_{sebssiwa}$ linearization quotient for anisotropic gene locus *CCN2* is 4.00. The sebs - sebssiwa residual for anisotropic gene locus *CCN2* is 91,067, 837,824, 90,880 and 256,983. The *uppesebssiwaa* and *dppesebssiwaa* for anisotropic gene locus *CCN2* are 3.0325E + 04 and 1.82468E + 05. The *esebssiwaagoT*$_Q$ for anisotropic gene locus *CCN2* is 0.166. Anisotropic gene locus *CNN2* is positioned at angle $\Theta_A = 70.0^0$ in the *z, y*-axis vertical plane (Table 2).

The *uppasebs*, *dppasebs*, *uppmsebs* and *dppasebs* for anisotropic gene locus *ESRRB* are 9.6129E + 04, 8.08599E + 05, 4.4321E + 04 and 9.0006E + 04. The *uppasebssiwa*, *dppasebssiwa*, *uppmsebssiwa* and *dppasebssiwa* for anisotropic gene locus *ESRRB* are 3.2043E + 04, 2.69533E + 05, 2.2161E + 04 and 4.5003E + 04. The sebs and sebssiwa exponential function pair for anisotropic gene locus *ESRRB* is 1.05918E+04 e^{1E-06x} and 3.4501E+04 e^{2E-06x}. The $b_{sebs}/b_{sebssiwa}$ linearization quotient for anisotropic gene locus *ESRRB* is 3.07. The sebs - sebssiwa residual for anisotropic gene locus *ESRRB* is 64,086, 539,533, 22,161 and 45,003. The *uppesebssiwaa* and *dppesebssiwaa* for anisotropic gene locus *ESRRB* are 2.7102E + 04 and 1.57268E + 05. The *esebssiwaagoT*$_Q$ for anisotropic gene locus *ESRRB* is 0.172. Anisotropic gene locus *ESRRB* is positioned at angle $\Theta_A = 69.2^0$ in the *z, y*-axis vertical plane (Table 2).

The *uppasebs*, *dppasebs*, *uppmsebs* and *dppasebs* for anisotropic gene locus *LMNB1* are 4.8020E + 04, 7.17938E + 05, 1.16027E + 05 and 2.71770E + 05. The *uppasebssiwa*, *dppasebssiwa*, *uppmsebssiwa* and *dppasebssiwa* for anisotropic gene locus *LMNB1* are 1.6007E + 04, 2.39313E + 05, 5.8014E + 04 and 1.35885E + 05. The sebs and sebssiwa exponential function pair for anisotropic gene locus *LMNB1* is 1.0E+05 e^{5E-07x} and 2.96910E+05 e^{1E-05x}. The $b_{sebs}/b_{sebssiwa}$ linearization quotient for anisotropic gene locus *LMNB1* is 3.37. The sebs - sebssiwa residual for anisotropic gene locus *LMNB1* is 32,013, 478,625, 58,014 and 135,885. The *uppesebssiwaa* and *dppesebssiwaa* for anisotropic gene locus *LMNB1* are 3.7010E + 04 and 1.87599E + 05. The *esebssiwaagoT*$_Q$ for anisotropic gene locus *LMNB1* is 0.197. Anisotropic gene locus *LMNB1* is positioned at angle $\Theta_A = 66.2^0$ in the *z, y*-axis vertical plane (Table 2).

The *uppasebs*, *dppasebs*, *uppmsebs* and *dppasebs* for anisotropic gene locus *EGR1* are 5.4733E + 04, 5.99581E + 05, 1.56904E + 05 and 3.55209E + 05. The *uppasebssiwa*, *dppasebssiwa*, *uppmsebssiwa* and *dppasebssiwa* for anisotropic gene locus *EGR1* are 1.8244E + 04, 1.99860E + 05, 3.9226E + 04 and 8.8802E + 04. The sebs and sebssiwa exponential function pair for anisotropic gene locus *EGR1* is 7.93682E+05 e^{5E-06x} and 4.04638E+05 e^{4E-05x}. The $b_{sebs}/b_{sebssiwa}$ linearization quotient for anisotropic gene locus *EGR1* is 1.96. The sebs - sebssiwa residual for anisotropic gene locus *EGR1* is 36,489, 399,721, 117,678 and 266,407. The *uppesebssiwaa* and *dppesebssiwaa* for anisotropic gene locus *EGR1* are 2.8735E + 04 and 1.44331E + 05. The *esebssiwaagoT*$_Q$ for anisotropic gene locus *EGR1* is 0.199. Anisotropic gene locus *EGR1* is positioned at angle $\Theta_A = 66.0^0$ in the *z, y*-axis vertical plane (Table 2).

The *uppasebs*, *dppasebs*, *uppmsebs* and *dppasebs* for anisotropic gene locus *PRKCH* are 5.2593E + 04, 9.42026E + 05, 1.52911E + 05 and 3.11633E + 05. The *uppasebssiwa*, *dppasebssiwa*, *uppmsebssiwa* and *dppasebssiwa* for anisotropic gene locus *PRKCH* are 1.7531E + 04, 3.14009E + 05, 7.6456E + 04 and 1.55816E + 05. The sebs and sebssiwa exponential function pair for anisotropic gene locus *PRKCH* is 1.129582E+06 e^{6E-06x} and 3.56470E+05 e^{1E-05x}. The $b_{sebs}/b_{sebssiwa}$ linearization quotient for anisotropic gene locus *PRKCH* is 3.17. The sebs - sebssiwa residual for anisotropic gene locus *PRKCH* is 35,062, 628,017, 79,455 and 155,817. The *uppesebssiwaa* and *dppesebssiwaa* for anisotropic gene locus *PRKCH* are 4.6994E + 04 and 2.34912E + 05. The *esebssiwaagoT*$_Q$ for anisotropic gene locus *PRKCH* is 0.200. Anisotropic gene locus *PRKCH* is positioned at angle $\Theta_A = 65.8^0$ in the *z, y*-axis vertical plane (Table 2).

The *uppasebs*, *dppasebs*, *uppmsebs* and *dppasebs* for anisotropic gene locus *LMNB2* are 2.0538E + 04, 2.16613E + 05, 3.4762E + 04 and 8.6623E + 04. The *uppasebssiwa*, *dppasebssiwa*, *uppmsebssiwa* and *dppasebssiwa* for anisotropic gene locus *LMNB2* are 5.135E + 03, 5.4153E + 04, 1.1587E + 04 and 2.8874E + 04. The sebs and sebssiwa exponential function pair for anisotropic gene locus *LMNB2* is 4.9363E+04 e^{4E-06x} and 2.9359E+04 e^{3E-06x}. The $b_{sebs}/b_{sebssiwa}$ linearization quotient for anisotropic gene locus *LMNB2* is 1.68. The sebs - sebssiwa residual for anisotropic gene locus *LMNB2* is 15,404, 162,460, 23,175 and 57,749. The *uppesebssiwaa* and *dppesebssiwaa* for anisotropic gene locus *LMNB2* are 8.361E + 03 and 4.1514E + 04. The *esebssiwaagoT*$_Q$ for anisotropic gene locus *LMNB2* is 0.201. Anisotropic gene locus *LMNB2* is positioned at angle $\Theta_A = 65.7^0$ in the *z, y*-axis vertical plane (Table 2).

The *uppasebs*, *dppasebs*, *uppmsebs* and *dppasebs* for anisotropic gene locus *IER3* are 2.3964E + 04, 2.05958E + 05, 5.3063E + 04 and 1.26140E + 05. The *uppasebssiwa*, *dppasebssiwa*, *uppmsebssiwa* and *dppasebssiwa* for anisotropic gene locus *IER3* are 1.1982E + 04, 1.02979E + 05, 1.7688E + 04 and 4.2047E + 04. The sebs and sebssiwa exponential function pair for anisotropic gene locus *IER3* is 6.75603E+05 e^{2E-05x} and 3.08411E+05 e^{9E-06x}. The $b_{sebs}/b_{sebssiwa}$ linearization quotient for anisotropic gene locus *IER3* is 2.78. The sebs - sebssiwa residual for anisotropic gene locus *IER3* is 11,982, 102, 979, 35,375 and 84,093. The *uppesebssiwaa* and *dppesebssiwaa* for anisotropic gene locus *IER3* are 1.4835E + 04 and 7.2513E + 04. The *esebssiwaagoT*$_Q$ for

anisotropic gene locus *IER3* is 0.205. Anisotropic gene locus *IER3* is positioned at angle Θ_A = 65.3^0 in the *z, y*-axis vertical plane (Table 2).

The *uppasebs*, *dppasebs*, *uppmsebs* and *dppasebs* for anisotropic gene locus *EMD* are 1.0617E + 04, 2.59446E + 05, 7.9224E + 04 and 1.96068E + 05. The *uppasebssiwa*, *dppasebssiwa*, *uppmsebssiwa* and *dppasebssiwa* for anisotropic gene locus *EMD* are 3.539E + 03, 8.6482E + 04, 3.9612E + 04 and 9.8034E + 04. The sebs and sebssiwa exponential function pair for anisotropic gene locus *EMD* is 2.70939E+05 $e^{4E\text{-}06x}$ and 8.5425E+04 $e^{3E\text{-}06x}$. The $b_{sebs}/b_{sebssiwa}$ linearization quotient for anisotropic gene locus *EMD* is 3.17. The sebs - sebssiwa residual for anisotropic gene locus *EMD* is 7,078, 172,964, 39,612 and 98,034. The *uppesebssiwaa* and *dppesebssiwaa* for anisotropic gene locus *EMD* are 2.1576E + 04 and 9.2258E + 04. The *esebssiwaagoT*$_Q$ for anisotropic gene locus *EMD* is 0.234. Anisotropic gene locus *EMD* is positioned at angle Θ_A = 61.7^0 in the *z, y*-axis vertical plane (Table 2).

The *uppasebs*, *dppasebs*, *uppmsebs* and *dppasebs* for anisotropic gene locus *COL6A1* are 1.614E + 03, 7.3320E + 04, 4.6541E + 04 and 1.31882E + 05. The *uppasebssiwa*, *dppasebssiwa*, *uppmsebssiwa* and *dppasebssiwa* for anisotropic gene locus *COL6A1* are 8.07E + 02, 3.6660E + 04, 2.3271E + 04 and 6.5941E + 04. The sebs and sebssiwa exponential function pair for anisotropic gene locus *COL6A1* is 7.1790E+04 $e^{1E\text{-}05x}$ and 3.5895E+04 $e^{3E\text{-}05x}$. The $b_{sebs}/b_{sebssiwa}$ linearization quotient for anisotropic gene locus *COL6A1* is 2.00. The sebs - sebssiwa residual for anisotropic gene locus *COL6A1* is 807, 36,660, 23,271 and 65,941. The *uppesebssiwaa* and *dppesebssiwaa* for anisotropic gene locus *COL6A1* are 1.2039E + 04 and 5.1301E + 04. The *esebssiwaagoT*$_Q$ for anisotropic gene locus *COL6A1* is 0.235. Anisotropic gene locus *COL6A1* is positioned at angle Θ_A = 61.6^0 in the *z, y*-axis vertical plane (Table 2).

The *uppasebs*, *dppasebs*, *uppmsebs* and *dppasebs* for anisotropic gene locus *COL1A1* are 3.0099E + 04, 2.10767E + 05, 2.6123E + 04 and 5.0936E + 04. The *uppasebssiwa*, *dppasebssiwa*, *uppmsebssiwa* and *dppasebssiwa* for anisotropic gene locus *COL1A1* are 1.0033E + 04, 7.0256E + 04, 1.3062E + 04 and 2.5468E + 04. The sebs and sebssiwa exponential function pair for anisotropic gene locus *COL1A1* is 4.4873E+04 $e^{1E\text{-}06x}$ and 4.8093E+04 $e^{2E\text{-}05x}$. The $b_{sebs}/b_{sebssiwa}$ linearization quotient for anisotropic gene locus *COL1A1* is 2.08. The sebs - sebssiwa residual for anisotropic gene locus *COL1A1* is 20,066, 140,511, 13,062 and 25,468. The *uppesebssiwaa* and *dppesebssiwaa* for anisotropic gene locus *COL1A1* are 1.1547E + 04 and 4.7862E + 04. The *esebssiwaagoT*$_Q$ for anisotropic gene locus *COL1A1* is 0.241. Anisotropic gene locus *COL1A1* is positioned at angle Θ_A = 69.2^0 in the *z, y*-axis vertical plane (Table 2).

Mesotropic gene intergene tropy sub-episode block sum exponential functions for linear two-dimensional *z, y*-plane anglemetry

The *uppasebs*, *dppasebs*, *uppmsebs* and *dppasebs* for mesotropic gene locus *CYGB* are 3.5180E + 04, 2.22499E + 05, 4.6604E + 04 and 1.07321E + 05. The *uppasebssiwa*, *dppasebssiwa*, *uppmsebssiwa* and *dppasebssiwa* for mesotropic gene locus *CYGB* are 1.7590E + 04, 1.11250E + 05, 2.3302E + 04 and 5.3661E + 04. The sebs and sebssiwa exponential function pair for mesotropic gene locus *CYGB* is 6.0565E+04 $e^{2E\text{-}06x}$ and 3.0282E+04 $e^{5E\text{-}06x}$. The $b_{sebs}/b_{sebssiwa}$ linearization quotient for mesotropic gene locus *CYGB* is 2.00. The sebs - sebssiwa residual for mesotropic gene locus *CYGB* is 17,590, 111,250, 23,302 and 53,661. The *uppesebssiwaa* and *dppesebssiwaa* for mesotropic gene locus *CYGB* are 2.0446E + 04 and 8.2455E + 04. The *esebssiwaagoT*$_Q$ for mesotropic gene locus *CYGB* is 0.248. Mesotropic gene locus *CYGB* is positioned at angle Θ_M = 60.0^0 in the *z, y*-axis vertical plane.

The *uppasebs*, *dppasebs*, *uppmsebs* and *dppasebs* for mesotropic gene locus *RGS1* are 1.79174E + 05, 1.237585E + 06, 3.68331E + 05 and 6.86424E + 05. The *uppasebssiwa*, *dppasebssiwa*, *uppmsebssiwa* and *dppasebssiwa* for mesotropic gene locus *RGS1* are 8.9587E + 04, 6.18793E + 05, 1.84166E + 05 and 3.43212E + 05. The sebs and sebssiwa exponential function pair for mesotropic gene locus *RGS1* is 9.03665E+05 $e^{1E\text{-}06x}$ and 4.51832E+05 $e^{3E\text{-}06x}$. The $b_{sebs}/b_{sebssiwa}$ linearization quotient for mesotropic gene locus *RGS1* is 2.00. The sebs - sebssiwa residual for mesotropic gene locus *RGS1* is 89, 587, 616,793, 184,166 and 343,212. The *uppesebssiwaa* and *dppesebssiwaa* for mesotropic gene locus *RGS1* are 1.36876E + 05 and 4.81002E + 05. The *esebssiwaagoT*$_Q$ for mesotropic gene locus *RGS1* is 0.285. Mesotropic gene locus *RGS1* is positioned at angle Θ_M = 55.6^0 in the *z, y*-axis vertical plane (Table 3).

The *uppasebs*, *dppasebs*, *uppmsebs* and *dppasebs* for mesotropic gene locus *ENPP1* are 2.7027E + 04, 1.71207E + 05, 6.1750E + 04 and 1.44916E + 05. The *uppasebssiwa*, *dppasebssiwa*, *uppmsebssiwa* and *dppasebssiwa* for mesotropic gene locus *ENPP1* are 9.009E + 03, 5.7169E + 04, 3.0875E + 04 and 7.2458E + 04. The sebs and sebssiwa exponential function pair for mesotropic gene locus *ENPP1* is 1.94930E+05 $e^{5E\text{-}06x}$ and 5.1723E+04 $e^{1E\text{-}05x}$. The $b_{sebs}/b_{sebssiwa}$ linearization quotient for mesotropic gene locus *ENPP1* is 3.77. The sebs - sebssiwa residual for mesotropic gene locus *ENPP1* is 18,018, 114,138, 30,875 and 72,458. The *uppesebssiwaa* and *dppesebssiwaa* for mesotropic gene locus *ENPP1* are 1.9942E + 04 and 6.4814E + 04. The *esebssiwaagoT*$_Q$ for mesotropic gene locus *ENPP1* is 0.308. Mesotropic gene locus *ENPP1* is positioned at angle Θ_M = 52.8^0 in the *z, y*-axis vertical plane (Table 3).

Table 3 Angulation of mesotropic genes in reference to the horizontal for the linear normal *esebssiwaagoT*$_Q$ effective intracellular pressure unit

Gene (no. of locus bases; no. of gene bases or n/a)	Gene locus (ch, strand)	Episode category (final SEB structure)	*sebs f(x)*[a]	*sebssiwa f(x)*[a]	$b_{sebs}/b_{sebssiwa}$[b]	sebs – sebssiwa (x_1, y_1; x_2, y_2), residual	*uppesebssiwaa*, *dppesebssiwaa* (P_{eff} *esebssiwaagoT*$_Q$)	Angulation (^{0})
CYGB, cytoglobin (30,336; 30,250)	17q25.1 (–)	2 A 4	6.0565E+ 04 e^{2E-06x}	3.0282E+ 04 e^{5E-06x}	2.00	17,590, 111,250; 23,302, 53, 661	20,446, 82,455 (0.248)	60
RGS1, regulator of g protein signaling 1 (4,305; n/a)	1q31.2 (+)	3 M 4	9.03665E+ 05 e^{1E-06x}	4.51832E+ 05 e^{3E-06x}	2.00	89,587, 616,793; 184,166, 343,212	136,876, 481,002 (0.285)	55.6
ENPP1, ectonucleotide pyrophosphatase phosphodiesterase 1 (87,140; n/a)	6q23.2 (+)	2 A 5	1.94930E+05 e^{5E-06x}	5.1723E+04 e^{1E-05x}	3.77	18,018, 114,138; 30,875, 72, 458	19,942,64,814 (0.308[c])	52.8
SOX18, SRY-Box 18 (2,060; n/a)	20q13.33 (–)	3 M 3 q term	–	–	*n/a*	*nil*, *nil*; 30,318, 61,868	21,741, 70,370 (0.309)	52.7
NUMA1, nuclear mitotic apparatus protein 1 (5,063; n/a)	11q13.3-q13.4 (–)	2 A 5	3.67204E+05 e^{1E-05x}	9.0203E + 04 e^{4E-06x}	4.07	21,080, 172,300; 39,809, 75, 825	25,175, 80,987 (0.311)	52.4
INSL3, insulin like 3 (5,063; n/a)	19p13.11 (–)	3 A 7	4.59932E+05 e^{7E-06x}	9.0816E+04 e^{8E-06x}	5.06	32,763, 248,680; 74,198, 133, 207	74,198, 133,207 (0.321)	51.2
NFE2L2, Nuclear Factor Erythroid 2-Related Factor 2 (880,745; n/a)	2q31.2 (–)	6 A 11	5.23516E+05 e^{2E-06x}	8.7324E+04 e^{1E-05x}	5.995	49,163, 482,332; 448,729, 1,087,741	61,007, 184,201 (0.331)	50.2
JUND, JunD proto-oncogene, AP-1 transcription factor subunit (1,963; n/a)	19p13.11 (–)	3 M 7	1.18726E+05 e^{7E-06x}	3.9484E+04 e^{2E-05x}	3.01	14,691, 92,423; 126,964, 294, 152	24,833, 72,144 (0.344)	48.4
PRDM1, PR/SET domain 1 (23,620; n/a)	6q21 (+)	2 A 5	1.55684E+05 e^{2E-06x}	4.5086E+04 e^{2E-05x}	3.45	22,702, 109,291; 39,270, 87, 689	25,311,71,167 (0.356[c])	47
RGS13, regulator of g protein signaling 1 (24,174; n/a)	1q31.2 (+)	2 M 5	2.77812E+05 e^{3E-06x}	1.39157E+05 e^{5E-06x}	1.996	9,939, 146,229; 294,492, 580, 065	78,592 218,130 (0.360)	46.5
CEACAM1, carcinoembryonic antigen-related cell adhesion molecule 1 (54,447; 53,931)	19q13.2 (–)	2 M 5	1.13842E+05 e^{7E-06x}	5.6780E+04 e^{1E-05x}	2.005	13,221, 67,686; 126,663, 263, 463	38,276, 99,708 (0.384)	43.6
GABPA, GA binding protein transcription factor subunit alpha (37,891; n/a)	21q21.3 (+)	2 M 3	–	–	*n/a*	*nil*, *nil*; 231,930, 438,396	120,417, 243,978 (0.494)	30.3
CD34, CD34 molecule (34,319; 30,431)	1q32.2 (–)	2 M 3	–	–	*n/a*	*nil*, *nil*; 97,262, 145,422	48,882, 75,493 (0.648[c])	11.7

[a]$f(x) = b{\cdot}e^{m{\cdot}x}$, where b is the downstream anisotropic effect (intercept and slope are absolute values); [b]$b_{sebs}/b_{sebssiwa}$ is the linearization quotient; and [c]previously reported episode and sub-episode block structure and *esebssiwaagoT*$_Q$ value as per references, *ENPP1*, *PRDM1* and *CD34* [26, 27]. Note: [1)] Gene loci sub-episode block structure (SEB) variations include non-contributory anisotropy (NCA), anisotropy converted to mesotropy (ACM), and/or 0.5-factor adjusted stabilizing mesotropy or anisotropy converted to stabilizing isotropy for anisotropy or mesotropy (stIAfM, stIMfA or stIMfM) that result in an initial to final SEB conversion; [2)] previously reported episode and sub-episode block structure is applied in all cases as per reference [25], in which gene/gene loci at cusps of the delineated base intervals, in which case *NFE2L2* (880.745) classifies into the adjacent interval; [3)] Sub-episode block structures for initial to final SEB converted genes are *CYGB*, 2 A 5 (–1) ACM; *RGS1*, 3 M 7 (–3) stIMfA stIMfA; *SOX18*, 3 M 7 (–4) q terminal end; *NFE2L2*, 6 A 13 (–2) ACM; *GABPA*, 2 M 5 (– 2) ACM; and *CD34*, 2 M 5(– 2) NCA; and [3)] the $b_{sebs}/b_{sebssiwa}$ for *CYGB* and *RGS1* is by reverse *x*-intercept plotting of the *uppasebs*, *uppamsebs*, *dppasebs* and *dppmsebs* and the corelate *uppasebssiwa*, *uppamsebssiwa*, *dppasebssiwa* and *dppmsebssiwa*

The *uppasebs*, *dppasebs*, *uppmsebs* and *dppasebs* for mesotropic gene locus *SOX18* are 1.3165E + 04, 7.8872E + 04, 6.0635E + 04 and 1.23734E + 05. The *uppasebssiwa*, *dppasebssiwa*, *uppmsebssiwa* and *dppasebssiwa* for mesotropic gene locus *SOX18* are 1.3165E + 04, 7.8872E + 04, 3.0318E + 04 and 6.1867E + 04. The $b_{sebs}/b_{sebssiwa}$ linearization quotient for *SOX18* is not applicable. The sebs - sebssiwa residual for mesotropic gene locus *SOX18* is *nil*, *nil*, 30,318 and 61,868. The *uppesebssiwaa* and *dppesebssiwaa* for mesotropic gene locus *SOX18* are 2.1741E + 04 and 7.0370E + 04. The *esebssiwaagoT*$_Q$ for mesotropic gene locus *SOX18* is 0.309. Mesotropic gene locus *SOX18* is positioned at angle $\Theta_M = 52.7^0$ in the *z*, *y*-axis vertical plane (Table 3).

The *uppasebs*, *dppasebs*, *uppmsebs* and *dppasebs* for mesotropic gene locus *NUMA1* are 3.1620E + 04, 2.58450E + 05, 7.9618E + 04 and 1.51649E + 05. The *uppasebssiwa*, *dppasebssiwa*, *uppmsebssiwa* and *dppasebssiwa* for mesotropic gene locus *NUMA1* are 1.0540E + 04, 8.6150E + 04, 3.9809E + 04 and 7.5825E + 04. The sebs and sebssiwa exponential function pair for mesotropic gene locus *NUMA1* is 3.67204E+05 $e^{1E\text{-}05x}$ and 9.0203E+04 $e^{4E\text{-}06x}$. The $b_{sebs}/b_{sebssiwa}$ linearization quotient for mesotropic gene locus *NUMA1* is 4.07. The sebs - sebssiwa residual for mesotropic gene locus *NUMA1* is 21,080, 172,300, 39,809 and 75,825. The *uppesebssiwaa* and *dppesebssiwaa* for mesotropic gene locus *NUMA1* are 2.5175E + 04 and 8.0987E + 04. The *esebssiwaagoT*$_Q$ for mesotropic gene locus *NUMA1* is 0.311. Mesotropic gene locus *NUMA1* is positioned at angle $\Theta_M = 52.4^0$ in the *z*, *y*-axis vertical plane (Table 3).

The *uppasebs*, *dppasebs*, *uppmsebs* and *dppasebs* for mesotropic gene locus *INSL3* are 4.3684E + 04, 3.31573E + 05, 1.11297E + 05 and 1.99810E + 05. The *uppasebssiwa*, *dppasebssiwa*, *uppmsebssiwa* and *dppasebssiwa* for mesotropic gene locus *INSL3* are 1.0921E + 04, 8.2893E + 04, 3.7099E + 04 and 6.6603E + 04. The sebs and sebssiwa exponential function pair for mesotropic gene locus *INSL3* is 4.59932E+05 $e^{7E\text{-}06x}$ and 9.0816E+04 $e^{8E\text{-}06x}$. The $b_{sebs}/b_{sebssiwa}$ linearization quotient for mesotropic gene locus *INSL3* is 5.06. The sebs - sebssiwa residual for mesotropic gene locus *INSL3* is 32, 763, 248,680; 74,198 and 133,207. The *uppesebssiwaa* and *dppesebssiwaa* for mesotropic gene locus *INSL3* are 7.4198E + 04 and 1.33207E + 05. The *esebssiwaagoT*$_Q$ for mesotropic gene locus *INSL3* is 0.321. Mesotropic gene locus *INSL3* is positioned at angle $\Theta_M = 51.2^0$ in the *z*, *y*-axis vertical plane (Table 3).

The *uppasebs*, *dppasebs*, *uppmsebs* and *dppasebs* for mesotropic gene locus *NFE2L2* are 5.8996E + 04, 5.78798E + 05, 5.60911E + 05 and 1.359677E + 06. The *uppasebssiwa*, *dppasebssiwa*, *uppmsebssiwa* and *dppasebssiwa* for mesotropic gene locus *NFE2L2* are 9.833E + 03, 9.6466E + 04, 1.12182E + 05 and 2.71935E + 05. The sebs and sebssiwa exponential function pair for mesotropic gene locus *NFE2L2* is 5.23516E+05 $e^{2E\text{-}06x}$ and 8.7324E+04 $e^{1E\text{-}05x}$. The $b_{sebs}/b_{sebssiwa}$ linearization quotient for mesotropic gene locus *NFE2L2* is 5.995. The sebs - sebssiwa residual for mesotropic gene locus *NFE2L2* is 49,163, 482, 332, 448,729 and 1,087,741. The *uppesebssiwaa* and *dppesebssiwaa* for mesotropic gene locus *NFE2L2* are 6.1007E + 04 and 1.84201E + 05. The *esebssiwaagoT*$_Q$ for mesotropic gene locus *NFE2L2* is 0.331. Mesotropic gene locus *NFE2L2* is positioned at angle $\Theta_M = 50.2^0$ in the *z*, *y*-axis vertical plane (Table 3).

The *uppasebs*, *dppasebs*, *uppmsebs* and *dppasebs* for mesotropic gene locus *JUND* are, 2.2037E + 04, 1.38709E + 05, 1.69285E + 05 and 3.92203E + 05. The *uppasebssiwa*, *dppasebssiwa*, *uppmsebssiwa* and *dppasebssiwa* for mesotropic gene locus *JUND* are 7.346E + 03, 4.6236E + 04, 4.2321E + 04 and 9.8051E + 04. The sebs and sebssiwa exponential function pair for mesotropic gene locus *JUND* is 1.18726E+05 $e^{7E\text{-}06x}$ and 3.9484E+04 $e^{2E\text{-}05x}$. The $b_{sebs}/b_{sebssiwa}$ linearization quotient for mesotropic gene locus *JUND* is 3.01. The sebs - sebssiwa residual for mesotropic gene locus *JUND* is 14, 691, 92,423, 126,964, and 294,152. The *uppesebssiwaa* and *dppesebssiwaa* for mesotropic gene locus *JUND* are 2.4833E + 04 and 7.2144E + 04. The *esebssiwaagoT*$_Q$ for mesotropic gene locus *JUND* is 0.344. Mesotropic gene locus *JUND* is positioned at angle $\Theta_M = 48.4^0$ in the *z*, *y*-axis vertical plane (Table 3).

The *uppasebs*, *dppasebs*, *uppmsebs* and *dppasebs* for mesotropic gene locus *PRDM1* are 3.4053E + 04, 1.63936E + 05, 7.8539E + 04 and 1.75378E + 05. The *uppasebssiwa*, *dppasebssiwa*, *uppmsebssiwa* and *dppasebssiwa* for mesotropic gene locus *PRDM1* are 1.1351E + 04, 5.4645E + 04, 3.9270E + 04 and 8.7689E + 04. The sebs and sebssiwa exponential function pair for mesotropic gene locus *PRDM1* is 1.55684E+05 $e^{2E\text{-}06x}$ and 4.5086E+04 $e^{2E\text{-}05x}$. The $b_{sebs}/b_{sebssiwa}$ linearization quotient for mesotropic gene locus *PRDM1* is 3.45. The sebs - sebssiwa residual for mesotropic gene locus *PRDM1* is 2.2702E + 04, 1.09291E + 05, 3.9270E + 04 and 8.7689E + 04. The *uppesebssiwaa* and *dppesebssiwaa* for mesotropic gene locus *PRDM1* are 2.5311E + 04 and 7.1167E + 04. The *esebssiwaagoT*$_Q$ for mesotropic gene locus *PRDM1* is 0.356. Mesotropic gene locus *PRDM1* is positioned at angle $\Theta_M = 47.0^0$ in the *z*, *y*-axis vertical plane (Table 3).

The *uppasebs*, *dppasebs*, *uppmsebs* and *dppasebs* for mesotropic gene locus *RGS13* are 1.9877E + 04, 2.92457E + 05, 4.41738E + 05 and 8.70097E + 05. The *uppasebssiwa*, *dppasebssiwa*, *uppmsebssiwa* and *dppasebssiwa* for mesotropic gene locus *RGS13* are 9.939E + 03, 1.46229E + 05, 1.47246E + 05 and 2.90032E + 05. The sebs and sebssiwa exponential function pair for mesotropic gene locus *RGS13* is 2.77812E+05 $e^{3E\text{-}06x}$ and 1.39157E+05 $e^{5E\text{-}06x}$. The $b_{sebs}/b_{sebssiwa}$ linearization

quotient for mesotropic gene locus *RGS13* is 1.996. The sebs - sebssiwa residual for mesotropic gene locus *RGS13* is 9,939, 146,229, 294,492 and 580,065. The *uppesebssiwaa* and *dppesebssiwaa* for mesotropic gene locus *RGS13* are 7.8592E + 04 and 2.18130E + 05. The *esebssiwaagoT*$_Q$ for mesotropic gene locus *RGS13* is 0.360. Mesotropic gene locus *RGS13* is positioned at angle $\Theta_M = 46.5^0$ in the *z, y*-axis vertical plane (Table 3).

The *uppasebs*, *dppasebs*, *uppmsebs* and *dppasebs* for mesotropic gene locus *CEACAM1* are 2.6442E + 04, 1.35371E + 05, 1.89995E + 05 and 3.95194E + 05. The *uppasebssiwa*, *dppasebssiwa*, *uppmsebssiwa* and *dppasebssiwa* for mesotropic gene locus *CEACAM1* are 13, 221, 67,686, 63,332 and 131,731. The sebs and sebssiwa exponential function pair for mesotropic gene locus *CEACAM1* is 1.13842E+05 $e^{2E\text{-}06x}$ and 5.6780E+04 $e^{1E\text{-}05x}$. The $b_{sebs}/b_{sebssiwa}$ linearization quotient for mesotropic gene locus *CEACAM1* is 2.005. The sebs - sebssiwa residual for mesotropic gene locus *CEACAM1* is 13,221, 67,686, 126,663 and 263,463. The *uppesebssiwaa* and *dppesebssiwaa* for mesotropic gene locus *CEACAM1* are 3.8276E + 04 and 9.9708E + 04. The *esebssiwaagoT*$_Q$ for mesotropic gene locus *CEACAM1* is 0.384. Mesotropic gene locus *CEACAM1* is positioned at angle $\Theta_M = 43.6^0$ in the *z, y*-axis vertical plane (Table 3).

The *uppasebs*, *dppasebs*, *uppmsebs* and *dppasebs* for mesotropic gene locus *GABPA* are 8.904E + 03, 4.9560E + 04, 4.63859E + 05 and 8.76791E + 05. The *uppasebssiwa*, *dppasebssiwa*, *uppmsebssiwa* and *dppasebssiwa* for mesotropic gene locus *GABPA* are 8.904E + 03, 4.9560E + 04, 2.31930E + 05 and 4.38396E + 05. The $b_{sebs}/b_{sebssiwa}$ linearization quotient for *GABPA* is not applicable. The sebs - sebssiwa residual for mesotropic gene locus *GABPA* is *nil*, *nil*, 231,930 and 438,396. The *uppesebssiwaa* and *dppesebssiwaa* for mesotropic gene locus *GABPA* are 1.20417E + 05 and 2.43978E + 05. The *esebssiwaagoT*$_Q$ for mesotropic gene locus *GABPA* is 0.494. Mesotropic gene locus *GABPA* is positioned at angle $\Theta_M = 30.3^0$ in the *z, y*-axis vertical plane (Table 3).

The *uppasebs*, *dppasebs*, *uppmsebs* and *dppasebs* for mesotropic gene locus *CD34* are 5.03E + 02, 5.565E + 03, 1.94524E + 05 and 2.90844E + 05. The *uppasebssiwa*, *dppasebssiwa*, *uppmsebssiwa* and *dppasebssiwa* for mesotropic gene locus *CD34* are 5.03E + 02, 5.565E + 03, 9.7262E + 04 and 1.45422E + 05. The $b_{sebs}/b_{sebssiwa}$ linearization quotient for *CD34* is not applicable. The sebs - sebssiwa residual for mesotropic gene locus *CD34* is *nil*, *nil*, 97,262 and 145,422. The *uppesebssiwaa* and *dppesebssiwaa* for mesotropic gene locus *CD34* are 4.8882E + 04 and 7.5493E + 04. The *esebssiwaagoT*$_Q$ for mesotropic gene locus *CD34* is 0.648. Mesotropic gene locus *CD34* is positioned at angle $\Theta_M = 11.7^0$ in the *z, y*-axis vertical plane (Table 3).

$b_{sebs}/b_{sebssiwa}$ linearization quotient and sebs - sebssiwa residual statistical significance by effective intracellular pressure gene *esebssiwaagoT*$_Q$ stratum

The $b_{sebs}/b_{sebssiwa}$ linearization quotient is 3.143 ± 0.688 for tier 1 ($P_{eff} \leq 0.200$, $n = 11$). The Σ intergene tropy for tier 1 is 1.162733E+06 ± 497,383 intergene bases. The $b_{sebs}/b_{sebssiwa}$ linearization quotient is 2.240 ± 0.463 for tier 2 ($P_{eff} > 0.200 \leq 0.300$, $n = 6$; $p = 0.006$ vs tier 1). The Σ intergene tropy for tier 2 is 7.34813E+05 ± 856,523 intergene bases ($p = 0.103$ vs tier 1). The $b_{sebs}/b_{sebssiwa}$ linearization quotient is 3.670 ± 1.393 for tier 3 ($P_{eff} > 0.300$, $n = 8$, non-*nil*; $p = 0.145$ vs tier 1; $p = 0.017$ vs tier 2). The Σ intergene tropy is 9.64537E+05 ± 749,407 intergene bases for tier 3 ($p = 0.248$ vs tier 1; $p = 0.301$ vs tier 2).

The *uppasebs*, *uppasebssiwa* residual is 4.4214E+04 ± 24,373 for tier 1 ($P_{eff} \leq 0.200$, $n = 11$). The *dppasebs*, *dppasebssiwa* residual is 5.47340E+05 ± 258,360 for tier 1 ($n = 11$). The *uppmsebs*, *uppmsebssiwa* residual is 5.3053E+04 ± 34,298 for tier 1 ($n = 11$). The *dppmsebs*, *dppmsebssiwa* residual is 1.24074E+05 ± 82,270 for tier 1 ($n = 11$).

The *uppasebs*, *uppasebssiwa* residual is 2.5470E+04 ± 32,476 for tier 2 ($P_{eff} > 0.200 \leq 0.300$, $n = 6$; $p = 0.098$ vs tier 1). The *dppasebs*, *dppasebssiwa* residual is 1.87595E+05 ± 217,367 for tier 2 ($n = 6$; $p = 0.006$ vs tier 1). The *uppmsebs*, *uppmsebssiwa* residual is 5.2179E+04 ± 65,457 for tier 2 ($n = 6$; $p = 0.486$ vs tier 1). The *dppmsebs*, *dppmsebssiwa* residual is 1.21333E+05 ± 112, 712 for tier 2 ($n = 6$; $p = 0.477$ vs tier 1).

The *uppasebs*, *uppasebssiwa* residual is 3.6877E+04 ± 38,272 for tier 3 ($P_{eff} > 0.300$, $n = 8$, non-*nil*; $p = 0.308$ vs tier 1; $p = 0.284$ vs tier 2). The *dppasebs*, *dppasebssiwa* residual is 2.03613E+05 ± 129,187 for tier 3 ($n = 8$, non-*nil*; $p = 0.002$ vs tier 1; $p = 0.433$ vs tier 2). The *uppmsebs*, *uppmsebssiwa* residual is 1.33445E+05 ± 156,526 for tier 3 ($n = 8$; $p = 0.057$ vs tier 1; $p = 0.129$ vs tier 2). The *dppmsebs*, *dppmsebssiwa* residual is 2.99853E+05 ± 364, 084 for tier 3 ($n = 8$, non-*nil*; $p = 0.068$ vs tier 1; $p = 0.136$ vs tier 2).

Heterochromatinization parameters for differentiated neural axis gene angulation positioning in linear 2-dimensional *z, y*-vertical plane

The *uppasebs*, *dppasebs*, *uppmsebs* and *dppasebs* for *UNC13A* are 5.888E + 03, 2.8975E + 04, 1.65112E + 05, 3.50047E + 05. The *uppasebssiwa*, *dppasebssiwa*, *uppmsebssiwa* and *dppasebssiwa* for *UNC13A* are 5.888E + 03, 2.8975E + 04, 8.2556E + 04 and 1.75024E + 05. The $b_{sebs}/b_{sebssiwa}$ linearization quotient for *UNC13A* is not applicable. The sebs - sebssiwa residual for *UNC13A* is *nil*, *nil*, 82,556 and 175,024. The *uppesebssiwaa* and *dppesebssiwaa* for *UNC13A* are 4.4222E + 04 and 1.01999E + 05. The *esebssiwaagoT*$_Q$ for *UNC13A* is

Table 4 Heterochromatinization parameters for *z*, *y*-plane gene angulation positioning and pressuromodulation mapping of effective cell pressures for neuroaxis gene expression of differentiated neuron cell sub-types in reference to tissue macro-compliance

Gene (no. of locus bases; no. of gene bases or n/a)	Gene locus (strand)	Episode category (final SEB structure)	*uppesebssiwaa*, *dppesebssiwaa* (P_{eff} *esebssiwaagoT*$_Q$)	$f(x)_{sebs}$ $f(x)_{sebssiwa}$[c]	b_{sebs}/ $b_{sebssiwa}$[b]	Angulation (^{0})	Neural axis overexpression (predicted range)[a]
UNC13A, unc-13 homolog A (87,038; n/a)	19p13.11 (–)	2 M 3	44,222, 101,999 (0.434)	– –	*n/a*	37.6	lmn (a)
RGS21, regulator of G protein signaling 21 (50,294; n/a)	1q31.2 (+)	2 M 5	62,631, 151,780 (0.413)	1.11284E+05 e^{4E-06x} 2.2137E+04 e^{3E-06x}	5.03	40.1	–
SOX1, SRY-Box 1 (160,765; 4,108)	13q34 (+)	2 M 7 q term end	24,498, 77,119 (0.318)	1.20477E+05 e^{7E-06x} 3.9963E+04 e^{2E-05x}	3.01	51.6	pituit, capc, bell (pj)
NGB, neuroglobin (5,830; n/a)	14q24.3 (–)	3 A 5	14,618, 48,000 (0.305)	2.50250E+05 e^{2E-05x} 6.6186E+04 e^{2E-05x}	3.78	53.2	thal, bral, umn (arc)
SHANK2, SH3 And Multiple Ankyrin Repeat Domains 2 (784,883; n/a)	11q13.3-q13.4 (–)	6 A 13	27,834, 92,467 (0.301)	6.12243E+05 e^{1E-07x} 8.2498E+04 e^{4E-06x}	7.42	53.6	umn (asc, dsc)
RGS2, regulator of G protein signaling 2 (3,245; n/a)	1q31.2 (+)	3 M 7	95,617, 321,146 (0.298)	6.84931E+05 e^{1E-06x} 2.31902E+05 e^{3E-06x}	2.95	54	bgnc
RGS16, regulator of G protein signaling 16 (5,791, n/a)	1q23.3 (–)	3 M 5	32,709, 130,446 (0.251)	2.45881E+05 e^{3E-06x} 1.56958E+05 e^{6E-06x}	1.57	59.7	–
DRD1, Dopamine Receptor D1 (4,170; n/a)	5q35.2 (+)	3 M 8	50,934, 204,294 (0.249)	6.93874E+05 e^{2E-06x} 1.73469E+05 e^{6E-06x}	4.00	59.9	–
SOX14, SRY-Box 14 (2,055; n/a)	3q22.3 (+)	3 A 7	43,588, 198,734 (0.219)	1.209365E+06 $e^{4.5E-06x}$ 3.34544E+05 e^{1E-05x}	3.62	63.5	–

Table 4 Heterochromatinization parameters for *z*, *y*-plane gene angulation positioning and pressuromodulation mapping of effective cell pressures for neuroaxis gene expression of differentiated neuron cell sub-types in reference to tissue macro-compliance *(Continued)*

Gene (no. of locus bases; no. of gene bases or n/a)	Gene locus (strand)	Episode category (final SEB structure)	*uppesebssiwaa*, *dppesebssiwaa* (P_{eff} *esebssiwaagoT*$_Q$)	$f(x)_{sebs}$ $f(x)_{sebssiwa}$[c]	$b_{sebs}/b_{sebssiwa}$[b]	Angulation (^{0})	Neural axis overexpression (predicted range)[a]
DRD2, Dopamine Receptor D2 (66,097; n/a)	11q23.2 (–)	2 A 5	38,628, 178,043 (0.217)	1.10192E+05 e^{4E-07x} 7.2871E+04 e^{4E-06x}	1.51	63.8	bgnc
RBFOX3, RNA Binding Fox-1 Homolog 3 (521,757, n/a)	17q25.3 (–)	5 M 13	21,887, 102,648 (0.213)	1.0E+06 e^{3E-06x} 2.08197E+05 e^{3E-05x}	4.29	64.3	bell (gr); bral, umn (arc)
RGS18, regulator of G protein signaling 18 (378,397; 28,716)	1q31.2 (+)	4 M 11	46,829, 227,894 (0.205)	2.0E+06 e^{2E-06x} 4.77757E+05 e^{2E-05x}	4.19	65.2	–
GRIN1, Glutamate Ionotropic Receptor NMDA Type Subunit 1 (30,373; n/a)	9q34.3 (+)	2 M 5	14,630, 72,035 (0.203)	1.86172E+05 e^{2E-06x} 1.27295E+05 e^{4E-05x}	1.46	65.5	–
DRD3, Dopamine Receptor D3 (347,501; 71,611)	3q13.31 (–)	4 A 9	16,088, 79,289 (0.203)	6.3965E+04 e^{3E-07x} 1.6772E+04 e^{5E-07x}	3.81	65.5	capc

[a]Neuroanatomic location cell-specific ranges of effective cell pressure for gene overexpression: lmn (a), lower motor neuron (afferent), P_{eff} 0.434 ≥ 0.301; umn (asc, dsc, arc), upper motor neuron (ascending, descending, arcuate association), $P_{eff} \leq 0.301$; pituit, hypothalamic posterior pituitary axis neurons, upper limit P_{eff} 0.331 ≥ 0.311; thal, peri-ventricular thalamic deep nuclei neurons, upper limit P_{eff} 0.311 ≥ 0.305; capc, cornu ammonis/Papez circuit (pyramidal neuron, 3-layer cortex), P_{eff} 0.318–0.203; bell, cerebellar cortex neurons [bell (pj), purkinje cell layer, P_{eff} 0.301; bell (gr), granule cell layer, P_{eff} 0.213]; bral, cerebral cortex (pyramidal neuron, 6-layer), $P_{eff} < 0.318 \geq 0.305$–0.213; and bgnc, basal ganglia nuclei substantia nigra circuit (spiny neuron, dopaminergic), P_{eff} 0.298 - < 0.217 > 0.213. [c]$f(x) = b \cdot e^{m \cdot x}$, where *b* is the downstream anisotropic effect (intercept and slope are absolute values). [b]$b_{sebs}/b_{sebssiwa}$ is the linearization quotient. Note: [1)] gene loci sub-episode block structure (SEB) variations include non-contributory anisotropy (NCA), anisotropy converted to mesotropy (ACM), and/or 0.5-factor adjusted stabilizing mesotropy or anisotropy converted to stabilizing isotropy for anisotropy or mesotropy (stlAfM, stlMfA or stlMfM) that result in an initial to final SEB conversion; [2)] previously reported episode and sub-episode block structure is applied in all cases as per reference [25], in which gene/gene loci at cusps of the delineated base intervals, *SHANK2* (784,883), *RBFOX3* (521,757) classify into the adjacent interval; [3)] Sub-episode block structures for initial to final SEB converted genes are as follows: *NGB*, 3 A 7 (−2) stlMfA NCA; *SOX1*, 2 M 5 (+2) ACM q terminal end; *RGS18*, 4 M 9 (+2) ACM; *RBFOX3*, 5 M 11 (+2) ACM; *RGS16*, 3 M 7 (−2) NCA; *DRD1*, 3 A 7 (+1) ACM; and *UNC13A*, 2 M 5 (−2) ACM; and [4)] $b_{sebs}/b_{sebssiwa}$ quotients for *DRD1*, *DRD2* and *DRD3* are by reverse *x*-intercept plotting the *uppasebs*, *uppamsebs*, *dppasebs* and *dppmsebs* and the corelate *uppasebssiwa*, *uppamsebssiwa*, *dppasebssiwa* and *dppmsebssiwa*

0.434. *UNC13A* is positioned at angle $\Theta_M = 37.6^0$ in the *z, y*-axis vertical plane.

The *uppasebs*, *dppasebs*, *uppmsebs* and *dppasebs* for *RGS21* are 1.3087E + 04, 2.29159E + 05, 3.56158E + 05 and 5.66939E + 05. The *uppasebssiwa*, *dppasebssiwa*, *uppmsebssiwa* and *dppasebssiwa* for *RGS21* are 6.544E + 03, 1.14580E + 05, 1.18719E + 05 and 1.88980E + 05. The sebs and sebssiwa exponential function pair for *RGS21* is 1.11284E+05 e^{4E-06x} and 2.2137E+04 e^{3E-06x}. The $b_{sebs}/b_{sebssiwa}$ linearization quotient for *RGS21* is 5.03. The sebs - sebssiwa residual for *RGS21* is 6,544, 114,580, 237,439 and 377,959. The *uppesebssiwaa* and *dppesebssiwaa* for *RGS21* are 6.2631E + 04 and 1.51780E + 05. The *esebssiwaagoT*$_Q$ for *RGS21* is 0.413. *RGS21* is positioned at angle $\Theta_M = 40.1^0$ in the *z, y*-axis vertical plane (Table 4; Additional file 1: Table S1).

The *uppasebs*, *dppasebs*, *uppmsebs* and *dppasebs* for *SOX1* are 1.6642E + 04, 1.36246E + 05, 1.73795E and 4.35291E + 05. The *uppasebssiwa*, *dppasebssiwa*, *uppmsebssiwa* and *dppasebssiwa* for *SOX1* are 5.547E + 03, 4.5415E + 04, 4.3449E + 04 and 1.08823E + 05. The sebs and sebssiwa exponential function pair for *SOX1* is 1.20477E+05e^{7E-06x} and 3.9963E+04 e^{2E-05x}. The $b_{sebs}/b_{sebssiwa}$ linearization quotient for *SOX1* is 3.01. The sebs - sebssiwa residual for *SOX1* is 11,095, 90,830, 130,346 and 326,468. The *uppesebssiwaa* and *dppesebssiwaa* for *SOX1* are 2.4498E + 04 and 7.7119E + 04. The *esebssiwaagoT*$_Q$ for *SOX1* is 0.318. *SOX1* is positioned at angle $\Theta_M = 51.6^0$ in the *z, y*-axis vertical plane (Table 4; Additional file 1: Table S1).

The *uppasebs*, *dppasebs*, *uppmsebs* and *dppasebs* for *NGB* are 1.6465E + 04, 1.68356E + 05, 4.7494E + 04 and 7.9764E + 04. The *uppasebssiwa*, *dppasebssiwa*, *uppmsebssiwa* and *dppasebssiwa* for *NGB* are 5.488E + 03, 5.6119E + 04, 2.3747E + 04 and 3.9882E + 04. The sebs and sebssiwa exponential function pair for *NGB* is 2.50250E+05 e^{2E-05x} and 6.6186E+04 e^{2E-05x}. The $b_{sebs}/b_{sebssiwa}$ linearization quotient for *NGB* is 3.78. The sebs - sebssiwa residual for *NGB* is 10,977, 112,238, 23,747 and 39,882. The *uppesebssiwaa* and *dppesebssiwaa* for *NGB* are 1.4618E + 04 and 4.8000E + 04. The *esebssiwaagoT*$_Q$ for *NGB* is 0.305. *NGB* is positioned at angle $\Theta_M = 53.2^0$ in the *z, y*-axis vertical plane (Table 4; Additional file 1: Table S1).

The *uppasebs*, *dppasebs*, *uppmsebs* and *dppasebs* for *SHANK1* are 7.9764E + 04, 8.2330E + 04, 6.05471E + 05, 2.63439E + 05 and 5.90625E + 05. The *uppasebssiwa*, *dppasebssiwa*, *uppmsebssiwa* and *dppasebssiwa* for *SHANK1* are 1.1761E + 04, 8.6496E + 04, 4.3907E + 04 and 9.8438E + 04. The sebs and sebssiwa exponential function pair for *SHANK1* is 6.12243E+05 e^{1E-07x} and 8.2498E+04 e^{4E-06x}. The $b_{sebs}/b_{sebssiwa}$ linearization quotient for *SHANK1* is 7.42. The sebs - sebssiwa residual for *SHANK1* is 70,569, 518,975, 219,533 and 492,188. The *uppesebssiwaa* and *dppesebssiwaa* for *SHANK1* are 2.7834E + 04 and 9.2467E + 04. The *esebssiwaagoT*$_Q$ for *SHANK1* is 0.301. *SHANK1* is positioned at angle $\Theta_M = 53.6^0$ in the *z, y*-axis vertical plane (Table 4; Additional file 1: Table S1).

The *uppasebs*, *dppasebs*, *uppmsebs* and *dppasebs* for *RGS2* are 7.9267E + 04, 7.56237E + 05, 6.59244E + 05 and 1.560848E + 06. The *uppasebssiwa*, *dppasebssiwa*, *uppmsebssiwa* and *dppasebssiwa* for *RGS2* are 2.6422E + 04, 2.52079E + 05, 1.64811E + 05 and 3.90212E + 05. The sebs and sebssiwa exponential function pair for *RGS2* is 6.84931E+05 e^{1E-06x} and 2.31902E+05 e^{3E-06x}. The $b_{sebs}/b_{sebssiwa}$ linearization quotient for *RGS2* is 2.95. The sebs - sebssiwa residual for *RGS2* is 52,845, 504,158, 494,433 and 1,170,636. The *uppesebssiwaa* and *dppesebssiwaa* for *RGS2* are 9.5617E + 04 and 3.21146E + 05. The *esebssiwaagoT*$_Q$ for *RGS2* is 0.298. *RGS2* is positioned at angle $\Theta_M = 54^0$ in the *z, y*-axis vertical plane (Table 4; Additional file 1: Table S1).

The *uppasebs*, *dppasebs*, *uppmsebs* and *dppasebs* for *RGS16* are 4.1927E + 04, 2.78410E + 05, 1.33362E + 05 and 6.5059E + 04. The *uppasebssiwa*, *dppasebssiwa*, *uppmsebssiwa* and *dppasebssiwa* for *RGS16* are 2.0964E + 04, 1.39205E + 05, 4.4454E + 04 and 1.21686E + 05. The sebs and sebssiwa exponential function pair for *RGS16* is 2.45881E+05 e^{3E-06x} and 1.56958E+05 e^{6E-06x}. The $b_{sebs}/b_{sebssiwa}$ linearization quotient for *RGS16* is 1.57. The sebs - sebssiwa residual for *RGS16* is 20,964, 139,205, 88,908 and 243,373. The *uppesebssiwaa* and *dppesebssiwaa* for *RGS16* are 3.2709E + 04 and 1.30446E + 05. The *esebssiwaagoT*$_Q$ for *RGS16* is 0.251. *RGS16* is positioned at angle $_M = 59.7^0$ in the *z, y*-axis vertical plane (Table 4; Additional file 1: Table S1).

The *uppasebs*, *dppasebs*, *uppmsebs* and *dppasebs* for *DRD1* are 1.27930E + 05, 1.062852E + 06, 2.79538E + 05 and 5.71499E + 05. The *uppasebssiwa*, *dppasebssiwa*, *uppmsebssiwa* and *dppasebssiwa* for *DRD1* are 3.1983E + 04, 2.65713E + 05, 6.9885E + 04 and 1.42875E + 05. The sebs and sebssiwa exponential function pair for *DRD1* is 6.93874E+05 e^{2E-06x} and 1.73469E+05 e^{6E-06x}. The $b_{sebs}/b_{sebssiwa}$ linearization quotient for *DRD1* is 4.00. The sebs - sebssiwa residual for *DRD1* is 95,948, 797,139, 209,654 and 428,624. The *uppesebssiwaa* and *dppesebssiwaa* for *DRD1* are 5.0934E + 04 and 2.04294E + 05. The *esebssiwaagoT*$_Q$ for *DRD1* is 0.249. *DRD1* is positioned at angle $\Theta_M = 59.9^0$ in the *z, y*-axis vertical plane (Table 4; Additional file 1: Table S1).

The *uppasebs*, *dppasebs*, *uppmsebs* and *dppasebs* for *SOX14* are 7.6621E + 04, 1.016347E + 06, 2.04065E + 05 and 4.30144E + 05. The *uppasebssiwa*, *dppasebssiwa*, *uppmsebssiwa* and *dppasebssiwa* for *SOX14* are 1.9155E + 04, 2.54087E + 05, 6.8022E + 04 and 1.43381E + 05. The sebs and sebssiwa exponential function pair for *SOX14* is 1.209365E+06 $e^{4.5E-06x}$ and 3.34544E+05

$e^{1E\text{-}05x}$. The $b_{sebs}/b_{sebssiwa}$ linearization quotient for *SOX14* is 3.62. The sebs - sebssiwa residual for *SOX14* is 57,466, 762,260, 136,043 and 286,763. The *uppesebssiwaa* and *dppesebssiwaa* for *SOX14* are 4.3588E + 04 and 1.98734E + 05. The *esebssiwaagoT*$_Q$ for *SOX14* is 0.219. *SOX14* is positioned at angle $\Theta_A = 63.5^0$ in the *z, y*-axis vertical plane (Table 4; Additional file 1: Table S1).

The *uppasebs*, *dppasebs*, *uppmsebs* and *dppasebs* for *DRD2* are 7.8907E + 04, 7.90658E + 05, 1.01906E + 05 and 1.85067E + 05. The *uppasebssiwa*, *dppasebssiwa*, *uppmsebssiwa* and *dppasebssiwa* for *DRD2* are 2.6302E + 04, 2.63553E + 05, 5.0953E + 04 and 9.2533E + 04. The sebs and sebssiwa exponential function pair for *DRD2* is 1.10192E+05 $e^{4E\text{-}07x}$ and 7.2871E+04 $e^{4E\text{-}06x}$. The $b_{sebs}/b_{sebssiwa}$ linearization quotient for *DRD2* is1.51. The sebs - sebssiwa residual for *DRD2* is 52,605, 527, 106, 50,953 and 92,533. The *uppesebssiwaa* and *dppesebssiwaa* for *DRD2* are 3.8628E + 04 and 1.78043E + 05. The *esebssiwaagoT*$_Q$ for *DRD2* is 0.217. *DRD2* is positioned at angle $\Theta_A = 63.8^0$ in the *z, y*-axis vertical plane (Table 4; Additional file 1: Table S1).

The *uppasebs*, *dppasebs*, *uppmsebs* and *dppasebs* for *RBFOX3* are 7.7745E + 04, 7.99501E + 05, 2.15712E + 05 and 5.04325E + 05. The *uppasebssiwa*, *dppasebssiwa*, *uppmsebssiwa* and *dppasebssiwa* for *RBFOX3* are 1.2957E + 04, 1.33250E + 05, 3.0816E + 04 and 7.2046E + 04. The sebs and sebssiwa exponential function pair for *RBFOX3* is 1.10192E+05 $e^{4E\text{-}07x}$ and 7.2871E+04 $e^{4E\text{-}06x}$. The $b_{sebs}/b_{sebssiwa}$ linearization quotient for *RBFOX3* is 4.80. The sebs - sebssiwa residual for *RBFOX3* is 64,787, 666,251, 184,896 and 432,278. The *uppesebssiwaa* and *dppesebssiwaa* for *RBFOX3* are 2.1887E + 04 and 1.02648E + 05. The *esebssiwaagoT*$_Q$ for *RBFOX3* is 0.213. *RBFOX3* is positioned at angle $\Theta_A = 64.3^0$ in the *z, y*-axis vertical plane (Table 4; Additional file 1: Table S1).

The *uppasebs*, *dppasebs*, *uppmsebs* and *dppasebs* for *RGS18* are 1.53005E + 05, 1.438692E + 06, 3.78343E + 05 and 1.008303E + 06. The *uppasebssiwa*, *dppasebssiwa*, *uppmsebssiwa* and *dppasebssiwa* for *RGS18* are 3.0601E + 04, 2.87738E + 05, 6.3057E + 04 and 1.68050E + 05. The sebs and sebssiwa exponential function pair for *RGS18* is 2.0E+06 $e^{2E\text{-}06x}$ and 4.77757E+05 $e^{2E\text{-}05x}$. The $b_{sebs}/b_{sebssiwa}$ linearization quotient for *RGS18* is 4.19. The sebs - sebssiwa residual for *RGS18* is 122,404, 1,150,953, 315,285 and 840,252. The *uppesebssiwaa* and *dppesebssiwaa* for *RGS18* are 4.6829E + 05 and 2.27894E + 05. The *esebssiwaagoT*$_Q$ for *RGS18* is 0.205. *RGS18* is positioned at angle $\Theta_A = 65.2^0$ in the *z, y*-axis vertical plane (Table 4; Additional file 1: Table S1).

The *uppasebs*, *dppasebs*, *uppmsebs* and *dppasebs* for *GRIN1* are 1.7024E + 04, 1.79509E + 05, 6.2241E + 04 and 1.62947E + 05. The *uppasebssiwa*, *dppasebssiwa*, *uppmsebssiwa* and *dppasebssiwa* for *GRIN1* are 8.512E + 03, 8.9755E + 04, 2.0747E + 04 and 5.4316E + 04. The sebs and sebssiwa exponential function pair for *GRIN1* is 1.86172E+05 $e^{2E\text{-}06x}$ and 1.27295E+05 $e^{4E\text{-}05x}$. The $b_{sebs}/b_{sebssiwa}$ linearization quotient for *GRIN1* is 1.46.

The sebs - sebssiwa residual for *GRIN1* is 8,512, 89, 755, 41,494 and 108,632. The *uppesebssiwaa* and *dppesebssiwaa* for *GRIN1* are 1.4630E + 04 and 7.2035E + 04. The *esebssiwaagoT*$_Q$ for *GRIN1* is 0.203. *GRIN1* is positioned at angle $\Theta_A = 65.5^0$ in the *z, y*-axis vertical plane (Table 4; Additional file 1: Table S1).

The *uppasebs*, *dppasebs*, *uppmsebs* and *dppasebs* for *DRD3* are 7.8218E + 04, 6.57108E + 05, 6.6128E + 04 and 1.08626E + 05. The *uppasebssiwa*, *dppasebssiwa*, *uppmsebssiwa* and *dppasebssiwa* for *DRD3* are 1.5644E + 04, 1.31422E + 05, 1.6532E + 04 and 2.7157E + 04. The sebs and sebssiwa exponential function pair for *DRD3* is 6.3965E+04 $e^{3E\text{-}07x}$ and 1.6772E+04 $e^{5E\text{-}07x}$. The $b_{sebs}/b_{sebssiwa}$ linearization quotient for *DRD3* is 3.81. The sebs - sebssiwa residual for *DRD3* is 62,574, 525, 686, 49,596 and 81,470. The *uppesebssiwaa* and *dppesebssiwaa* for *DRD3* are 1.6088E + 04 and 7.9289E + 04. The *esebssiwaagoT*$_Q$ for *DRD3* is 0.203. *DRD3* is positioned at angle $\Theta_A = 65.5^0$ in the *z, y*-axis vertical plane (Table 4; Additional file 1: Table S1).

Discussion

Linear normalized determination of gene positioning angulation in the *z, y*-plane by the *esebssiwaagoT*$_Q$ method effective intracellular pressure unit

The $b_{sebs}/b_{sebssiwa}$ sebs intercept-to-sebssiwa intercept quotient and residual adjustments have been determined in this study by *x*-, *y*- or hybrid intercept exponential function plotting for specific detection of the predominant paired linearization effect as either the *dppasebs*, *dppmsebs*, *uppasebs*, *uppmsebs*, or dual *uppasebs*, *uppmsebs*, *dppasebs*, *dppmsebs* due to normalizing primary weighted averaging. Since the $b_{sebs}/b_{sebssiwa}$ linearization quotient for tier 1 sub-group analysis genes within the P_{eff} stratum ≤ 0.200 is 3.143 ± 0.688 (n = 11), and that for tier 3 sub-group analysis genes within the P_{eff} stratum > 0.300 is 3.670 ± 1.393 (n = 8; p = 0.145 vs tier 1), whereas that for tier 2 sub-group analysis genes within the P_{eff} stratum > 0.200 ≤ 0.300 is 2.240 ± 0.463 (n = 6; p = 0.006 vs tier 1); these pairwise comparisons are consistent with primary linearization of the *dppasebs*, *dppmsebs* anisotropy effect for tier 1 ≤ 0.200 P_{eff} genes and of the *uppasebs*, *uppamsebs* mesotropy effect for tier 3 > 0.300 P_{eff} genes, in contrast to dual linearization for tier 2 intermediate P_{eff} stratum genes due to the presence of downstream and upstream tropy effects of equivalence. The pairwise statistical significance of the subtractive sebs, sebssiwa residual comparisons between tier 2 and tier 1 genes (p = 0.098, p = 0.006, p = 0.486, p = 0.477), and between tier 3 and

tier 1 genes (p = 0.308, p = 0.002, p = 0.057, p = 0.068) is further consistent with the primary weighted averaging linearization due to *uppmsebs* and *dppmsebs* normalizing of the *uppasebs* and *uppmsebs* effects in tier 3 > 0.300 P_{eff} genes as probability for significance approaches alpha (α = 0.05). Therefore, primary linearization adheres to the rule of split-integrated averaging to linearization of mutually exclusive upstream (*upp*-) and downstream (*dpp*-) parts within the respective anisotropic or mesotropic gene category inclusive of SEB interconversions; in which case, normalization of the *dppasebs*, *dppmsebs* effect predominates in anisotropic gene *MYC* ($b_{\text{sebs}}/b_{\text{sebssiwa}}$: 3.63), the *uppasebs*, *uppmsebs* effect predominates in mesotropic gene *PRDM1* ($b_{\text{sebs}}/b_{\text{sebssiwa}}$: 3.45), while both the *dppasebs*, *dppmsebs* and *uppasebs*, *uppmsebs* effects are linear normalized in *PRKCH* ($b_{\text{sebs}}/b_{\text{sebssiwa}}$: 3.17).

Secondary linearization of the anisotropic effect for both types of genes is by the mesotropic effect at the second weighted averaging stage of the *uppesebssiwaa* and *dppesebssiwaa*; as in the example of mesotropic gene *INSL3* ($b_{\text{sebs}}/b_{\text{sebssiwa}}$: 5.06) in which there is further linearization of the split-integrated final anisotropic effect of 1.0921E + 04 (*uppasebssiwa*) and 8.2893E + 04 intergene bases (*dppmsebssiwa*) by the mesotropic effect of 3.7099E + 04 (*dppasebssiwa*) and 6.6603E + 04 (*dppmsebssiwa*), which results in an *uppasebssiwaa*, *dppesebssiwaa* of 2.4010E + 04 and 7.4748E + 04 (P_{eff}, 0.321) for horizontal alignment from the z, y-plane (θ_{M} = 51.2^0); and as another example, anisotropic gene *CCN2* ($b_{\text{sebs}}/b_{\text{sebssiwa}}$: 4.00) in which there is the further linearization of the split-integrated final anisotropic effect of 3.0356E + 04 and 2.79275E + 05 with a mesotropic effect of 4.2913E + 04 and 1.13936E + 05 intergene bases that results in an *uppasebssiwaa*, *dppesebssiwaa* of 30293E + 04 and 1.82468E + 05 (P_{eff}, 0.166) for z, x-plane transcriptive alignment ($\theta_{\text{A}} = 70.0^0$).

Therefore, since the *esebssiwaago*T_{Q} method is based on the normalization of the anisotropy effect at two distinct stages and predicts the temporality of gene expression in linear normal effective intracellular pressure units (P_{eff}) at which eukaryotic heterochromatin strand segments of DNA horizontally align for transcription with respect to the gene it can be applied to study gene positioning angulation in linear normal 2-D space, which implies that the process of horizontal z, x-plane alignment of a gene is linear normalized in the nucleoplasm of an eukaryotic cell.

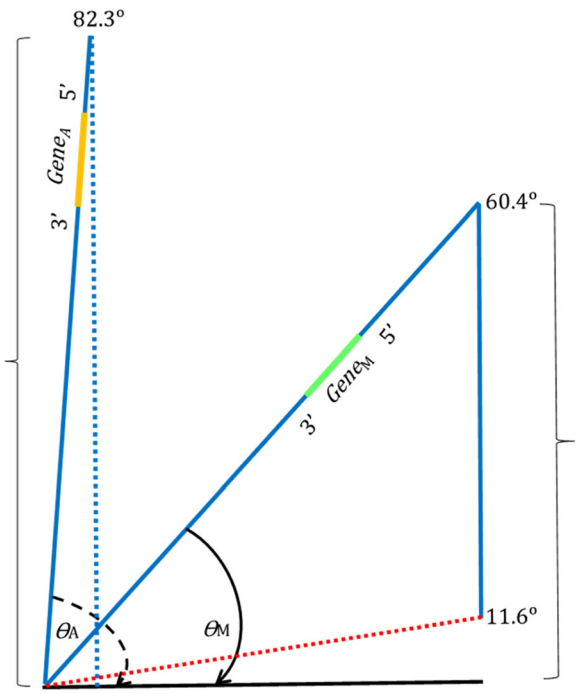

Fig. 4 Vectormetry for horizontal alignment of anisotropic and mesotropic genes by heterochromatin strand structural pressurotopy. Anisotropic gene loci are positioned between angles 82.3 and 60.5^0 in the z, y-vertical plane encounter the chromatin-associated protein viscosity effect at intergene segments. The effective momentum ($\boldsymbol{m}_{\text{eff}}$) in anisotropic gene alignment to the z, x-horizontal plane is $\boldsymbol{m}_{\text{A}} = \boldsymbol{m}_{\text{ch tropy}}$ (- $\boldsymbol{m}_{\text{pro-grav ch tropy}}$) as indicated by the left bracket. Mesotropic gene loci are positioned between angles 60.4 and 11.7^0 in the z, y-vertical plane encounter dual chromatin-associated protein viscosity effect at intergene segments and the nuclear membrane nucleoplasm chromatin-associated protein viscosity effect at intergene segments. The effective momentum ($\boldsymbol{m}_{\text{eff}}$) in mesotropic gene alignment to the z, x-horizontal plane is $\boldsymbol{m}_{\text{M}} = \boldsymbol{m}_{\text{ch tropy}} + \boldsymbol{m}_{\text{ch nmn tropy}}$ (- $\boldsymbol{m}_{\text{pro-grav ch tropy}}$) as indicated by the right bracket. The effective momentum ($\boldsymbol{m}_{\text{eff}}$) in gene transcription will be inversely proportional to the effective cell pressure (P_{eff}) required for horizontal alignment of gene intergene loop segment tropy, P_{eff} ($0.064 \geq x < 0.245$) · $\boldsymbol{m}_{\text{A}} = P_{\text{eff}}$ ($0.245 \geq x \leq 0.648$) · $\boldsymbol{m}_{\text{M}}$. The initial momentum vector for anisotropic gene alignment, $\boldsymbol{m}_{\text{ch tropy}}$, will be greater as the origination point of anisotropic genes is 7.7 degrees (^{0}) from the z, y-vertical, which require lesser applied pressure for horizontal alignment; whereas, the initial momentum vector for mesotropic gene alignment, $\boldsymbol{m}_{\text{ch tropy}} + \boldsymbol{m}_{\text{ch nmn tropy}}$ ($\boldsymbol{m}_{\text{M}}$), will be lesser as the origination point of mesotropic genes is between 29.6^0 and 78.3 degrees (^{0}) to the z, y-vertical plane, which require lesser applied pressure for horizontal alignment. Therefore, the effective momentum ($\boldsymbol{m}_{\text{eff}}$; $\boldsymbol{m}_{\text{A}}$, $\boldsymbol{m}_{\text{M}}$) for gene transcription is inversely proportional to the effective cell pressure (P_{eff}) required for horizontal alignment of gene intergene loop segment tropy. Legend. $\boldsymbol{m}_{\text{ch tropy}}$, left bracket; $\boldsymbol{m}_{\text{ch tropy}} + \boldsymbol{m}_{\text{ch nmn tropy}}$, right bracket; $\boldsymbol{m}_{\text{pro-grav ch tropy}}$, pro-gravitational momentum vector (not shown); $P_{\text{effective intracellular pressure}}$ (P_{eff}) = $P_{\text{effective intranuclear pressure}}$

Arrangement of genes in native positions is pressurotopic by heterochromatin gene loop segments of differing nano-compliance

The upstream 5' end intergene and downstream 3' end intergene base segments with respect a gene are subject to peptide, microRNA and functional pseudogene RNA affinity binding viscosity weighting effects in both forward transcribing and reverse anti-transcribing directions that are asymmetric [25], in which case each gene exists at angulation with reference to the z, x-axis

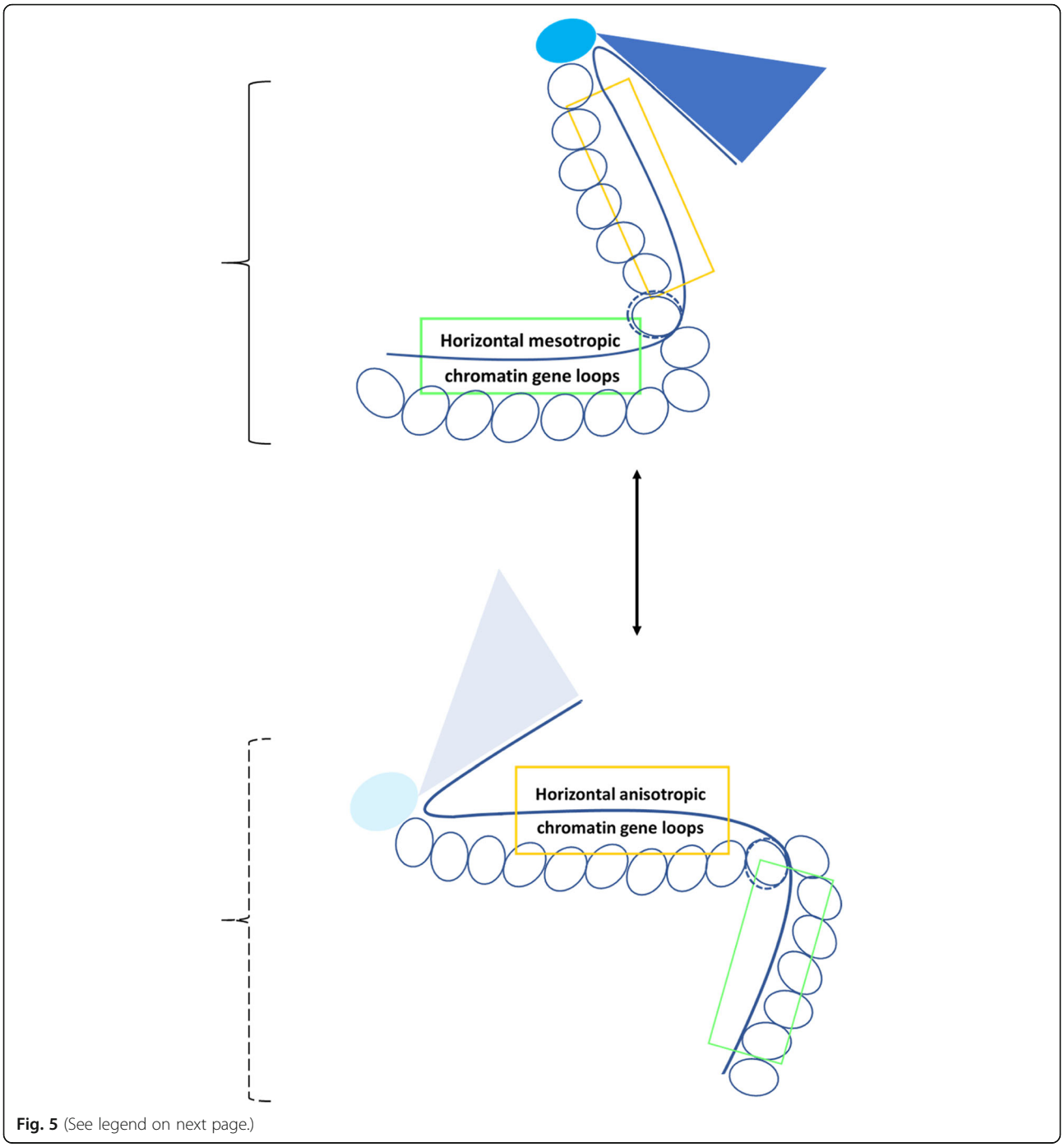

Fig. 5 (See legend on next page.)

(See figure on previous page.)
Fig. 5 Pressurotopic model for binomial always-on heterochromatin gene transcription by anisotropic or mesotropic DNA strand loop micro-structural segmentation. In the binomial always-on model of gene transcription by micro-structural segmentation pressurotopy, mesotropy and amorphousity loop form heterochromatin loop tropy strand genes positioned between 11.7 and 60.4^0 degrees in the *z*, *y*-vertical plane perceiving asymmetric viscosity effects of the same align for transcription during increases of P_{eff} to between 0.245 and 0.648 $esebssiwaagoT_Q$ units within inner nuclear membrane (INM)-associated heterochromatin; whereas, anisotropy and amorphousity loop form heterochromatin loop tropy strand genes positioned between 60.5 and 82.3^0 in the *z*, *y*-vertical plane perceiving lesser grade asymmetric viscosity effects of the same align for transcription during decreases in P_{eff} to between 0.064 and 0.2445 $esebssiwaagoT_Q$ units within peripheral nucleoplasm heterochromatin in association with un-limiting nuclear pore subunits. Heterochromatin shifts towards the inner nuclear envelope margin following the transcription of *EMD* (P_{eff}, 0.234; $\theta_A = 61.7^0$) during which positive pressuromodulation at the cell membrane regulates mechanotransduction apparatus sensitivity for linear increases in nuclear effective pressure (P_{eff}) and resultant mesotropic gene transcription; whereas, heterochromatin shifts towards the central peripheral nucleoplasm edge due to negative pressuromodulation at the cell membrane and mitochondrial oxidative challenge-exothermy, during which transcription of inner nuclear envelope peptide-coding genes *LMNB1* (P_{eff}, 0.197; $\theta_A = 66.2^0$) → *LMNA* (P_{eff}, 0.184; $\theta_A = 67.8^0$) to *LMNB2* (P_{eff}, 0.167; $\theta_A = 69.8^0$) regulates sensitivity for linear increases (or decreases) in mechanotransduction pressure $esebssiwaagoT_Q$ units. Legend. Cyan oval, complete nuclear pore complex with all subunits; light cyan oval, partial nuclear pore complex with some subunits; dark blue triangle, lamin and lamin-associated proteins; light blue triangle, lamin and lamin-associated proteins; transparent ovals, nucleosome with histone proteins; solid gold rectangle, anisotropic chromatin strand loop segment DNA with transcription ready infra-pressuromodulated genes; bright green rectangle, mesotropic chromatin strand loop segment DNA with transcription ready supra-pressuromodulated genes; solid bracket, nuclear membrane nucleoplasm chromatin; dashed bracket, central peripheral edge nucleoplasm chromatin

horizontal plane at the line of unity (θ_H) as a result of forward paired point tropy fulcrum weighting ($prpT_Q$) with underlying baseline reverse anisotropy.

The segmentation of strand heterochromatin for positive strand (+) native configuration genes of human 1q22 located between position -12 and +15 in reference to *LMNA* (pos 0) has been studied by the determinations of the $esebssiwaagoT_Q$ of sequentially situated genes. As it has been determined herein, the gene loop segment structure for the *LMNA* gene (P_{eff}, 0.184; $\theta_A = 68.4^0$)-containing forward strand (+) from 5' to 3' has been determined is: 5'-0.234-(a_{-12})-0.272 (m_{-11})-0.229 (a_{-10})-0.211 (a_{-9})-0.269 (m_{-8})-0.144 (a_{-7})-0.314 (m_{-6})-0.268 (m_{-5})-0.176 (a_{-4})-0.260 (m_{-3})-0.259 (m_{-2})-0.270 (m_{-1})-0.184 (a_0)-0.135 (m_{+1})-0.395 (m_{+2})-0.146 (a_{+3})-0.212 (a_{+4})-0.336 (m_{+5})-0.287 (m_{+6})-0.153 (a_{+7})-0.283 (m_{+8})-0.193 (a_{+9})-0.269 (m_{+10})-0.199 (a_{+11})-0.146 (a_{+12})-0.190 (a_{+13})-0.188 (a_{+14})-0.243 (a_{+15})-3', which begins at the 5' end with *DAP3* (P_{eff} 0.234) in the form of a 9-in series anisotropy alternating mesotropy amorphous loop segment (a-m-a-a-m-a-m-m-a) followed by a 3-in series mesotropy loop segment (m), and then a 11-in series anisotropy alternating anisotropy amorphous loop segment (a-m-m-a-a-m-m-a-m-a-m) with *LMNA* followed by a 5-in series anisotropy loop segment (a) with 3' end *BCAN* (P_{eff} 0.234). These findings of the study are further supported by the retrospective analysis of micro-segmentation of negative strand (-) human 14q32.3 B-cell heavy chain immunoglobin locus genes in native positions (n = 42) [26, 27], in which there are two instances of sequential alternating tropy in-series amorphousity (n = 5, n = 4), two instances of sequential mesotropy in-series (n = 8, n = 3), as well as several instances of sequential micro-structural anisotropy (n = 5, n = 3, 3, 3).

Therefore, based on the findings of this study on the micro-segmentation of a 0.73-mm length plus (+) strand *LMNA* gene-containing heterochromatin strand loop segment and a 0.25 mm length minus (-) strand *IGH_* locus-containing DNA strand loop segment, there is segmental difference in DNA strand nano-compliance, in which case intergene tropy loop segments with differences nano-compliance overlap as there exists micron (μm) scale segmentation of alternating mesotropy and anisotropy; as such, heterochromatin DNA strand loops can be characterized as anisotropy, mesotropy or amorphousity loop forms with micro-segmentation perceiving various grades of the asymmetric tropy viscosity effect for genes in juxtaposition separated by intergene base distance of between 11.6 and 14 nanometers (nm; 13 - 15 bases), if two nucleic acid bases and a primed half-phosphodiester bond in-tandem is considered to be ~1.75 nm in length.

Anglemetry of gene positioning angulation in the *z, y*-plane and vectormetry for *z, x*-plane horizontal alignment in two-dimensional linear space

Gene intergene tropy anglemetry is performed in 2-D linear angulation space utilizing the strand specific effective intracellular pressure unit (P_{eff})-to-angle regression conversion, based on which it has been determined that anisotropic genes are situated between 60.5 and 82.3^0 in the *z*, *y*-vertical plane and mesotropic genes are situated between 60.4 and 11.7^0 in the *z*, *y*-vertical axis plane; in which case the initial momentum vector for anisotropic gene alignment, $\boldsymbol{m}_{\text{ch tropy}}$, from origination is between 82.3 and 60.5^0 in the *z*, *y*-vertical, whereas the initial momentum vector for mesotropic gene alignment, $\boldsymbol{m}_{\text{ch tropy}} + \boldsymbol{m}_{\text{ch nmn tropy}}$ ($\boldsymbol{m}_M$), from origination is 60.4 and 11.7^0 from above the *z*, *x*-horizontal plane.

Therefore, the effective momentum ($\boldsymbol{m}_{\text{eff}}$; $\boldsymbol{m}_{\text{A}}$, $\boldsymbol{m}_{\text{M}}$) for gene transcription is inversely proportional to the effective cell pressure (P_{eff}) required for horizontal alignment of gene intergene loop segment tropy (Fig. 4).

Based on these findings of the study, sequentially located anisotropic genes in a gene intergene tropy segment of the same will transition into the *z*, *x*-horizontal plane reading frame for gene transcription from between origination angulations of between 60.5 and 82.3^0 in the *z*, *y*-vertical plane where the originating momentum vector (***m***ch tropy) will encounter a singular viscosity effect at intergene base tropy segments, in comparison to mesotropic genes situated between 60.4 and 11.7^0 in the *z*, *y*-vertical axis plane that will align within the inner nuclear membrane (INM) nucleoplasm where dual viscosity effects are encountered at intergene base tropy segments, in which case the additional inner nuclear membrane nucleoplasm chromatin viscosity tropy effect for mesotropic gene alignment is attributable to the additive effect of nuclear pore traffic-related to peptide synthesis rough endoplasmic reticular network of the inner nuclear envelope. Therefore, the pressurotopic model for a binomial always-on heteroeuchromatin transcription is proposed in which mesotropic DNA loop segments of supra-pressuromodulated genes are transcriptionally active at the inner nuclear membrane (INM), while anisotropic DNA loop segments of infra-pressuromodulated genes are transcriptionally active at the at the nucleolar peripheral nucleoplasm interface. The pressurotopic loop segment-dependent eukaryotic gene transcription builds on the static heterochromatin-dynamic euchromatin model in which chromatin is inactive at the nuclear envelope and active in the nucleoplasm in proximity to mobile nuclear pore complex subunits [11, 14–16] (Fig. 5).

There exists significant variance of Σ intergene base segment loop tropy, although genes are positioned at similar angulation in the *z*, *y*-vertical plane as has been determined in the study; for example, the Σ intergene base segment loop tropy for *CYGB* is 4.11804E + 05 (P_{eff} 0.248), whereas that for *DRD1* is 2.041819E + 06 intergene bases (P_{eff} 0.249), which align to $\theta_{\text{H}} = 0^0$ from angulations of 60.0^0 and 59.9^0. Therefore, based on such determinations gene angulation distances to the *z*, *x*-horizontal plane line of unity can be determined from the hypotenusal tropy inclusive of the interposed gene bases, as in the example of *MIR4537*, a 3 A 7 gene positioned at an angle of 82.3^0 (P_{eff} 0.064), for which the hypotenusal tropy length inclusive of intervening genes is 3.55373E + 05 bases, and thus the reverse extrapolated arc tropy distance from angulation to the *z*, *x*-horizontal plane (*Ho*) is 2.465E + 02 microns. Therefore, study findings are applicable to further study of heteroeuchromatin loop segment *z*, *x*-plane alignment kinetics when the inverse relationship between effective pressure and momentum, P_{eff} $(0.064 \geq x < 0.245) \cdot \boldsymbol{m}_{\text{A}} = P_{\text{eff}}$ $(0.245 \geq x \leq 0.648) \cdot \boldsymbol{m}_{\text{M}}$ ($P_{\text{eff}} \cdot \boldsymbol{m}_{\text{ch tropy}} = P_{\text{eff}} \cdot \boldsymbol{m}_{\text{ch tropy}} + \boldsymbol{m}_{\text{ch nmn tropy}}$) for DNA strand loop alignment in nuclear protoplasm.

Differentiated neuron cell sub-types differ in the range of effective cell pressures for neuroaxis gene expression in reference to tissue macro-compliance

During retinoic acid-mediated neural differentiation of NT2/D1embryonal lineage pluripotent cells ($SOX1^+$/$SOX14^-$) *in vitro* [42], it has been shown that *SOX1* (P_{eff} 0.318; $\theta_{\text{M}} = 51.6^0$), expression re-increases at 2-weeks in response to RA, while *SOX14* (P_{eff} 0.219; $\theta_{\text{A}} = 63.5^0$) expression increases over the same 4-week period, which is plasmid-expressed in HeLa cells at anisotropic pressure. Since *SOX1* determines neuronal lineage analogous to *SOX2*, and *SOX14* determines neural differentiation state analogous to homolog *TUBB3* in differentiated radial pre-cursor cells (RPs) [43], the P_{eff} interval for differentiating neural cells can be delineated as being between 0.219 and 0.318 *esebssiwaagoT*$_{\text{Q}}$ units, in which case the P_{eff} interval for differentiated neuron sub-types from distal to proximal in the neuroaxis is between a P_{eff} of 0.434 to 0.203 *esebssiwaagoT*$_{\text{Q}}$ units based on pressuromodulation mapping. Furthermore, since glial cell marker, *BCAN* (P_{eff} 0.243, $\theta_{\text{A}} = 60.6^0$) [44, 45], and neuronal markers, *SOX14* and *RBFOX3* (P_{eff} 0.213; $\theta_{\text{M}} = 59.7^0$; NeuN), are differentially expressed in symbiotic cell types; brain-specific protein of the Aggrecan class, Brevican (*BCAN*, P_{eff} 0.243; $\theta_{\text{A}} = 60.6^0$), is proposed to be the CNS hyaluronic acid-stabilizing chondroitin sulfate proteoglycan that increases the P_{eff} interval for certain differentiated neuronal cell types (ie hippocampal/Papez circuit).

The upper limit of effective intracellular pressure for proprioceptive afferent lower motor neuron [lmn (a)] gene expression is at that of gene *UNC13A* (P_{eff} 0.434; $\theta_{\text{M}} = 37.6^0$); ortholog, *munc13-1*), a nuclear membrane-associated heterochromatinized gene required for presynaptic vesicle docking exocytosis, which has been shown to be under-expressed following application of sodium channel blocker tetrodotoxin (TTX) in a standard *in vitro* culture model for study of pre-to-post synaptic neuronal activity [46]. In addition, post-synaptic scaffold protein *SHANK2* ($P_{\text{eff}} \leq 0.301$; $\theta_{\text{M}} = 53.6^0$) has been shown to be over-expressed in the model, and represents the effective intracellular pressure upper limit for gene expression in secondary upper motor neurons [umn (asc)] to thalamic nuclei. Furthermore, since it has been shown in a murine model of regulator of G protein signaling gene differential expression in the *corpus striatum* basal ganglia nigral mesencephalic dopaminergic circuit (bgnc) in response to D1R antagonist/D2R

agonist pharmacological modulation *in vivo* [47], and *RGS2* (P_{eff} 0.298; θ_{M} = 54.0^0) shown to be differentially expressed by high density array following synaptogenesis of plated neuronal precursors *in vitro* [46], the effective cellular pressure interval range for gene expression in basal ganglia nigral circuit deep brain nuclei neurons includes genes *RGS2* and *RGS16* (P_{eff} 0.251; θ_{M} = 59.7^0), which implies that *RGS4* (P_{eff} 0.118; θ_{M} = 75.8^0) is the murine paralog for the human *RGS16* gene based on the findings of this study. Dopamine receptor 1 gene *DRD1* (P_{eff} 0.249; θ_{M} = 59.7^0) co-expresses with *RGS16*, and *DRD2* is expressed at a P_{eff} of 0.217 (θ_{A} = 63.8^0)], the effective intracellular pressure range for basal ganglia nigral neuronal circuit neuronal gene expression is delineable as being between 0.217 and 0.298 *esebssiwaagoT*$_{\text{Q}}$ units, which are overexpressed on spiny neurons of the basal ganglia circuit by the late telencephalic development stage [48].

Neuronal nuclei protein (NeuN; *RBFOX3,* P_{eff} 0.213) has been shown to be expressed in pyramidal neuron layers (I-VI) of the cerebrum [bral, pyr umn (arc)], granule cell layer neurons (gr) of the cerebellum (bell) and 3-layered hippocampal formation Papez circuit (capc) by high affinity antibody histochemistry [49]. In the murine *Sox1*$^{\text{lacz/+}}$ model, early neuronal differentiation gene *SOX1* (P_{eff} 0.318; θ_{M} = 51.6^0) is maximally expressed in the periventricular zone and hippocampal Papez circuit [50], but does not appear to be expressed in the cerebral cortex (bral), while *NGB* (P_{eff} 0.305; θ_{M} = 53.2^0) globin is minimally expressed in human brain cortex and *CYGB* (P_{eff} 0.248; θ_{M} = 60^0) globin shows positive expression in the hippocampus [51]. Thus, the effective intracellular pressure interval for cortical telencephalon neuronal gene expression is determined to range between 0.213 and 0.305 *esebssiwaagoT*$_{\text{Q}}$ units (bral); whereas, the P_{eff} range for hippocampal formation Papez circuit (capc) neuronal gene expression is delineated as being between a P_{eff} of 0.318 and the effective cell pressure for expression of dopaminergic receptor *DRD3* (P_{eff} 0.203; θ_{A} = 65.2^0) [52], which is also the P_{eff} for expression of *GRIN1* (P_{eff} 0.203; θ_{A} = 65.2^0), a *NFE2L2* (P_{eff} 0.331; θ_{M} = 50.2^0) target gene, as has been shown by DNA complex/transcription factor to NRF-1 antibody by electromobility super-shift assay [53]. Furthermore, since *NUMA1* (P_{eff} 0.311; θ_{M} = 52.4^0) is shown to be differentially upregulated in cryptorchidism by qRT-PCR [54, 55], and ovarian theca cell origin *INSL3* (P_{eff} 0.321; θ_{M} = 51.2^0) is shown to be expressed in the hypothalamic neuron projections to the posterior pituitary by *in situ hybridization* [56], the upper limit of the P_{eff} range for gene transcription for peri-ventricular thalamic deep nuclei neurons will be in-between a P_{eff} of 0.305 and 0.311, whereas that for the hypothalamic pituitary axis (pituit) will be inclusive to 0.331 P_{eff} *esebssiwaagoT*$_{\text{Q}}$ units.

Based on the pressuromapping findings of the study, the upper limit interval for peripheral lower motor neuron (lmn) gene expression is definable as being between a P_{eff} of 0.434 and 0.311 (> 0.305); whereas, the range for gene expression is between a P_{eff} of 0.305 and 0.213 for cerebrocortical upper motor neurons, between a P_{eff} of 0.318 and 0.203 for hippocampocortical neurons, and between a P_{eff} of 0.298 and 0.217 for basal ganglia spiny neurons. Therefore, there exists an inverse relationship between effective range of whole cell compliance and tissue macro-compliance ($R_{\text{effective whole cell compliance}} \cdot T_{\text{macro-compliance}}$ = k), which is attributable to differences in regional negative macro-pressuromodulation in a tissue with cell populations arranged in the form of nuclear groups (ie hyaluronate matrix), and attributable to differences in the same across tissue types with differences in stromal stiffness (ie calcified matrix). In corollary, the effective cell pressure range for mesenchymal stem cell (MSC) gene expression is delineable as being between a Peff of 0.648 and <= 0.118, in which case the upper limit is attraibutable to cell-to-cell focal adhesion formation within myeloid bone caverns. Furthermore, based on the study findings, *RGS18* (P_{eff} 0.205; θ_{M} = 65.2^0), *RGS16* (P_{eff} 0.251; θ_{M} = 59.7^0; human paralog of murine *RGS4*), *lnc-RXFP4-5* (P_{eff}, 0.314; θ_{M} = 52.1^0; pituit), *RGS13* (P_{eff}, 0.360, θ_{M} = 46.5^0), *CEACAM1* (P_{eff}, 0.384; θ_{M} = 43.6^0), *SLC25A44* (P_{eff}, 0.395; θ_{M} = 42.3^0) and *RGS21* (P_{eff}, 0.413; θ_{M} = 40.1^0) are expressed within the lower motor neuron (lmn)-upper motor neuron (umn) neural cell axis; and *TSACC* (P_{eff}, 0.336; θ_{M} = 49.4^0) and *JUND* (P_{eff}, 0.344; θ_{M} = 48.4^0) are non-cell specific developmental biomarkers.

Expression of inner nuclear envelope and anti-apoptosis pathway genes in response to dynamic strain-mediated alterations in cellular compliance

Micropipette aspiration studies on nuclear envelope elasticity utilizing fluorescent nuclear protein expression plasmid transfectants to study rates of DNA displacement over time and resultant changes in the surface area expansion alpha power (α) as a measure of alterations in nuclear envelope deformability [29–31]. Study of nuclear stress response to tonicity in TC7 renal epithelial cell transfectants in which sub-nuclear displacement rates of GFP-lamin B1 during constant aspiration pressure application (*J*, creep compliance; kPa^{-1}· sec^{-1}) [30] has shown more significant heterochromatin displacement in hypertonic and isotonic nuclei (α = 0.28-0.32) in comparison to hypotonic nuclei (α = 0.21), in which case shrunken and unswollen nuclei are less deformable at the onset (J_{initial} = 0.1) in comparison to swollen nuclei (J_{initial} = 1, kPa^{-1}) with a greater initial elastic dilation modulus (*K*, mN/m), implying that hypo-osmolar nuclear swelling increases cell membrane compliance. And, subsequent

study of sub-nuclear GFP-fibrillarin (or upstream binding factor 1, UBF1-GFP) displacement in which whole cells, Saos-2 carcinoma, HeLa and human venous endothelial (HuVec), exposed to shear stress from 10 to 40 dyn/cm^2 (1 to 4 Pa) or to compressive stress of 0.1 MPa over 60 minutes [31] have shown discordant results in alpha power (α) response to 10 dyn/cm^2 physiologic shear strain for HeLa cells as compared to in HuVec cells in which there is a parabolic comparative increase in mean standard displacement (MSD) alpha power at 40 dyn/cm^2, as the equivalently-increased alpha response due to 10 dyn/cm^2 of shear stress in HeLa cells or 100 kPa of compressive stress in the same will be a result of mitochondrial challenge oxidative stress-exothermy due to differences in the initial effective cell pressure (P_{eff}) setpoints of Hela carcinoma cells and HuVec endothelial cells. Furthermore, by the study of nucleus mechanical properties in *EMD* gene-deficient (-/y) differentiated embryonic fibroblasts, it has been determined that sex-linked deficient MEFs have a lower nuclear membrane dilation modulus (K)-to shear modulus (μ) ratio than wild-type (WT) fibroblasts, 2.1 as compared to 5.1 [32], in which case it has been shown that *EMD* gene-deficient cell nuclear envelope is more rigid in mechanical stain-free conditions, as it has a more significant decay exponential ($e^{-a \mid K/\mu}$) than that for the wild-type fibroblast (WT), -0.21 and -0.04, based on nuclear GFP-lamin A/C signal intensity. Therefore, since *EMD* gene-deficient fibroblasts are less sensitive to mechanotransduction in comparison to wild-type MEFs, and the $EMD^{+/y}$ wild-type fibroblast gene P_{eff} is 0.234 (*EMD*, $\theta_A = 61.7^0$), the cellular effective pressure in $EMD^{-/y}$ is predictable as being relatively constant at a P_{eff} of ≤ 0.234 *esebssiwaagoT*$_Q$ units during mitochondrially-mediated apoptosis.

Cell nucleus deformability in dynamic strain conditions has been studied in *LMNA* gene (-/-)- or *EMD* gene (-/y)-deficient fibroblasts as compared to wildtype (WT) fibroblasts, in which anti-apoptosis pathway-related gene expression has been studied in MEFs subject to low-frequency (1 Hz) low-grade biaxial mechanical strain (4 to 10%) at for one to 24 hours and [33–35]. Based on the findings of studies considered altogether, both *LMNA* gene- and *EMD* gene-deficient MEFs are mechanotransduction-impaired [34]; however, in the former due to increased nuclear envelope deformability as nuclear envelope perceived mechanical strain correlates with applied strain in lamin A/C-deficient cells, whereas in wildtype MEFs applied strain is cell membrane perceived and mechanotranduced to comparatively less deformable nucleus of WT fibroblasts. Furthermore, based on cells studied over in mechanical strain-free conditions by phase contrast time-lapse [33], of the two inner nuclear envelope protein deficient cell types with discordant nuclear envelope rigidity, lamin A/C-deficient cells show increased nuclear dynamics as early as 1 hour, during which neither *LMNA* gene-deficient nor WT fibroblasts express immediate early response 3 (*IER3*, *IEX-1* homolog; P_{eff} 0.204, $\theta_A = 65.4^0$) or early growth response-1 (*EGR1*; P_{eff} 0.199, $\theta_A = 66.0^0$), whereas emerin (*EMD*)-deficient fibroblasts express *IER3* as they must transcribe at a P_{eff} of between 0.204 and 0.199 at baseline. In fibroblasts subject to between 2 to 4 hours of 4% biaxial cyclic strain, qRT-PCR shows significantly increased expression of both NF-κB pathway genes *IER3* and *EGR1* in WT MEFs [33], which indicates that mechanical strain decreases P_{eff} from > 0.234 to in-between 0.199 and 0.204 units in mechanotransduction-sensitive $EMD^{+/y}/LMNA^{+/+}$ fibroblasts at which *IER3* and *EGR1* gene transcription occurs; whereas, *LMNA* gene (P_{eff} 0.184; $\theta_A = 67.8^0$)-deficient fibroblasts transcribe at a relatively constant $P_{eff} \leq 0.184$ units during which neither *IER3* nor *EGR1* is transcribed similar to WT fibroblasts. Since $LMNA^{-/-}$ fibroblasts become qRT-PCR positive for *IER3* and *EGR1* in response to mechanical strain, then it can be supposed that cellular pressure initially is around a P_{eff} of 0.167 with applied dynamic stain during which *LMNB2* ($\theta_A = 69.8^0$) is expressed in the mechanotransduction in-sensitive interval, followed by an increase in P_{eff} into the 0.197 – 0.204 units range in which *LMNB1* (P_{eff}, 0.197; $\theta_A = 66.2^0$) is expressed, due to which the mechanotransduction sensitivity of the *LMNA* gene-deficient fibroblast nuclear envelope is maintained within the same. Based on these findings considered together, the P_{eff} interval between 0.172 - 0.184 *esebssiwaagoT*$_Q$ units would be the mechanotransduction insensitive range for cellular gene expression.

Expression of inner nuclear envelope and extracellular matrix pathway genes in response to substrate stiffness

The effect of gel stiffness on cell morphology has been studied *in vitro* for contrasting cells grown on collagen I or fibronectin-coated 3 to 7.5% poly-acrylamide gels varying with shear elastic moduli for cross-linked stiffness (G', Pa) ranging between 0.002 to 55 kPa, in which it has been determined that actin stress fibers begin to develop in GFP-actin expressing fibroblasts (MEFs) at a stiffness of between 1.6 and 3.6 kPa or in synergism with EGFP-actin wildtype (WT) transfectants of the same [36]. Based on these findings on altered cellular phenotype as a result of gel stiffness mechanotransduction force (G'), it can be inferred that the physiologic range of effective cellular pressure is between 0.180 and 2.9 kPa in-between the G_0 to S phase of the cell cycle during which endothelial cell (EC) sprouting occurs during formation of cytoskeletal stress fibers; and that an additional increase in cellular pressure to between 2.9 and 28.6 kPa results in progression to binucleation followed by

EC diaphragmed fenestration-associated with mitogenesis multi-nucleation. Based on MMTV-*Her2/neu*, *myc*, *ras* mammary tumor stiffness studied *in situ* (*E*, kPa) and tensional homeostasis studied in response to applied shear force *in vitro* (dynes/cm^2) [37], when solid tumor tissue pressure is at 4.05 kPa, then it can be inferred that 1.59 kPa of synergistic positive mechanotransduction pressure will be attributable to secreted collagen I fibril matrix if maximum concentration is 4.0 mg/mL, which will be expressed at an effective cell pressure (P_{eff}) range of 0.235 – 0.241 for the expression of tumor tissue collagen ligand genes *COL1A1* (P_{eff} 0.241; $\theta_A = 60.9^0$) and *COL6A1* (P_{eff} 0.235; $\theta_A = 61.6^0$) preceded by expression of integrin receptor (ie αvβ3) that requires between 1.1 and 1.6 kPa of applied force for ectopic vector expression [36, 37]. Additionally, since an applied shear force of 140 dynes/cm^2 that results in focal adhesion formation (FAK$^+$) parallels an increase in fibronectin (FN) matrix rigidity (G') with an increase in Ki67 proliferative index during MEK inhibitor application (ie PD98059) [37], therefore the shear force interval between 40 and 140 dynes/cm^2 will be the effective intracellular pressure interval between the G_2 and S cell cycle phase, which is between 0.235 to 0.283 *esebssiwaagoT*$_Q$ units [26, 27]. Furthermore, since during the differentiation of human adipose tissue stromal progenitor cells (HADSCs) or myeloid marrow mesenchymal stem cells (MSC) into chondroblasts results in the spatial expression of *COL2A1* isoforms 1 and 2 as early day 5 as chondrocyte cell-specific marker [57, 58], then the transcriptional activation of *COL2A1* (P_{eff}, 0.118; $\theta_A = 75.8^0$) both directly and indirectly by Sox1 and Nkx3.2 respectively [59] will be the initial positive pressuro-modulation event that increases effective cell pressure in MSCs upwards and then to an P_{eff} of around 0.184 *esebssiwaagoT*$_Q$ units (*LMNA*) with resultant chondrocyte lineage differentiation, after an initial decrease in P_{eff} by retinoic acid (RA) pathway activation [38].

The relationship between stoichiometry of lamin A/C to lamin-B1 protein and mRNA expression across tissue cell types (ie MSC, HSCP; U251, brain) and cellular microelasticity (kPa^{-1}) has been studied in parallel with modeling of the time constant ($1/\tau$; sec^{-1}) for lamin A:B expression relationship [38], in which it has been determined that the lamin A/C : lamin B1 expression ratio follows $E^{0.6}$ with lamin B1 expression follows $E^{0.2}$ for the spectrum of cell types, and in parallel that the lamin A:B time constant (τ) proportionality is viscosity/elasticity. Based on the findings of this study, osteo-prone human mesenchymal stem cells from marrow (MSC) express *LMNA* (P_{eff}, 0.184; $\theta_A = 67.8^0$) but at a substrate stiffness of 12 kPa, which would be due to synergistic negative macro-pressurization, which further implies that cellular focal adhesionogenesis is required for expression of toti-pluripotency marker *CD34* (P_{eff}, 0.648; $\theta_M = 11.7^0$) in the myeloid marrow cavern [26, 27], for a cell type that is functional over a wider range of cellular compliance. Hematopoietic stem cell progenitors from marrow (HSCP), normal brain cells (unspecific) and orthotopic xenograft GBM (U251) express *LMNB1* (P_{eff} 0.197, $\theta_A = 66.2^0$; ~ constant *LMNB2*, P_{eff} 0.167) at a substrate pressure between 0.1 and 0.2 kPa; moreover, based on the correlation between application of synergistic pressure and *LMNB1* gene expression across the spectrum of cell types inclusive of osteo-prone cell types ($E^{0.2}$) [38], the effective intracellular pressure (P_{eff}) at baseline is greater than extracellular stromal pressure in osteo-prone mesenchymal stem cells (MSC), whereas the effective intracellular pressure (P_{eff}) at baseline approximates extracellular stromal pressure in the latter. Furthermore, the lamin A/C: lamin B1 expression ratio that favors (cart >) skull > femur > MSC for comparative osteo-prone cell types in response to 12 kPa of MSC equivalent applied pressure for *LMNB1* expression (P_{eff} 0.197) is attributable to a narrower functional range of cellular compliance in comparative cell types inclusive of osteocytes and chondrocytes.

Nuclear envelope mechanotransduction in response to dynamic strain and pharmacological signaling

The dynamic strain responsiveness of the cell nucleus in mesenchymal stem cells (MSCs) subject to 0.2 to 2 Hz cyclic dynamic loading (3% strain, 10 min) has been studied with the application of inhibitors of molecular signaling such as lysophosphatidic acid (LPA), myosin light chain kinase inhibitor (ML-7), F-actin inhibitor (cytochalasin D) and rho-associated protein kinase inhibitor (Y-27632); studies in which nuclear deformability has been measured with the nuclear aspect ratio and index (NAR, b/a, a/b; NDI, %) in combination with ATP exocytosis and sarcolemmal Ca^{2+} release measurements, and the condensation chromatin parameter (CCP, %) utilized to detect nuclear mechanotransduction sensitivity in parallel [39–41] in pluripotent stem cells (MSC) cultured on hydrogels with a substrate stiffness of between 5 and 10 kPa.

Based on the study of mechanotransduction strain transfer in load-stressed MSCs following pre-treatment with ML-7, nuclear deformability (NDI) is increased and the yes-associated protein (YAP) pathway is activated as during dynamic loading (DL), in contrast to with the application of LPA, Y-27632 or CytoD during which nuclear deformability is decreased, and in the case of lysophosphatidic acid (LPA), pERK/ERK ratio trends towards decrease between control and dynamic loading comparison groups [39] as does matrix stiffness [38];

and by the study of alteration in chromatin condensation in dynamic strain-loaded (DL) MSCs following pre-treatment ML-7 and Y27632, CCP is indifferent at 30 sec in comparison to conditioned media (CM) + DL controls however cellular traction force (nN) decreases in response to TGFβ inhibitors or Y-27632, whereas LPA + DL increases the chromatin condensation by 1.64-fold during mitochondrial ATP exocytosis, intracellular Ca^{2+} oscillation and increase in autocrine TGF-β [40]. Therefore, these findings considered together are consistent with the heterochromatinization of DNA effect of LPAR agonist, lysophosphatidic acid (LPA) during dynamic loafing, being towards the inner nuclear membrane due to increased rigidity of the nuclear envelope as result of the positive pressurization effect of LPA; and furthermore, the increase in nuclear envelope deformability however an indifferent heterochromatinization DNA effect of cell membrane (CM) receptor inverse agonist myosin light chain kinase inhibitor (ML-7) being a result of the negative pressurization effect of ML-7 in synergism with dynamic loading (DL) that remains in the anisotropic pressure range, $P_{\text{eff}} < 0.245$.

Mechanotransduction sensitivity alterations due to dynamic loading and resultant changes in lamin A/C protein expression have been studied under during the treatment of MSCs cultured *in vitro* with positive pressuromodulators HDAC inhibitor trichostatin A (TSA), CytoD and *D*-mannitol [41], in which it has been determined that deformation of the undifferentiated MSC nucleus in response to applied dynamic strain is lessened within the lamin-A/C protein transcription interval, *LMNA* (P_{eff}, 0.184; $\theta_{\text{A}} = 67.8^0$), as determined in the study. Since in dynamic strain-stressed cells there is a cell membrane compliance-mediated decrease in nuclear P_{eff} into the nadir pressure range for mesenchymal stem cells as determined by pressuromodulation mapping [24, 26], *COL2A1* gene transcription occurs (P_{eff}, 0.118; $\theta_{\text{A}} = 75.8^0$) with resultant MSC origin CTGF gene *CCN2* (P_{eff}, 0.166; $\theta_{\text{A}} = 70^0$) transcription within the mechanotransduction in-sensitive cellular P_{eff} range ($> 0.118 \leq 0.167$ *esebssiwaagoT*$_{\text{Q}}$ units); therefore, the P_{eff} pressuromodulation setpoint in toti-pluripotent cells (ie MSCs) will be at that for transcription factor *ESRRB* gene transcription (P_{eff}, 0.172), which is required for re-initiation of pluripotency in a differentiated cell [60, 61], from which P_{eff} decreases to a peri-nadir P_{eff} around 0.118 *esebssiwaagoT*$_{\text{Q}}$ units in part by mitochondrial oxidative stress-mediated exothermy, or increases to a peak at 0.648 *esebssiwaagoT*$_{\text{Q}}$ units during the expression of a MSC origin matched limiting focal adhesion component (ie integrin subunit : collagen fibril subunit).

Conclusions

In this research, heterochromatin shift during euchromatin gene transcription has been studied by parallel determinations of DNA strand loop segmentation tropy nano-compliance (*esebssiwaagoT*$_{\text{Q}}$ units, linear nl), gene positioning angulation in linear normal two-dimensional (2-D) *z*, *y*-vertical plane (anglemetry, ^{0}), horizontal alignment to the *z*, *x*-plane (vectormetry; $\boldsymbol{m}_{\text{A}}$, $\boldsymbol{m}_{\text{M}}$, a.u.), and by pressuromodulation mapping of differentiated neuron cell sub-class operating range for neuroaxis gene expression in reference to tissue macro-compliance (P_{eff}).

Heterochromatin strand DNA loop micro-segmentation structural nano-compliance is either amorphousity, anisotropy or mesotropy loop segment forms perceiving various grades of the asymmetric tropy viscosity effect, where between 3-to-5 and 8-to-11 genes are arranged as one or two in-tandem alternating anisotropic and mesotropic gene(s), or as in-tandem anisotropic or mesotropic genes in juxtaposition separated by intergene tropy base distance; for example, the amorphousity loop segment form between positions -12 to -4 in reference *LMNA* (P_{eff}, 0.184; $\theta_{\text{A}} = 68.4^0$) on human 1q22 (+) is 5'-0.234-(a_{-12})-0.272 (m_{-11})-0.229 (a_{-10})-0.211 (a_{-9})-0.269 (m_{-8})-0.144 (a_{-7})-0.314 (m_{-6})-0.268 (m_{-5})-0.176 (a_{-4})-3'. Based on this arrangement of stranded chromatin DNA, an always-on pressurotopic model for gene transcription is proposed, in which either mesotropy loop form genes positioned between 11.7 and 60.4^0 (*CD34*) in the *z*, *y*-vertical plane are transcriptionally active when heterochromatin shifts towards the inner nuclear envelope margin following the transcription of *EMD* (P_{eff}, 0.234; $\theta_{\text{A}} = 61.7^0$), during which mechanotransduction apparatus sensitivity for linear increases in nuclear effective pressure (P_{eff}) into the expression range for collagen fibril genes *COL6A1* (P_{eff} 0.235; $\theta_{\text{A}} = 61.6^0$) and *COL1A1* ($P_{\text{eff}}$ 0.241; $\theta_{\text{A}} = 60.9^0$) for focal adhesion (FA) formation and resultant cell specific increases in nuclear pressure; or, anisotropy loop form genes positioned between 60.5 and 82.3^0 (*MIR4537*) in the *z*, *y*-vertical plane are transcriptionally active when heterochromatin shifts towards the central peripheral nucleoplasm edge, during which transcription of inner nuclear envelope peptide-coding genes *LMNB1* (P_{eff}, 0.197; $\theta_{\text{A}} = 66.2^0$) → *LMNA* ($P_{\text{eff}}$, 0.184; $\theta_{\text{A}} = 67.8^0$) to *LMNB2* ($P_{\text{eff}}$, 0.167; $\theta_{\text{A}} = 69.8^0$) regulates sensitivity for linear increases (or decreases) in mechanotransduction pressure *esebssiwaagoT*$_{\text{Q}}$ units. Based on momentum vectormetry, the relationship between effective pressure and momentum is inverse proportionality, $P_{\text{eff}}\ (0.064 \geq x < 0.245) \cdot \boldsymbol{m}_{\text{A}} = P_{\text{eff}}\ (0.245 \geq x \leq 0.648) \cdot \boldsymbol{m}_{\text{M}}$ ($P_{\text{eff}} \cdot \boldsymbol{m}_{\text{ch tropy}} = P_{\text{eff}} \cdot \boldsymbol{m}_{\text{ch tropy}} + \boldsymbol{m}_{\text{ch nmn tropy}}$) for DNA strand loop alignment in nuclear

protoplasm, which are applicable to further study of heteroeuchromatin loop segment *z*, *x*-plane alignment kinetics.

The episodic sub-episode block sums (SEB) split-integrated weighted average-averaged gene overexpression tropy quotient is a linear normal measure of effective intracellular pressure (P_{eff}) for determination of gene positioning anglemetry due to primary and secondary linearization effects, validation of the primary linearization effect is the sebs intercept-to-sebssiwa intercept linearization quotient ($b_{\text{sebs}}/b_{\text{sebssiwa}}$); in which case, normalization of the *dppasebs*, *dppmsebs* effect predominates in anisotropic gene *MYC* ($b_{\text{sebs}}/b_{\text{sebssiwa}}$: 3.63; P_{eff} 0.157; $\theta_{\text{A}} = 71^{0}$), the *uppasebs*, *uppmsebs* effect predominates in mesotropic gene *PRDM1* ($b_{\text{sebs}}/b_{\text{sebssiwa}}$: 3.45; P_{eff} 0.356; $\theta_{\text{M}} = 47^{0}$), while both the *dppasebs*, *dppmsebs* and *uppasebs*, *uppmsebs* effects are linear normalized in *PRKCH* ($b_{\text{sebs}}/b_{\text{sebssiwa}}$: 3.17; P_{eff} 0.200; $\theta_{\text{A}} = 65.8^{0}$) as examples.

Based on the findings of this study considered together, the precise mechanistic basis for alterations in chromatin gene transcription eukaryotic stranded heterochromatin arranged by structural pressurotopy nano-compliance in DNA stand loop segments is effective cell pressure (P_{eff}) regulated shifting of transcriptionally active DNA in-between the inner nuclear envelope margin and the peripheral nucleoplasm edge and the *z*, *x*-plane horizontal alignment of a gene by gene specific P_{eff} within the cell specific effective range of whole cell compliance in reference to tissue macro-compliance. The findings of this study are therefore applicable to the further study of changes in gene transcription in response to applied mechanical strain-mediated alterations in nuclear envelope deformability *in silico*.

Additional file

Additional file 1: Table S1. Sequential episodic sub-episode block sum split-integrated weighted average gene overexpression tropy quotients to final $esebssiwaagoT_{\text{Q}}$ for predicted neural axis gene overexpression [1)] Gene loci sub-episode block structure variations include non-contributory anisotropy (NCA), anisotropy converted to mesotropy (ACM), and/or 0.5-factor adjusted stabilizing mesotropy or anisotropy converted to stabilizing isotropy for anisotropy or mesotropy (stIAfM, stIMfA or stIMfM) that result in an initial to final SEB conversion; and [2)] previously reported episode and sub-episode block structure is applied in all cases as per reference [25], in which gene/gene loci at cusps of the delineated base intervals, *SHANK2* (784,883), *RBFOX3* (521,757) classify into the adjacent interval. (DOC 66 kb)

Abbreviations

ACM: Anisotropy converted to mesotropy; $b_{\text{sebs}}/b_{\text{sebssiwa}}$: Intercept sebs/intercept sebssiwa linearization quotient; *d*, d_{M} , d_{A}: Distance of gene intergene base tropy; *dppasebs*: Downstream part anisotropic sub-episode block sum; *dppasebs*: Downstream part anisotropic sub-episode block sum; *dppasebssiwa*: Downstream part anisotropic sub-episode block sum split integrated weighted average; *dppasebssiwa*: Downstream part anisotropic sub-episode block sum split integrated weighted average; NCA: Non-contributory anisotropy; P_{eff}: Effective intracellular pressure, $esebssiwaagoT_{\text{Q}}$; $prpT_{\text{Q}}$: Paired point tropy quotient; SEB: Sub-episode block; stIAfM, stIMfA or stIMfM: 0.5-factor adjusted stabilizing isotropy for anisotropy or mesotropy; *uppasebs*: Upstream part anisotropic sub-episode block sum; *uppasebssiwa*: Upstream part anisotropic sub-episode block sum split integrated weighted average; *uppmsebs*: Upstream part mesotropic sub -episode block sum; *uppmsebssiwa*: Upstream part mesotropic sub-episode block sum split integrated weighted average; Θ, Θ_{M}, Θ_{A}, Θ_{H}: Gene angle; m_{eff}, m_{A} ($m_{\text{ch tropy}}$), m_{M} ($m_{\text{ch tropy}} + m_{\text{ch nmn tropy}}$): Effective momentum

Acknowledgements

Not applicable

Authors' contributions

HS conceptualized the research, developed the methodology, analyzed the data, and wrote the manuscript. The author read and approved the final manuscript.

Funding

No funding was applied for this research.

Availability of data and materials

All data analysed in this study are included in the table files of this article.

Ethics approval and consent to participate

Not applicable

Consent for publication

Not applicable.

Competing interests

The author declares that he has no competing interests.

Received: 5 April 2019 Accepted: 22 July 2019
Published online: 02 August 2019

References

1. German J. The pattern of dna synthesis in the chromosomes of human red blood cells. J Cell Biol. 1964;20(1):37–55.
2. Comings DE. The rationale for an ordered arrangement of chromatin in the interphase nucleus. Am J Hum Genet. 1968;34(5):757–80.
3. Camargo M, Cervenka J. Patterns of DNA replication of human chromosomes. II. Replication map and replication model. Am J Hum Genet. 1982;34(5):757–80.
4. Holmquist GP. Role of replication time in the control of tissue-specific gene expression. Am J Hum Genet. 1987;40:153–73.
5. Rocchi A. On the heterogeneity of heterochromatin. Caryologia. 1982;35(2):169–89.
6. Sarin H. Permeation thresholds for hydrophilic small biomolecules across microvascular and epithelial barriers are predictable on the basis of conserved biophysical properties. In Silico Pharmacol. 2014;3:5.
7. Comings DE, Wallack AS. DNA-binding properties of nuclear matrix proteins. J Cell Sci. 1978;34(1):233–46.
8. Fawcett DW. On the occurrence of a fibrous lamina on the inner aspect of the nuclear envelope in certain cells of vertebrates. Am J Anat. 1966;119(1):129–45.
9. Markovics J, Glass L, Maul GG. Pore patterns on nuclear membranes. Exp Cell Res. 1974;55(2):443–51.
10. Gerace L, Blum A, Blobel G. Immunocytochemical localization of the major polypeptides of the nuclear pore complex-lamina fraction: interphase and mitotic distribution. J Cell Biol. 1978;79(3):545–66.
11. Blobel G. Gene gating: a hypothesis. Proc Natl Acad Sci U S A. 1985;82:8527–9.
12. Fisher DZ, Chaudhary N, Blobel G. cDNA sequencing of nuclear lamins A and C reveals primary and secondary structural homology to intermediate filament proteins. Proc Natl Acad Sci U S A. 1986;83:6450–4.
13. Wydner KL, McNeil JA, Lin F, Worman HJ, Lawrence JB. Chromosomal assignment of human nuclear envelope protein genes LMNA, LMNB1, and LBR by fluorescencein *in situ* hydridization. Genomics. 1996;32(3):474–8.
14. Kavlverda B, Roling MD, Fornerod M. Chromatin organization in relation to the nuclear periphery. FEBS Lett. 2008;582:2017–22.
15. Finlan LE, Sproul D, Thomson I, Boyle S, Kerr E, Perry P, Yistra B, Chubb JR, Bickmore WA. Recruitment to the nuclear periphery can alter expression of genes in human cells. PLoS Genet. 2008;4(3):e1000039.

16. Kalverda B, Pickersgill H, Shloma VV, Fornerod M. Nucleoporins directly stimulate expression of developmental and cell-cycle genes inside the nucleoplasm. Cell. 2010;140(3):360–71.
17. Miroshnikova YA, Nava MM, Wickstrom SA. Emerging roles of mechanical forces in chromatin regulation. J Cell Sci. 2017;130:2243–50.
18. Berk JM, Tift KE, Wilson KL. The nuclear envelope LEM-domain protein emerin. Nucleus. 2013;4(4):298–314.
19. Macgregor HC, Callan HG. The actions of enzymes on lampbrush chromosomes. J Cell Sci. 1962;s3-103:173–203.
20. Laemmli UK, Marsden MPF. Metaphase chromosome structure: evidence for a radial loop model. Cell. 1979;17(4):849–58.
21. Gall JG. Are lampbrush chromosomes unique to meiotic cells? Chromosom Res. 2012;20(8):905–9.
22. Kołowerzo-Lubnau A, Niedojadło J, Świdziński M, Bednarska-Kozakiewicz E, Smoliński DJ. Transcriptional activity in Diplotene larch microsporocytes, with emphasis on the diffuse stage. PLoS One. 2015;10(2):e0117337.
23. Sobecki M, Mrouj K, Camasses A, Parisis N, Nicolas E, Llères D, Gerbe F, Prieto S, Krasinska L, David A, Eguren M, Birling M-C, Urbach S, Hem S, Déjardin J, Malumbres M, Jay P, Dulic V, Lafontaine DLJ, Feil R, Fisher D. The cell proliferation antigen Ki-67 organises heterochromatin. eLife. 2016;5:e13722.
24. Sarin H. Pressuromodulation at the cell membrane as the basis for small molecule hormone and peptide regulation of cellular and nuclear function. J Transl Med. 2015;13:372.
25. Sarin H. Horizontal alignment of 5′ -> 3′ intergene distance segment tropy with respect to the gene as the conserved basis for DNA transcription. Future Sci OA. 2016;3(1):FSO160.
26. Sarin H. B-cell differentiation is pressuromodulated as determined by pressuromodulation mapping: part I, cell differentiation. Trans Med Comms. 2018;3(3).
27. Sarin, H. B-cell antibody class switchings are pressuromodulated events: part II, gene recombination. Trans Med Comms. 2018;3(2).
28. Belaadi N, Aurene J, Guilluy C. Under pressure: mechanical stress management in the nucleus. Cells. 2016;5(2):E27.
29. Dahl KN, Engler AJ, Pajerowski DJ, Discher DE. Power-law rheology of isolated nuclei with mapping of nuclear substructures. Biophys J. 2005;89:2855–4.
30. Booth-Gauthier EA, Alcoser TA, Yang G, Dahl KN. Force-induced changes in subnuclear movement and rheology. Biophys J. 2012;103(12):2423–31.
31. Dahl KN, Kahn SM, Wilson KL, Discher DE. The nuclear envelope lamina network has elasticity and a compressibility limit suggestive of a molecular shock absorber. J Cell Sci. 2004;117:4779–86.
32. Rowat AC, Lammerding J, Ipsen JH. Mechanical properties of the cell nucleus and the effect of emerin deficiency. Biophys J. 2006;91:4649–64.
33. Lammerding J, Schulze CP, Takahashi T, Kozlov S, Teresa Sullivan T, Kamm RD, Stewart CL, Lee RT. Lamin A/C deficiency causes defective nuclear mechanics and mechanotransduction. J Clin Invest. 2004;113:370–8.
34. Lammerding J, Hsiao J, Schulze PC, Kozlov S, Stewart CL, Lee RT. Abnormal nuclear shape and impaired mechanotransduction in emerin-deficient cells. J Cell Biol. 2005;170:781–91.
35. Rowat AC, Foster LJ, Nielsen MM, Weiss M, Ipsen JH. Characterization of the elastic properties of the nuclear envelope. J R Soc Interface. 2005;2:63–9.
36. Yeung T, George PC, Flanagan LA, Marg B, Ortiz M, Funak M, Zahir N, Ming W, Weaver V, Janmey PA. Effects of substrate stiffness on cells morphology cytoskeletal structure and adhesion. Cell Motil Cytoskeleton. 2005;60:24–34.
37. Paszek MJ, Zahir N, Johnson KR, Lakins JN, Rozenberg GL, Gefen A, Reinhart-King CA, Margulies SS, Dembo M, Boettiger D, Hammer DA, Weaver VM. Tensional homeostasis and the malignant phenotype. Cancer Cell. 2005;8:241–54.
38. Swift J, Ivanovska IL, Buxboim A, Harada T, Dingal PC, Pinter J, Pajerowski JD, Spinler KR, Shin J-W, Manorama T, Rehfeldt F, Speicher DW, Discher DE. Nuclear Lamin-A scales with tissue stiffness and enhances matrix-directed differentiation. Science. 2013;341(6149):1240104.
39. Driscoll TP, Cosgrove BD, Heo S-J, Shurden ZE, Mauck RL. Cytoskeletal to nuclear strain transfer regulates YAP signaling in mesenchymal stem cells. Biophys J. 2015;118:2783–93.
40. Heo S-J, Han WM, Szczesny SE, Cosgrove BD, Elliot DM, Lee DA, Duncan RL, Mauck RL. Mechanically induced chromatin condensation requires cellular contractility in mesenchymal stem cells. Biophys J. 2016;111:864–74.
41. Heo S-J, Driscoll TP, Thorpe SD, Nerurkar NL, Baker BM, Yang MT, Chen CS, Lee DA, Mauck RL. Differentiation alters stem cell nuclear architecture, mechanics, and mechano-sensitivity. eLife. 2016;5:e18207.
42. Popovic J, Stanisavljevic D, Schwirtlich M, Klajn A, Marjanovic J, Stevanovic M. Expression analysis of *SOX14* during retinoic acid induced neural differentiation of embryonal carcinoma cells and assessment of the effect of its ectopic expression on *SOXB* members in HeLa cells. PLoS One. 2014;9(3):e91852.
43. Yuzwa S, Borrett MJ, Innes BT, Voronova A, Ketela T, Kaplan DR, Bader GD, Miler FD. Developmental emergence of adult neural cells as revealed by single-cell transcriptional profiling. Cell Rep. 2017;21:3970–86.
44. Yamada H, Fredette B, Shitara K, Hagihara K, Miura R, Ranscht B, Stallcup WB, Yamaguchi Y. The brain chondroitin sulfate proteoglycan brevican associates with astrocytes ensheathing cerebellar glomeruli and inhibits neurite outgrowth from granule neurons. J Neurosci. 1997;17(20):7784–95.
45. Ruoslahti E. Brain extracellular matrix. (1996). Glycobiology. 1996;6(5):489–92.
46. Kitamura C, Takahashi M, Kondoh Y, Tashiro H, Tashiro T. Identification of synaptic activity-dependent genes by exposure of cultured cortical neurons to tetrodotoxin followed by its withdrawal. J Neurosci Res. 2007;85(11):2385–99.
47. Taymans JM, Leysen JE, Langlois X. Striatal gene expression of RGS2 and RGS4 is specifically mediated by dopamine D1 and D2 receptors: clues for RGS2 and RGS4 functions. J Neurochem. 2003;84(5):1118–27.
48. Straccia M, Barriga G-D, Phil Sanders P, Bombau G, Carrere J, Mairal PB, Vinh N-N, Yung S, Kelly CM, Svendsen CN, Kemp PJ, Arjomand J, Schoenfeld RC, Alberch J, Allen ND, Rosser AE, Canals JM. Quantitative high-throughput gene expression profiling of human striatal development to screen stem cell–derived medium spiny neurons. Mol Ther Methods Clin Dev. 2015;2:15030.
49. Mullen RJ, Buck CR, Smith AM. NeuN, a neuronal specific nuclear protein in vertebrates. Development. 1992;116:201–11.
50. Lixin K, Jalali A, Zhao L-R, Zhou X, McGuire T, Kazanis I, Episkopou V, Bassuk AG, Kessler JA. Dual function of Sox1 in Telencephalic progenitor cells. Dev Biol. 2007;310(1):85–98.
51. Hundahl CA, Kelsen J, Hay-Schmidt A. Neuroglobin and cytoglobin expression in the human brain. Brain Struct Funct. 2013;218(2):603–9.
52. Heintz N. Gene expression nervous system atlas (GENSAT). Nature Neurosci. 2004;7(5):483.
53. Dhar SS, Wong-Riley MTT. Coupling of energy metabolism and synaptic transmission at the transcriptional level: role of nuclear respiratory factor 1 in regulating both cytochrome c oxidase and NMDA glutamate receptor subunit genes. J Neurosci. 2009;29(2):483–92.
54. Kojima Y, Kurokawa S, Maruyama T, Sasaki S, Kohri K, Hayashi Y. Identification of differentially expressed genes in human cryptorchid testes using suppression subtractive hybridization. J of Urology. 2009;181(3):1330–7.
55. Homem CCF, Knoblich JA. Drosophila neuroblasts: a model for stem cell biology. Development. 2012;139:4297–310.
56. Carol B, Hanna CB, Yao S, Patta MC, Jensen JT, Wu X. Expression of insulin -like 3 (INSL3) and differential splicing of its receptor in the ovary of rhesus macaques. Reprod Biol Endocrinol. 2010;8:150.
57. McAlinden A, Johnstone B, Kollar J, Kazmi N, Hering TM. Expression of two novel alternatively spliced Col2a1 isoforms during chondrocyte differentiation. Matrix Biol. 2008;27(3):254–66.
58. Zhao Q, Eberspaecher H, Lefebvre V, Crombrugghe BE. Parallel expression of Sox9 and Col2a1 in cells undergoing chondrogenesis. Dev Dynam. 1997;209:377-86.
59. Kawato Y, Hirao M, Ebina K, Shi K, Hashimoto J, Honjo Y, Yoshikawa H, Myoui A. Nkx3.2 promotes primary chondrogenic differentiation by upregulating Col2a1 transcription. PLoS One. 2012;7(4):e34703.
60. Festuccia N, Osorno R, Halbritter F, Karwacki-Neisius V, Navarro P, Colby D, Wong F, Yates A, Tomlinson SR, Chambers I. Esrrb is a direct Nanog target gene that can substitute for Nanog function in pluripotent cells. Cell Stem Cell. 2012;11:477–90.
61. Takahashi K, Tanabe K, Ohnuki M, Narita M, Ichisaka T, Tomoda K, Yamanaka S. Induction of pluripotent stem cells from adult human fibroblasts by defined factors. Cell. 2007;131(5):861–72.

Publisher's Note